Identification of drugs targeting multiple viral and human proteins using computational analysis for repurposing against COVID-19

Sugandh Kumar
Institute of Life Sciences https://orcid.org/0000-0001-7000-4718
Pratima Kumari
Institute of Life Sciences https://orcid.org/0000-0001-7015-7837
Geetanjali Agnihotri
KIITS University: Kalinga Institute of Industrial Technology https://orcid.org/0000-0001-8887-4009
Preethy V Kumar
Institute of Life Sciences https://orcid.org/0000-0002-0443-7985
Bharti Singh
Institute of Life Sciences https://orcid.org/0000-0002-8817-5387
Shaheerah Khan
Institute of Life Sciences https://orcid.org/0000-0003-3146-0440
Tushar Kant Beuria
Institute of Life Sciences https://orcid.org/0000-0003-3352-4508
Gulam Hussain Syed
Institute of Life Sciences https://orcid.org/0000-0001-8540-6162
Anshuman Dixit (anshumandixit@ils.res.in)
Institute of Life Sciences https://orcid.org/0000-0001-8063-7893

Research article

Keywords: Coronavirus, COVID-19, Drug repurposing, Network analysis, Docking, polypharmacology, molecular dynamics

Posted Date: November 13th, 2020

DOI: https://doi.org/10.21203/rs.3.rs-101778/v1

Abstract

The SARS-CoV2 is a highly contagious pathogen that causes COVID-19 disease. It has affected millions of people globally with an average lethality of ~3%. Unfortunately, there is no standard cure for the disease, although some drugs are under clinical trial. Thus, there is an urgent need of drugs for the treatment of COVID-19.

In the current studies, we have used state of the art bioinformatics techniques to screen the FDA approved drugs against nine SARS-CoV2 proteins to identify drugs for quick repurposing. The strategy was to identify potential drugs that can target multiple viral proteins simultaneously.

Additionally, we analyzed if the identified molecules can also affect the human proteins whose expression is differentially modulated during SARS-CoV2 infection. The differentially expressed genes (DEGs) as a result of SARS-CoV2 infection were identified using NCBI-GEO data (GEO-ID: GSE-147507). Targeting such genes may also be a beneficial strategy to curb disease manifestation. We have identified 74 molecules that can bind to various SARS-CoV2 and human host proteins. Their possible use in COVID-19 have also been reviewed in detail. We hope that this study will help development of multipotent drugs, simultaneously targeting the viral and host proteins, for the treatment of COVID-19.

1. Introduction:

Novel zoonotic viruses with potential for rapid spread and significant pathology pose a grave threat to humans. During the last few decades many epidemics of viral diseases have occurred such as Ebola, Zika, Nipah, Avian influenza (H7N9), HIN1, Severe Acute Respiratory Syndrome Coronavirus 1 (SARS-CoV1), and Middle East Respiratory Syndrome Coronavirus (MERS-CoV) (1).

In the end of 2019, mysterious pneumonia cases begin to emerge in China's Wuhan city. A novel coronavirus, which was later renamed as severe acute respiratory syndrome coronavirus 2 (SARS-CoV2) was found to be the causative organism and the disease was termed "coronavirus disease-19" (COVID-19) (2). COVID-19 is the world's worst pandemic and has so far affected about 35 million people globally (identified cases as on 5th Oct 2020), with average lethality of ~ 3%. Infection with SARS-CoV2 results in acute respiratory distress syndrome (ARDS) leading to lung injury, respiratory distress and lethality. Elderly patients and those with comorbidities have been reported to be at risk of higher mortality. The extremely infectious nature of the disease, emergence of new hyperinfective strains and the fact that there is no vaccine or effective drug is a serious cause of concern.

The SARS-CoV2, SARS-CoV1 and MERS-CoV belongs to the family of Coronaviridae and β-coronavirus genus (3). While bats are considered to be the origin of SARS-CoV1 and SARS-CoV2, the intermediate host that led to human transmission of SARS-CoV2 is still unknown. Sequence analysis reveals that SARS-CoV2 is similar to coronavirus identified in Malayan pangolins (*Manis javanica*) (4). The SARS-CoV2 genome is 29.8–29.9 kb positive-sense single stranded RNA with 5'-cap and 3'-poly-A tail. Its genome is organised into two segments that encode non-structural (Nsp) and structural proteins. The first

segment is directly translated by ribosomal frameshifting into polyprotein 1a (486 kDa) or 1ab (790 kDa) (ORF1a, ORF1ab) which results in generation of non-structural proteins and formation of replication-transcription complex (RTC) (5, 6). Discontinuous transcription of the viral genome results in formation of subgenomic RNAs (sgRNAs) containing common 5'- and 3'- leader and terminal sequences which serve as the template for subgenomic mRNA production (6). The ORF1a/1ab covers two-thirds of the whole genomic length and encodes for the 16 non-structural proteins (Nsp1-16), which play critical role in various viral processes. The second segment at the 3'-terminus of the genome encodes the four main structural proteins: spike (S), membrane (M), envelope (E), and nucleocapsid (N) proteins (6). The life cycle of SARS-CoV2 starts with its entry into the host cell through receptor mediated endocytosis initiated by the binding of its Spike protein to the ACE2 receptor (7). Subsequently, uncoating of the virus particle releases the genome, which is translated to generate replication-transcription complex proteins. The viral RTC complex then generates full length negative sense RNA which is subsequently transcribed into full length genome. The viral genome and structural proteins are assembled into virions near the ER and Golgi interface and are transported out of the cell through vesicles by the process of exocytosis (8).

The detailed understanding of the clinical manifestations and the underlying molecular mechanisms that drive disease pathogenesis are still unclear. There is no standard cure for the disease and currently the therapeutic regimen involves symptomatic treatment and drugs approved for emergency use such as remdesivir, favipiravir and ivermectin etc(9). Worldwide efforts to develop vaccines and drug against SARS-CoV2 are ongoing. Based on the similarity and information available from other coronaviruses, repurposing of approved drugs is among the best and rapid strategies to identify potential drug candidates (10). In this context, the computational techniques can quickly identify novel molecules that target viral proteins to suggest candidates for repurposing. Hence, during the COVID pandemic a lot of studies have been reported using a variety of such strategies (11, 12)

The *in-silico* studies have identified many drugs that can target viral proteins viz. RNA-dependent RNA polymerase (RdRp), Spike, proteases ($3CL^{pro}$ and PL^{pro}) and human proteins such as angiotensin converting enzyme 2 (ACE2), transmembrane serine protease (TMPRSS2), and PIKfyve etc. (13). Among them zanamivir, indinavir, saquinavir, and lopinavir are notable (14, 15). There are many drugs such as baricitinib (16), remdesivir (17, 18), favipiravir (19), duvelisib, ivermectin (20) and arbidol (21) etc., that are currently under clinical trials (https://clinicaltrials.gov/) to treat SARS-CoV-2 infection.

Recent reports suggests that the SARS-CoV2 not only causes infection in the lungs but may also cause infection in brain tissues (22). The experiments on mice have shown that the SARS-CoV2 infections can cause neuronal distruction and death (23). In COVID-19 also similar effects have been seen (24). In light of the above, the therapeutic agents with good CNS penetration ability could have additional advantage (25).

Only a few studies have reported targeting more than one viral protein with a single molecule or using combination therapy. In this study, we attempted to identify molecules that can simultaneously bind to multiple proteins of the SARS-CoV2. The strategy to target multiple proteins originates from the fact that

individual viral proteins play specific role in multiple aspects of viral lifecycle such as attachment, entry, replication, morphogenesis and egress. Single molecules that can potentially target many viral proteins can perturb viral lifecycle at multiple points and thereby can be highly efficient in curbing SARS-CoV2 infection. Such strategy will also have a higher barrier towards emergence of resistant mutants.

In this work, we have used the 3D-structures of the SARS-CoV2 proteins to identify FDA approved drugs that can bind to these proteins using bioinformatics methods. The FDA approved drugs were chosen so that they can be quickly repurposed for treating COVID19. Additionally, we also analyzed if the identified molecules can affect the host proteins that get differentially expressed as a result of SARS-CoV2 infection. These molecules can be used as modulators of both the SARS-CoV2 and human proteins.

2. Methods:

2.1. Protein structure modelling:

The SARS-CoV2 proteins for which there is no crystal structure reported were modelled using Modeller v9.22(26) (homology modeling). The modelling template for each protein was identified by performing Delta-BLAST against the PDB database. Proteins were modelled using either single or multiple templates based on the query coverage. Further, the model stereochemistry and other structural parameters were assessed using standalone PROCHECK tool.

2.2. Molecular docking of FDA approved drugs in SARS-CoV2 proteins:

The ensemble docking approach increases the efficiency by allowing virtual screening against multiple conformations (27). Therefore, the selected protein structures were subjected to 20 ns MD run (total 180 ns) using NAMD2.6 (28) to explore the flexibility of the binding site. Snapshots were generated at equal time points during MD simulation for each protein. The structures of the FDA approved drugs were obtained from the e-drugs (https://chemoinfo.ipmc.cnrs.fr/TMP/tmp.13454/e-Drug3D_1993.sdf) repository containing 1993 molecules in the current library (updated till July 2020). The molecules were prepared by Schrödinger LigPrep wizard ligands using the default parameters. The protein structures were prepared by addition of missing atoms, hydrogens, assignment of bond orders and proper protonation states. The structure of each of the protein was minimized by keeping heavy atoms fixed and then the whole structure was minimized until a RMS gradient of 0.3 kcal/mol/Å as implied in Schrodinger.

The active site of the modelled proteins were identified using either of the following methods 1) the ligand binding pocket, if the co-crystal structure is available or 2) the ligand bound co-crystal structure of a close homolog or 3) the active site was predicted using sitemap algorithm in Schrodinger v9.3 molecular modelling software (29). The proteins with active site pocket volume of < 150 $Å^3$ were removed as smaller pockets may not be amenable to docking. The pockets were further selected by sequence comparisons and available literature. Finally, 9 proteins were selected for docking. The molecular docking

was performed using the Glide module of Schrodinger molecular modelling software (www.schrodinger.com/glide). The docking was performed using default settings except that the formation of intramolecular hydrogen bonds was rewarded and the enhancement of planarity of conjugated π groups was checked on. Strain correction terms were applied and a maximum of 10 poses were generated for each of the molecules. The final ranking of the molecules was obtained by calculating the average glide score in the five snapshots of a viral protein generated by molecular dynamics simulation to include the effect of binding site dynamics. The molecules showing a docking score of -8.5 (roughly corresponding to 1 μm)(12) or better were selected for further analysis.

2.3. Binding free energy calculation (MM-GBSA):

The obtained hits were subjected to MM-GBSA analysis as implied in Glide module of Schrodinger modeling software for further selection of better hits. The receptor residues within 5 Å of the ligands were considered flexible for the MM-GBSA procedure with other default settings. Since the MM-GBSA binding energies reflect approximate free energies of binding, a more negative value indicates stronger binding. Similar to average glide score, average MMGBSA score was also calculated for each of the ligand for each viral protein.

2.4. The differential gene expression (DEGs) and protein-protein interaction network analysis:

The differentially expressed genes were obtained from the data reported by Blanco-Melo *et al* (30). The identified DEGs were mapped for their interactions with other human proteins using HIPPIE v2.2 which contains 14855 proteins and 411430 interactions. The reported protein-protein interactions with a minimum score of 0.63 (medium confidence, 2nd quartile)(31) were used for creation of the network using Cytoscape v3.7.2. The largest interconnected component was extracted and degree for individual nodes was calculated to assess their importance in the network.

2.5. Interaction with human proteins:

The drug-gene interaction database (DGIdb) that contains information about the drugs and their target genes was employed to identify the drugs that can modulate the differentially expressed genes in COVID-19. The drug gene interaction was obtained from various online resources such as Drugbank, BindingDB. It was utilized to identify the drugs that can target both the viral as well as human proteins. Further, it was analysed whether a drug is agonist or antagonist for a given human protein for optimum therapeutic effect.

The calculations were performed on the high performance Linux cluster. The flowchart of the methodology is presented in Fig. 1.

3. Results

As stated earlier a total of nine viral proteins (Table 1) were selected for molecular docking.

Table 1
The details of the proteins selected for screening.

S. No.	Protein Name	Length*	RefSeq ID	Source[$]
1	Spike protein	1273	YP_009724390.1	PDB: 6VSB
2	Nucleocapsid phosphoprotein	419	YP_009724397.2	PDB:6WJI
3	PL^{Pro} (Nsp3)	1945	YP_009724389.1	PDB:6W02
4	Main protease ($3CL^{Pro}$, Nsp5)	306	YP_009725301.1	PDB:6W63
5	RNA-dependent RNA polymerase (Nsp12)	932	YP_009725307.1	PDB:7BV2
6	Helicase (Nsp13)	601	YP_009725308.1	PDB:6XEZ
7	3'-to-5' exonuclease (Nsp14)	527	YP_009725309.1	Homology modelled
8	EndoRNAse (Nsp15)	346	YP_009725310.1	PDB:6VWW
9	2'-O-ribose methyltransferase (Nsp16)	298	YP_009725311.1	PDB:6W4H

*Number of amino acids. [$]PDB/homology modelling

The computational analysis of ligands binding to various proteins is a powerful method to quickly identify potential molecules for further analysis. These methods have been successfully used in various studies (32). In the first stage, the molecules were docked into the SARS-CoV2 protein snapshots using Glide module of Schrodinger in standard precision (SP) mode. The molecules were then ranked using average Glide score. The MM-GBSA was then performed to ensure the appropriate selection of top hits. All hits were visually inspected for interactions with receptor residues.

We adapted the following notion for our drug repurposing analysis: **1**. drugs that can inhibit viral entry into host cell by perturbing the function of surface glycoproteins like the spike. **2.** blocking the functions of viral enzymes that plays a vital role in replication such as 2'-O-ribose methyl transferase, RNA-dependent RNA polymerase, endoRNAse, helicase, 3'-to-5' exonuclease, 3C-like main protease and papain-like protease. **3.** drugs that can also affect differentially expressed host proteins in COVID-19 along with the viral proteins.

3.1 Molecules docking to SARS-CoV2 Structural proteins:

The hallmark feature of coronaviruses is their transmembrane **spike (S) glycoprotein** as this protein is reason for its name “Corona” in Latin meaning, "Crown". SARS-CoV-2 uses the spike (S) protein to attach to host cells. The spike protein exists as homo-trimers. Each monomer is about 180 kDa and has two distinct subunits S1 and S2. While the receptor binding is mediated by S1 subunit with the help of

receptor binding domain (RBD), the fusion between the viral envelope and the host cellular membranes is facilitated by the S2 subunits upon the cleavage of S1-S2 junction by host proteases (33). The S1 subunit of spike protein in SARS-CoV2 has four distinct domains: NTD, CTD1, CTD2 and CTD3, of these the “up” conformation of CTD1 is responsible for binding with ACE2 receptor (34). The S protein, due to its important role in the very first stage of infection, is an important target for development of therapeutics and vaccines. The co-crystal structure of the S-protein with small molecule ligand is not available, therefore we used the sitemap algorithm in Schrodinger to identify the active site on S-protein. The sitemap revealed a site that is very close to the receptor binding domain and trimerization interface lined by the residues Ser 46, Leu 48, Leu 303, Lys 304, Ser 305, Glu 309, Thr 732, Asn 758, Thr 827, Phe 833, Tyr 837, Arg 847, Lys 854, Asn 856, Val 860, Gln 949, Val 952, Asn 955, Gln 957, Asn 960, Val 963, and His 1058. Many of these residues are highly conserved among coronaviruses. The site is overlapping to the site suggested by Kalathiya *et al* (35). Recently, some of the SARS-CoV2 strains containing mutants of the S-protein (D614G) with high infectivity have been reported. This mutant does not change the structure of S-protein but increases its binding with human TMPRSS2 protein (36). This mutation is away from the identified binding site.

Our molecular docking analysis suggest that capreomycin, posaconazole, mefloquine, nebivolol, angiotensin II, celecoxib and trimethoprim bind to spike protein with appreciable affinity (Supplementary Table 1) (Fig. 2). Other groups have also predicted the binding of posaconazole to spike protein which further substantiates our analysis (37). Posaconazole is an antifungal agent used in the prevention of invasive fungal infections and is also shown to inhibit the entry of Chikungunya virus (38) and replication of Zika and Dengue viruses by binding to oxysterol-binding protein (sterol transporter) (39). Mefloquine is an antimalarial drug used in chloroquine resistant malaria. Nebivolol is an antihypertensive molecule with a very good safety profile in subjects with obstructive respiratory comorbidities (40) and can be an important drug to consider in SARS like diseases. Capreomycin is a polypeptide (isolated from *Streptomyces capreolus*) used in the treatment of multidrug resistant tuberculosis. Its mechanism is similar to aminoglycosides and used in the inhalation therapy of pulmonary tuberculosis by spray-drying technology (41, 42). It can be a promising prophylactic agent against SARS-CoV2 using similar application strategy (Fig. 2).

The nucleocapsid (N) protein is crucial for the viral RNA packaging. It is made up of two distinct RNA-binding domains (the N-terminal and the C-terminal domain) linked by serine/arginine-rich (SR-rich) domain (SRD)(43). Previous studies with SARS-CoV1 suggest that N protein inhibits TGF-beta, AP-1, NF-kB signaling and type 1 interferon production but induces apoptosis. The sera of COVID-19 patients shows the presence of IgG, IgA, and IgM antibodies against N protein suggesting its role in eliciting humoral immune response (44, 45). In the current study the crystal structure of N-terminal dimerization domain of nucleocapsid phosphoprotein with a ligand (PDB ID: 6WKP) is used. The ligand binds at the dimer interface and has interactions with residues of both of the chains. The active site was defined as residues lying within 5 Å of the cocrystallized ligand. Our study predicts that nelarabine, paclitaxel, regadenoson, quinaprilat and bromfenac are among top molecules binding to N protein (Supplementary Table 1) (Fig. 3).

3.2. Molecules docking to SARS-CoV2 enzymes:

2'-O-Methyl Transferase (Nsp16) of SARS-CoV2 belongs to the S-adenosylmethionine-dependent methyl transferase family and is activated upon binding to Nsp10. Capping of viral mRNA at 5'-end is one of the viral strategy for protecting viral transcripts from host 5' exoribonucleases and escaping the host innate immune response by mimicking as host mRNAs, thus Nsp16 is the potential target for antiviral therapeutics (46).

The crystal structure of SARS-CoV2 Nsp16 (PDB ID: 6W4H, co-crystallized with S-adenosyl methionine) was used in the current studies. The binding site was found to be lined by the residues Phe 70, Gly 71, Ala 72, Gly 73, Asp 99, Leu 100, Leu 111, Gly 113, Met 131, Tyr 132, Asp 133, Phe 149, Asp 114, Ala 116, Cys 115, and Val 118. Our study shows that methotrexate, viomycin, saralin, saquinavir, venetoclax, vidarabine, histrelin, triptorelin and ribavirin binds to Nsp16 with high affinity (Supplementary Table 1). Methotrexate forms hydrogen bonds with Asn6841, Asp6928, Lys6968, Asp6897, Asn6899 and Asp6876 of NSP16. (Fig. 4).

Methotrexate acts as an antimetabolite and thus used as an antineoplastic drug. It is also used in treatment of inflammatory diseases like rheumatoid arthritis. It decreases the de novo synthesis of purines and pyrimidines and forms dimers with thymidylate synthase (TS), hence also has anti-parasitic effect (47). Methotrexate is also shown to effectively reduce replication of Zika and Dengue viruses (48). Zidovudine is used in HIV1 treatment (21), histrelin and triptorelin are gonadotropin-releasing hormone analogs used in the treatment of central precocious puberty and endometriosis (49). Lanreotide is a long-acting analog of somatostatin and is used for the management of acromegaly, a condition caused by excess secretion of growth hormone. Octreotide is also a somatostatin analog currently used for the treatment of watery diarrhoea and flushes caused by certain carcinoid tumors. Vidarabine (ara-A) is a purine analog and an antiviral drug used for infections caused by herpes simplex and varicella zoster viruses.

Among all the proteins encoded by SARS-CoV2 genome, **PL^{pro} (papain-like protease) and $3CL^{pro}$ (3C chymotrypsin-like protease)** are two important viral proteases that cleave the two polyproteins (pp1a and pp1ab) into individual functional viral proteins (Nsp2-Nsp16). The two proteases are important for replication and controlling the host cell response and hence they are among the key targets for the development of therapeutics against SARS-CoV2. These proteases have cysteine in the active site that has also been targeted for the development of covalent inhibitors. There are many small molecules, peptides and peptidomimetics that have been developed against these proteases (50–52).

The $3CL^{pro}$ is a cysteine protease having three domains: β-barrel Domain I (residues 8–101) and II (residues 102–184) and α-helix domain III (residues 201–306) similar in structure to chymotrypsin (53). The functional protease is a dimer that cleaves polyprotein 1ab in 11 regions at its specific cleavage site (P1) of Leu-Gln↓(Ser, Ala, Gly). The sequences of SARS-CoV2 and SARS-CoV main protease are highly similar (96% identity) and so their 3D structures, barring some surface residues. However, enigmatically

the inhibitors of SARS-CoV $3CL^{pro}$ lopinavir and ritonavir that were also recommended for use against SARS-CoV2 have not shown expected results in the clinical trials for COVID-19 (54). The binding site for $3CL^{pro}$ was defined as residues falling within 5 Å of the co-crystallized ligand (PDB: 6W63). The residues Thr 25, His 41, Cys 44, Thr 45, Ser 46, Met 49, Asn 142, Gly 143, Ser 144, Cys 145, His 164, Met 165, Glu 166, Leu 167, Pro 168, Asp 187, Arg 188, Gln 189, and Gln 192 were used for defining the active site. Rupintrivir, alatrofloxacin, cangrelor, capreomycin, naldemedine, lopinavir and indinavir are among the drugs predicted to bind to $3CL^{pro}$ (Supplementary Table 1) (Fig. 5). It is important to note that most of the molecules are making HB interactions with the oxyanion hole residues (Asn 142, **Gly 143**, Ser 144) of the $3CL^{pro}$.

Previous studies report α-ketoamides, lopinavir and ritonavir as inhibitor of $3CL^{pro}$ (55, 56). Ruprintrivir inhibits human rhinovirus (HRV) 3C protease and has shown broad-spectrum anti-HRV activity (57). Others have also indicated it to be useful against SARS-CoV2 main protease (58). Indinavir is shown to inhibit HIV protease by blocking its active site and leads to immature virus particle formation, however high doses have been linked to lipodystrophy syndrome (59). Naldemedine, is a μ-opioid receptor antagonist used for the treatment of opioid-induced constipation (60).

PL^{pro} is a domain within nsp3 of pp1a/pp1ab with proteolytic activity. It cleaves three sites at 181–182, 818–819, and 2763–2764 at the N-terminus of PP1ab (61). It is the least explored among coronavirus proteins and only a few inhibitors are known for this protein (62). Our study predicts that galidesivir, pralatrexte, methotrexate, daunorubicin, ganciclovir, folic acid, montelukast and itraconazole are among interesting molecules binding to the protease PL^{pro} (Supplementary Table 1). Galidesivir has broad-spectrum antiviral activity (in vitro) against many RNA viruses in nine different families, including the coronaviruses (63). The binding of galidesivir with PL^{pro} is shown in Fig. 6. This drug has been under clinical trials for COVID-19 (NCT03891420). Daunorubicin (DNR) is the anthracycline compound used in the Kaposi's sarcoma and lymphomas treatment of HIV-1 infected patients (64). Moreover its derivative N,N-dimethyl daunomycin (NDMD) is used as the inhibitor of Herpes simplex virus (HSV) (65). Montelukast is shown to reduce proinflammatory cytokines e.g. TNF-α, IL-6 and IL-1β levels (66, 67). A previous study suggests that it inhibits Zika virus by disrupting the integrity of the virions (68). It has been predicted by other groups as well to bind to main protease of SARS-CoV2 (69). An interesting observation is the identification of folic acid as a high affinity ligand of PL^{pro}.

Helicase enzyme (Nsp13) of SARS-CoV2 is motor protein essential for unwinding of both dsDNA and dsRNA and has metal binding (Zn2+) N-terminal and helicase domain (Hel). It is involved in formation of RTC of SARS-CoV2 along with RdRp, which is known to enhance its activity (70). The SARS-CoV2 helicase has 99.8% sequence similarity with that of SARS-CoV. Since it is one of the most conserved proteins in Nidoviruses and is essential for viral RNA synthesis, it is an attractive target for antiviral drug development. A recent review summarizes its importance as a drug target in COVID-19 (71). In the current studies the cryo electron microscope structure of helicase-RdRp (PDB: 6XEZ) was used. The residues within 5 Å of the ADP bound to helicase enzyme were defined as the active site. Our analysis shows that

eratapenem, methotrexate, clofarabine, trimethoprim, ascorbic acid, cefixime, and pibrentasvir bind to the helicase with high affinity (Fig. 7). Clofarabine is a potent HIV-1 inhibitor (72). Pibrentasvir, is a HCV NS5A inhibitor effective against all HCV genotypes (73).

The most vital enzyme responsible for the replication/transcription of the viral genome is the **RNA-dependent RNA polymerase (RdRp)** also known as Nsp12. The primer for RdRp RNA synthesis is synthesized by Nsp8 (74). It has two main functional domains namely nidovirus RdRp associated nucleotidyl transferase (NIRAN) domain and RNA dependent RNA polymerase (RdRp) domain. The NIRAN domain helps in nucleotide transfer while RdRp domain is involved in the polymerisation. The RdRp is conserved in structure and function among RNA viruses (75). This enzyme, due to its importance in viral replication and also to the fact that humans are devoid of it, is a very attractive target (76, 77). Moreoever due to the availability of its structure with cofactors Nsp7 and Nsp8 (PDB: 6M71) and remdesivir (PDB: 7BV2) the structure based design is feasible. A number of studies have been done on development of RdRp inhibitors and some molecules e.g. remdesivir, favipiravir etc. have been approved for emergency use in COVID-19.

In the current studies, we have used the structure of RdRp complexed with remdesivir (PDB: 7BV2). The residues falling withing 5 Å of the remdesivir were defined as active site. Our analysis shows that fludarabine, cobicistat, capreomycin, regadenoson, doxazocin, pibrentasvir, elbasvir, indinavir and remdesivir among others that can bind with RdRp (Fig. 8).

Fludarabine is used for the treatment of hematological malignancies. It inhibits various critical enzymes and results in the inhibition of DNA synthesis. It has been predicted to be ative against SARS-CoV2 RdRp by other groups as well (69, 78). Ribavirin is broad spectrum antiviral used for treatment of RSV infection, hepatitis C and viral hemorrhagic fevers (79). It is a well known RdRp inhibitor. Cobicistat is known to inhibit the cytochrome-mediated metabolism of HIV protease and was approved in 2012 by FDA as pharmacoenhancer for HIV treatment (80). Other groups have also predicted that cobicistat and capreomycin can inhibit SARS-CoV2 protease (81) (82). Pibrentasvir and elbasvir are HCV NS5A inhibitors and indinavir is potent HIV protease inhibitor (83). Another molecule monteleukast, a leukotrine inhibitor used as antihistaminic was also showing good affinity towards RdRp (docking score − 9.42). The molecules we identified to bind to RdRp can serve as potential alternatives to remdesivir.

The Nsp15 is EndoRNase with endoribonuclease activity. It cleaves the 5' and 3' of uridylate residues in RNA by forming 2'-3'cyclic phosphodiester. Its mechanism is similar to that of RNase A, RNAse T1 and XendoU (84). Its NendoU activity can interfere with the host’s innate immune response and masks the exposure of viral dsRNA to host dsRNA sensors (85). The crystal structure of SARS-CoV2 Nsp15 cocrystallized with U5P (PDB: 6WLC) was used in the current studies. The active site was defined by the residues falling with 5 Å of the co-crystallized ligand. The active site is situated near the N-terminal and is surrounded by beta sheets and a helix. In our analysis, drugs such as quinapril, octreotide, folic acid, and macimorelin were found to bind to Nsp15 with appreciable affinity (Fig. 9). Quinapril is an angiotensin converting enzyme (ACE) inhibitor and the ACE inhibitors have been suggested to be beneficial for COVID-

19 patients (86). Folic acid is essential for DNA and protein synthesis and in the adaptive immune response (87). The dose dependent effect of folic acid on rotavirus infected mice has been reported indicting its antiviral activity (88). Additionally, the role of folic acid in the prevention of cellular entry of SARS-CoV2 has been reported (89). Macimorelin is used for the diagnosis of adult growth hormone deficiency (90). Interestingly other groups have also predicted it to be active against SARS-CoV2 (91, 92).

Nsp14 is the 3'-5'exonuclease that plays a role in proofreading mechanism (93). Nsp14 contains four conserved DE-D-D acidic and a zinc-finger (ZnF) domain (94). The homology model of Nsp14 based on the crystal structure of closely related Nsp14 of SARS CoV (PDB: 5C8T_chainB, 95.07% identity) was used for the current studies. The binding site was defined by comparison with the cocrystallized ligand (PDB: 5C8T, chainB). The SARS-CoV2 Nsp14 active site was found to be lined by the residues Arg289, Trp292, Asn306, Arg310, Asp324, Lys336, Asp362, Ala363, Leu366, Asn386, Asn388, Phe401, Tyr419, Asn422, Phe426, His455, Arg476, Tyr491, and Phe506.

Our molecular docking predicted that cangrelor, venetoclax, pimozide, nilotinib, droperidol, nebivolol, indacaterol, ezetimibe, simeprevir, siponimod, lapatinib, elagolix bind to Nsp14 (Fig. 10).

Pimozide, a calmodulin inhibitor is shown to inhibit Chikungunya virus secretion (95). Moreover, it binds to the envelope protein of HCV and inhibits infection with many HCV genotypes (96). Droperidol is also predicted by other groups to be effective against SARS-CoV2 infection (97). Ezetimibe is shown to inhibit formation of capsid-associated relaxed circular DNA of Hepatitis B Virus (HBV) (98) and is also shown to inhibit Dengue infection by interfering in formation of replication complex (99). Indacaterol is the β2-adrenoceptor agonist and used in the treatment of chronic obstructive pulmonary disease (COPD) since it induces bronchodilation (100). It is a promising candidate for therapeutics against SARS-CoV2 due to its ability to regulate genes involved in suppressing proinflammatory cytokine production and attenuation of airway hyper-responsiveness (101). However, dose and treatment schedule needs to be evaluated due to its counter effect on the expression of RNase L which is vital for antiviral response.

Since one of our major objectives was modeling of the intrinsic flexibility of the SARS-CoV2 proteins by molecular dynamics simulation and finding drugs that can adjust with the site flexibility. We provide a summary of the top drugs for individual proteins and their docking scores in the frames generated by molecular dynamics along with the average MMGBSA score Table 2. The drugs with consistently good docking scores will have a better average. This approach is novel and is not reported anywhere before for screening of drugs against SARS-CoV2 as per the best of our knowledge.

Table 2
Docking and MMGBSA scores of top drugs targeting different SARS-CoV2 proteins.

RdRp							
Drugs/Frames	**F1$^{\$}$**	**F2$^{\$}$**	**F3$^{\$}$**	**F4$^{\$}$**	**F5$^{\$}$**	**Avg_score***	**MMGBSA_Avg$^{\#}$**
Fludarabine	-11.32	-10.85	-9.83	-11.34	-11.86	-11.04	-126.47
Ribavirin	-10.83	-9.63	-10.24	-10.06	-11.38	-10.43	-110.14
Acrobase	-12.94	-10.58	-8.08	-9.28	-10.63	-10.30	-99.25
Remdesivir	-10.53	-9.69	-8.49	-10.02	-10.21	-9.79	-107.23
Cangrelor	-9.39	-8.36	-9.03	-9.42	-10.36	-9.31	-118.86
Nebivolol	-9.56	-9.89	-8.69	-7.98	-10.13	-9.25	-88.87
Spike							
Capreomycin	-9.61	-8.82	-9.16	-8.24	-9.68	-9.10	-168.25
Trimethoprim	-9.39	-9.02	-8.97	-8.14	-9.26	-8.96	-85.29
Mefloquine	-8.56	-8.69	-7.89	-9.02	-9.10	-8.65	-105.84
Nebivolol	-8.56	-8.59	-8.47	-7.89	-9.26	-8.55	-135.63
Angiotensin II	-10.77	-8.68	-7.28	-8.02	-7.89	-8.53	-96.82
Celecoxib	-9.23	-7.58	-8.08	-7.89	-8.95	-8.35	-83.21
Main Protease (3CL^{pro})							
Octreotide	-11.08	-11.58	-11.03	-11.03	-10.25	-10.99	-78.23
Rupintrivir	-10.68	-10.56	-9.87	-10.78	-11.03	-10.58	-110.61
Lopinavir	-11.04	-9.58	-9.97	-10.89	-11.31	-10.56	-92.06
Lapatinib	-10.03	-10.56	-10.00	-10.97	-11.03	-10.52	-87.03
Ritonavir	-10.77	-10.26	-10.36	-10.02	-10.98	-10.48	-85.06
Fosaprepitant	-9.89	-9.85	-10.24	-10.36	-10.58	-10.18	-93.05
Exonuclease							
Cangrelor	-11.79	-10.58	-11.06	-11.03	-11.28	-11.15	-147.54
Venetoclax	-9.90	-10.03	-10.07	-9.58	-10.01	-9.92	-165.58
Pimozide	-9.68	-9.50	-9.89	-10.05	-10.21	-9.87	-90.28

$^{\$}$docking score in individual snapshots generated from molecular dynamics (F1-F5), *average docking score. $^{\#}$average MMGBSA score.

RdRp							
Nebivolol	-9.23	-9.45	-10.25	-10.84	-9.58	-9.87	-115.42
Nilotinib	-9.46	-9.65	-9.89	-10.58	-9.25	-9.77	-105.87
Droperidol	-9.34	-9.26	-10.21	-9.87	-8.51	-9.44	-100.52
EndoNuclease							
Octreotide	-9.40	-8.12	-8.58	-10.87	-11.03	-9.60	-86.25
Quinapril	-9.63	-8.69	-9.02	-9.36	-10.02	-9.34	-108.02
Metaraminol	-9.47	-9.57	-8.24	-10.24	-9.02	-9.31	-98.57
Ribavirin	-8.06	-9.28	-8.26	-10.03	-10.58	-9.24	111.58
Folic Acid	-8.89	-8.98	-9.36	-8.14	-10.28	-9.13	-99.58
Macimorelin	-8.52	-7.85	-9.28	-8.97	-10.03	-8.93	-108.20
Helicase							
Eratapenem	-10.34	-9.51	-9.67	-10.21	-9.58	-9.86	-120.58
Methotrexate	-9.99	-8.28	-10.69	-9.14	-10.78	-9.78	-111.21
Trimethoprim	-8.25	-8.59	-9.41	-9.26	-9.57	-9.02	-105.13
Cefixime	-9.03	-8.52	-8.66	-8.87	-9.25	-8.87	-60.25
Clofarabine	-8.33	-8.55	-8.69	-8.78	-9.87	-8.84	-99.58
Ascorbic Acid	-8.56	-8.77	-8.69	-8.96	-9.09	-8.81	-88.26
PL^{pro}							
Methotrexate	-11.99	-11.99	-11.99	-11.99	-12.00	-11.99	-80.26
Galidesivir	-12.36	-11.39	-12.06	-11.03	-12.68	-11.90	-126.95
Pralatrexate	-11.10	-11.25	-11.54	-12.02	-12.24	-11.76	-92.36
Ganciclovir	-10.84	-10.76	-10.76	-10.76	-10.76	-10.78	-83.26
Daunonubicin	-9.42	-9.04	-8.98	-10.06	-11.06	-9.71	-82.06
Itraconazole	-8.95	-8.78	-9.06	-10.25	-10.17	-9.44	-69.20
Methyl transferase							
Methotrexate	-8.57	-8.98	-9.26	-8.98	-9.58	-9.07	-90.58

$docking score in individual snapshots generated from molecular dynamics (F1-F5), *average docking score. #average MMGBSA score.

RdRp							
Vinadarabine	-8.56	-9.12	-8.56	-8.69	-8.77	-8.74	-65.89
Saquinavir	-8.36	-8.55	-8.45	-8.60	-9.02	-8.60	-92.05
Venetoclax	-8.10	-8.68	-8.96	-8.45	-8.78	-8.59	-74.28
Viomycin	-7.85	-7.89	-8.26	-8.65	-8.79	-8.29	-100.60
Saralasin	-8.29	-8.88	-8.76	-8.23	-7.26	-8.28	-95.28
Nucleocapsid							
Nelarabine	-8.51	-8.56	-8.40	-9.02	-9.14	-8.73	-90.58
Thioguanine	-8.48	-8.55	-8.50	-8.56	-8.66	-8.55	-80.25
Paclitaxel	-8.20	-8.54	-8.64	-8.42	-8.74	-8.51	-77.01
Quinaprilat	-8.75	-8.79	-7.95	-8.40	-8.51	-8.48	-94.02
Regadenoson	-8.95	-8.05	-8.74	-8.09	-7.99	-8.36	-65.84
Bromfenac	-8.41	-8.96	-8.10	-7.58	-8.74	-8.36	-84.85

$docking score in individual snapshots generated from molecular dynamics (F1-F5), *average docking score. #average MMGBSA score.

3.3. Drugs targeting multiple SARS-CoV2 proteins

A heatmap (Fig. 11) was generated using the docking scores to summarize the binding of important drugs to multiple proteins. Individually or combinations of these drugs can serve as potential therapeutics as dual modulators for viral as well as human proteins. The identification of molecules targeting multiple proteins simultaneously should result in synergistic activity with less chances of emergence of resistance alleviating a common problem with many direct acting antivirals (DAA) against RNA viruses. The detailed list of drugs and their docking scores is given in **Supplementary table 1**.

Figure 11: Drugs binding to multiple proteins. The drugs are shown along the X-axis while the proteins are shown along Y-axis. The white-red colour spectrum shows increasing binding affinity.

3.4. Analysis of the transcriptome data and drug interactions of few differentially expressed genes:

As stated earlier, the differentially expressed genes (DEGs) were obtained from the data reported by Blanco-Melo *et al* (30). The DEGs were selected based on the following criteria:

$|\log_2 FC| \geq 1$, adj-P-value ≤ 0.001 (Supplementary Table 2). This criteria was chosen to select genes showing the most significant variation. The gene ontology (GO) enrichment analysis on these DEGs indicates immune system processes, such as type II interferon signaling (IFNG), innate defence response,

cytokine and chemokine siganling, RAGE receptor binding, secretary granuale are among the most enriched ontologies (Supplementary Table 3). It is important to note that these are among the processes usually activated in infection associated inflammation. Protein-protein-interaction network analysis was done using Cytoscape to identify the network hubs based on their interactions with other proteins. The giant component was extracted from the network with 1823 nodes containing 2546 interactions. Top 5% of the proteins (total 91) were selected based on the connections they make to other nodes in the network for further analysis (Supplementary Table 4).

It is worth to mention that among the human proteins many of them (e.g. ARRB2, JUN, CDC73, SUMO, TNFα, IL2RG, MCM7, IFIT1, FOS and ISG15 etc.) with prominent role in inflammation and immune response are hubs i.e. very important proteins in the generated protein-protein-interaction network. A search for the selected DEGs (292) at drug-gene interaction database (DGIdb) resulted in the identification of 658 unique drugs for 97 proteins (Supplementary table 5). An intersection of these with drugs binding with viral proteins (docking score≤-8.5) resulted in identification of 74 drugs that can target at least one viral protein whereas there are 31 drugs that can target atleast two viral proteins and one or more human proteins differentially expressed as a result of SARS-CoV2 infection. It is interesting to find many drugs with multi-targeting ability against hub proteins as well as SARS-CoV2 proteins. Such drugs can have a significant therapeutic utility for COVID-19 (Fig. 12).

4. Discussion

The overall goal of this study was to identify molecules that can bind with multiple SARS-CoV2 proteins that play vital role(s) in the viral lifecycle as well as target the host factors that drive viral persistence and disease pathogenesis. Our analysis predicted drugs that can bind to viral proteins (both the structural and non-structural proteins) with high affinity and can effectively inhibit viral entry as well as the post entry events like viral genome replication and transcription. Capreomycin is a promising candidate with potential to inhibit SARS-CoV2 at mutltiple stages of viral lifecycle, as it can bind with high affinity to spike protein and the viral proteases and methyl transferase, which play a crucial role in viral entry, replication and transcription. Our analysis indicated that some drugs identified to bind to viral proteins also target some of host proteins modulated/upregulated during SARS-CoV2 infection. The predicted drug candidates that interact with the viral protein or proteins, in parallel can also specifically target the host signalling pathways vital to control viral infection or disease manifestation. For instance, nebivolol a β-adrenoreceptor blocker, which stimulates nitric oxide production by endothelial nitric oxide synthase (40) is found to bind to PL^{pro} and exonuclease of SARS-CoV2. Nitric oxide is used to reverse pulmonary hypertension and shown to improve severe hypoxia in SARS-CoV1 (102) and SARS-CoV2 patients. Hence, nebivolol can be a promising therapeutic strategy with dual benefit; i) to curb SARS-CoV2 infection and ii) reversal of severe hypoxia manifestation in critical Covid-19 patients via its direct effect on nitric oxide synthase. Similarly, celecoxib a selective cyclooxygenease-2 (COX-2) inhibitor, which lowers the effect of proinflammatory cytokines IL-6 and IL-1β (103) can also target Spike and RdRp protein of SARS-CoV2. Hyper-inflammation and cytokine hyperactivity is a major contributor of COVID-19 pathology. Thus

administrating celecoxib to COVID-19 patients can have dual benefit of reducing systemic inflammation as well as inhibition of viral replication. It has been shown that COX inhibitors, in dose dependent manner, can inhibit the synthesis of RNA, proteins and production of virus particles in other coronaviruses (104). Therefore, celecoxib can be promosing therapeutic option for COVID-19. Both the celecoxib and nebivolol can cross blood brain barrier (105, 106), which gives additional advantage to counter neurological manifestations of COVID-19. Similarly, Lapatinib binds to Nsp14, a viral protein crucial for primary viral RNA synthesis (107). Lapatinib is a HER2 inhibitor which can also trigger TBK1 activation that plays a crucial role in anti-viral innate immune signalling. Thereby, lapatinib has the dual advantage of inhibiting SARS-CoV2 replication as well as upregulating anti-viral signalling (108–110). Saralasin belongs to a class of drugs called angiotensin receptor blockers (ARBs). It is worth mentioning some other ARBs (e.g. losartan) are also in clinical trials as therapeutics for COVID-19 (https://clinicaltrials.gov, IDs: NCT04287686, NCT04312009, NCT04311177). Moreover, it is reported to bind to many other SARS-CoV2 targets (111, 112). Therefore, it is also a good candidate worth consideration.

Similarly, bronchodialator indacaterol which targets the exonuclease is also a promising agent due to its ability to regulate genes involved in suppressing pro-inflammatory cytokine production and attenuation of immune response (113–115). We also observed that the molecules that bind to helicase, methyltransferase and nucleocapsid proteins can also bind to human proteins that play a pivotal role in disease pathogenesis by promoting inflammatory signalling leading to cytokine storm thereby suggesting that the molecules such as a paclitaxel, and zidovudine can have a dual beneficial effect in the management of COVID19.

The transcription complex Activator protein 1 (AP1) is composed of homo/hetero dimers of Fos, Jun, CREB and others activated transcription factors (ATFs). The studies on the SARS-CoV1 infection in the Vero and Huh7 cell shows that nucleocapsid protein is the potent activator of (AP-1) (116). Interestingly, asthmatic patients show higher expression of c-Fos in their epithelial cells. It is also observed that TNF-α induced ROS and intracellular glutathione depletion in the airway epithelial cells induces the production of AP-1 and leads to the pulmonary fibrosis (117, 118). Our analysis suggests that paclitaxel and bromocriptine which dock with nucleocapsid and Nsp4 proteins can also effectively bind to c-Fos and thereby would be beneficial in inhibiting the SARS-CoV2 as well as in alleviating lung injury observed in COVID19. The transcriptome analysis revealed that S100/calgranulin is upregulated during SARS-CoV2 infection. This protein is also found in higher quantity in the Bronchoalveloar Lavage Fluid (BALF) and sputum of patients with inflamed lungs, COPD, and ARDS (119). Calgranulin is polypeptide released by the activated inflammatory cells such as leukocytes, PBMC phagocytes and lymphocytes and is accumulated at the sites of chronic inflammation. It is the ligand for RAGE receptors and is the major initiator of cascading events that amplify inflammation (120). Our analysis suggests that the anti-inflammatory agent methotrexate which has high affinity to the Nsp16 protein of SARS-CoV2 also shows appreciable binding to calgranulin and can thereby be useful to curtail systemic inflammation observed in lungs during COVID19 in addition to its inhibitory effect on SARS-CoV2. The expression of endogenous prolactin is also upregulated during SARS-CoV2, which leads to prolactin induced STAT5 activation and its pathways. Prolactin has a dual role in human physiology functioning as a hormone (secreted from

anterior pituitary gland) and cytokine (secreted by immune cells). It causes anti-apoptotic effect and induces proliferation in immune cells in response to antigens leading to increased production of immunoglobulin, cytokines, and autoantibodies (121). We envisage that prolactin may be one of the significant player in trigger of cytokine storm implicated in COVID19. Interestingly, our study suggests that zidovudine which target the O'-methyl transferase (Nsp16) can also bind to prolactin and can be of high significance in management of COVID19 due to dual ability to affect Nsp16 and prolactin.

The COVID-19 creates an inflammatory state involving proinflammatory cytokines e.g. IL-6, TNF-α etc. The IL-6 stimulate ferritin and hepcidin synthesis (122). The hyper-ferritinemia is associated with generation of ROS and RNS leading to increased systemic inflammation. As a result a devastating cycle is propogated where increased ferritin leads to higher inflammation (incresed IL6) resulting in further increase in ferritin levels (123). Hyper-ferritinemia has been linked with poor prognosis in COVID-19 patients, evidenced by high levels of ferritin in non-survivors as compared to survivors (124, 125). In this milieu, iron chelators can be extremely helpful by reducing the hyper-ferritinemia and systemic inflammation. Deferoxamine is an iron chelator that also increases degradation of ferritin by lysosomes leading to reduction of free radicals and subsequently inflammation. It also limits the chances of ARDS and tissue fibrosis. Our analysis indicates that deferoxamine binds to RdRp and PL^{pro} protein of SARS-CoV2 with good affinity. Therefore it can be a good candidate for the therapeutics of COVID-19.

5. Conclusions

Currently, there are no approved coronavirus treatments and therefore there is a pressing need for drugs that can be effective therapeutics for COVID-19. Our study predicted several promising drug candidates with high binding affinity towards many of SARS-CoV2 proteins. These drugs are expected to be more effective than drugs that target single viral proteins due to their ability to affect multiple aspects of viral lifecycle and enhance the barrier towards the evolution of drug-resistant mutants, a usual phenomenon observed in RNA viruses.

Overall our study predicts promising agents with potential to inhibit crucial viral processes, upregulate anti-viral host response and alleviate severe lung disease condition thereby providing attractive avenues for design of potential and multipronged therapeutic strategies against COVID 19.

Declarations

Author Contribution

The work is designed and conceptualized by SK, AD, GA and GHS. Data generation and work performed by SK, PK and AD. The manuscript was prepared by SK, AD, PK, GA, PVK, BS, TKB and GHS.

Acknowledgment

All authors acknowledge Director, Institute of Life Sciences (ILS), Bhubaneswar and Dept. of Biotechnology, Govt. of India for providing necessary facilities for this work. AD and TKB acknowledge Dept. of Biotechnology, Govt. of India for infrastructure support (Grant No. BT/PR5430/MED/29/566/2012). SK and PK are thankful to the University Grant Commission (UGC) for fellowship. GA is thankful to DST for fellowship (No. SR/WOS-A/CS-129/2016). GHS is thankful to DBT-Wellcome trust India alliance for fellowship (IA/I/15/1/501826).

Conflict of Interest

Authors has no conflict of interest.

References

1. Guo D. Old Weapon for New Enemy: Drug Repurposing for Treatment of Newly Emerging Viral Diseases. Virologica Sinica. 2020 Feb 11. PubMed PMID: 32048130.
2. Chen Y, Li L. SARS-CoV-2: virus dynamics and host response. The Lancet Infectious diseases. 2020 Mar 23. PubMed PMID: 32213336. Pubmed Central PMCID: 7156233.
3. Neuman BW, Kiss G, Kunding AH, Bhella D, Baksh MF, Connelly S, et al. A structural analysis of M protein in coronavirus assembly and morphology. Journal of structural biology. 2011;174(1):11-22.
4. Lam TT, Shum MH, Zhu HC, Tong YG, Ni XB, Liao YS, et al. Identifying SARS-CoV-2 related coronaviruses in Malayan pangolins. Nature. 2020 Mar 26. PubMed PMID: 32218527.
5. Khailany RA, Safdar M, Ozaslan M. Genomic characterization of a novel SARS-CoV-2. Gene reports. 2020 Apr 16:100682. PubMed PMID: 32300673. Pubmed Central PMCID: 7161481.
6. Chen Y, Liu Q, Guo D. Emerging coronaviruses: Genome structure, replication, and pathogenesis. J Med Virol. 2020 Apr;92(4):418-23. PubMed PMID: 31967327. Pubmed Central PMCID: 7167049.
7. Li XT, Liu Y, Song JJ, Zhong JC. Letter to the Editor: Increased plasma ACE2 concentration does not mean increased risk of SARS-CoV-2 infection and increased fatality rate of COVID-19. Acta pharmaceutica Sinica B. 2020 Sep 7. PubMed PMID: 32923317. Pubmed Central PMCID: 7476560.
8. Shereen MA, Khan S, Kazmi A, Bashir N, Siddique R. COVID-19 infection: Origin, transmission, and characteristics of human coronaviruses. Journal of advanced research. 2020 Jul;24:91-8. PubMed PMID: 32257431. Pubmed Central PMCID: 7113610.
9. He C, Qin M, Sun X. Highly pathogenic coronaviruses: thrusting vaccine development in the spotlight. Acta pharmaceutica Sinica B. 2020 Jul;10(7):1175-91. PubMed PMID: 32834948. Pubmed Central PMCID: 7260574.
10. Asai A, Konno M, Ozaki M, Otsuka C, Vecchione A, Arai T, et al. COVID-19 Drug Discovery Using Intensive Approaches. International journal of molecular sciences. 2020 Apr 18;21(8). PubMed PMID: 32325767.
11. Enmozhi SK, Raja K, Sebastine I, Joseph J. Andrographolide As a Potential Inhibitor of SARS-CoV-2 Main Protease: An In Silico Approach. Journal of biomolecular structure & dynamics. 2020 Apr 24:1-

10. PubMed PMID: 32329419.

12. Wang J. Fast Identification of Possible Drug Treatment of Coronavirus Disease-19 (COVID-19) through Computational Drug Repurposing Study. Journal of chemical information and modeling. 2020 May 4. PubMed PMID: 32315171. Pubmed Central PMCID: 7197972.

13. Kang S, Yang M, Hong Z, Zhang L, Huang Z, Chen X, et al. Crystal structure of SARS-CoV-2 nucleocapsid protein RNA binding domain reveals potential unique drug targeting sites. Acta pharmaceutica Sinica B. 2020 Jul;10(7):1228-38. PubMed PMID: 32363136. Pubmed Central PMCID: 7194921.

14. Sheahan TP, Sims AC, Leist SR, Schafer A, Won J, Brown AJ, et al. Comparative therapeutic efficacy of remdesivir and combination lopinavir, ritonavir, and interferon beta against MERS-CoV. Nat Commun. 2020 Jan 10;11(1):222. PubMed PMID: 31924756. Pubmed Central PMCID: 6954302.

15. Hall DC, Jr., Ji HF. A search for medications to treat COVID-19 via in silico molecular docking models of the SARS-CoV-2 spike glycoprotein and 3CL protease. Travel medicine and infectious disease. 2020 Apr 12:101646. PubMed PMID: 32294562. Pubmed Central PMCID: 7152904.

16. Favalli EG, Biggioggero M, Maioli G, Caporali R. Baricitinib for COVID-19: a suitable treatment? The Lancet Infectious diseases. 2020 Apr 3. PubMed PMID: 32251638.

17. Wang M, Cao R, Zhang L, Yang X, Liu J, Xu M, et al. Remdesivir and chloroquine effectively inhibit the recently emerged novel coronavirus (2019-nCoV) in vitro. Cell research. 2020 Mar;30(3):269-71. PubMed PMID: 32020029. Pubmed Central PMCID: 7054408.

18. Al-Tawfiq JA, Al-Homoud AH, Memish ZA. Remdesivir as a possible therapeutic option for the COVID-19. Travel medicine and infectious disease. 2020 Mar 5:101615. PubMed PMID: 32145386. Pubmed Central PMCID: 7129391.

19. Agrawal U, Raju R, Udwadia ZF. Favipiravir: A new and emerging antiviral option in COVID-19. Medical journal, Armed Forces India. 2020:10.1016/j.mjafi.2020.08.004. PubMed PMID: 32895599. eng.

20. Caly L, Druce JD, Catton MG, Jans DA, Wagstaff KM. The FDA-approved drug ivermectin inhibits the replication of SARS-CoV-2 in vitro. Antiviral Res. 2020 Apr 3;178:104787. PubMed PMID: 32251768. Pubmed Central PMCID: 7129059.

21. Glowacka I, Bertram S, Herzog P, Pfefferle S, Steffen I, Muench MO, et al. Differential downregulation of ACE2 by the spike proteins of severe acute respiratory syndrome coronavirus and human coronavirus NL63. J Virol. 2010 Jan;84(2):1198-205. PubMed PMID: 19864379. Pubmed Central PMCID: 2798380.

22. Li YC, Bai WZ, Hashikawa T. The neuroinvasive potential of SARS-CoV2 may play a role in the respiratory failure of COVID-19 patients. J Med Virol. 2020 Jun;92(6):552-5. PubMed PMID: 32104915. Pubmed Central PMCID: 7228394.

23. Netland J, Meyerholz DK, Moore S, Cassell M, Perlman S. Severe acute respiratory syndrome coronavirus infection causes neuronal death in the absence of encephalitis in mice transgenic for

human ACE2. J Virol. 2008 Aug;82(15):7264-75. PubMed PMID: 18495771. Pubmed Central PMCID: 2493326.

24. Baig AM, Khaleeq A, Ali U, Syeda H. Evidence of the COVID-19 Virus Targeting the CNS: Tissue Distribution, Host-Virus Interaction, and Proposed Neurotropic Mechanisms. ACS chemical neuroscience. 2020 Apr 1;11(7):995-8. PubMed PMID: 32167747. Pubmed Central PMCID: 7094171.
25. Danta CC. CNS Penetration Ability: A Critical Factor for Drugs in the Treatment of SARS-CoV-2 Brain Infection. ACS chemical neuroscience. 2020 Aug 5;11(15):2137-44. PubMed PMID: 32639711. Pubmed Central PMCID: 7359671.
26. Eswar N, John B, Mirkovic N, Fiser A, Ilyin VA, Pieper U, et al. Tools for comparative protein structure modeling and analysis. Nucleic Acids Res. 2003 Jul 1;31(13):3375-80. PubMed PMID: 12824331. Pubmed Central PMCID: PMC168950. Epub 2003/06/26.
27. Dixit A, Verkhivker GM. Integrating ligand-based and protein-centric virtual screening of kinase inhibitors using ensembles of multiple protein kinase genes and conformations. J Chem Inf Model. 2012 Oct 22;52(10):2501-15. PubMed PMID: 22992037.
28. Phillips JC, Braun R, Wang W, Gumbart J, Tajkhorshid E, Villa E, et al. Scalable molecular dynamics with NAMD. Journal of computational chemistry. 2005 Dec;26(16):1781-802. PubMed PMID: 16222654. Pubmed Central PMCID: 2486339.
29. Le Guilloux V, Schmidtke P, Tuffery P. Fpocket: an open source platform for ligand pocket detection. BMC Bioinformatics. 2009 Jun 2;10:168. PubMed PMID: 19486540. Pubmed Central PMCID: PMC2700099. Epub 2009/06/03.
30. Blanco-Melo D, Nilsson-Payant BE, Liu WC, Uhl S, Hoagland D, Moller R, et al. Imbalanced Host Response to SARS-CoV-2 Drives Development of COVID-19. Cell. 2020 May 28;181(5):1036-45 e9. PubMed PMID: 32416070. Pubmed Central PMCID: 7227586.
31. Alanis-Lobato G, Andrade-Navarro MA, Schaefer MH. HIPPIE v2. 0: enhancing meaningfulness and reliability of protein–protein interaction networks. Nucleic acids research. 2016:gkw985.
32. Meng XY, Zhang HX, Mezei M, Cui M. Molecular docking: a powerful approach for structure-based drug discovery. Curr Comput Aided Drug Des. 2011 Jun;7(2):146-57. PubMed PMID: 21534921. Pubmed Central PMCID: PMC3151162. Epub 2011/05/04.
33. Walls AC, Park Y-J, Tortorici MA, Wall A, McGuire AT, Veesler D. Structure, function, and antigenicity of the SARS-CoV-2 spike glycoprotein. Cell. 2020.
34. Song W, Gui M, Wang X, Xiang Y. Cryo-EM structure of the SARS coronavirus spike glycoprotein in complex with its host cell receptor ACE2. PLoS pathogens. 2018;14(8):e1007236.
35. Kalathiya U, Padariya M, Mayordomo M, Lisowska M, Nicholson J, Singh A, et al. Highly Conserved Homotrimer Cavity Formed by the SARS-CoV-2 Spike Glycoprotein: A Novel Binding Site. Journal of clinical medicine. 2020 May 14;9(5). PubMed PMID: 32422996. Pubmed Central PMCID: 7290299.
36. Korber B, Fischer WM, Gnanakaran S, Yoon H, Theiler J, Abfalterer W, et al. Tracking Changes in SARS-CoV-2 Spike: Evidence that D614G Increases Infectivity of the COVID-19 Virus. Cell. 2020 Aug 20;182(4):812-27 e19. PubMed PMID: 32697968. Pubmed Central PMCID: 7332439.

37. Wu C, Liu Y, Yang Y, Zhang P, Zhong W, Wang Y, et al. Analysis of therapeutic targets for SARS-CoV-2 and discovery of potential drugs by computational methods. Acta Pharmaceutica Sinica B. 2020.
38. Varghese FS, Meutiawati F, Teppor M, Merits A, van Rij RP. Posaconazole is a novel inhibitor for alphavirus viral entry. Access Microbiology. 2019;1(10):41.
39. Meutiawati F, Bezemer B, Strating JR, Overheul GJ, Žusinaite E, van Kuppeveld FJ, et al. Posaconazole inhibits dengue virus replication by targeting oxysterol-binding protein. Antiviral research. 2018;157:68-79.
40. Dal Negro R. Pulmonary effects of nebivolol. Therapeutic advances in cardiovascular disease. 2009 Aug;3(4):329-34. PubMed PMID: 19638367.
41. Ramanathan MR, Sanders JM. Drugs used in TB and leprosy. Side Effects of Drugs Annual. 39: Elsevier; 2017. p. 283-93.
42. Hirota K, Terada H. Particle-manufacturing technology-based inhalation therapy for pulmonary diseases. Colloid and interface science in pharmaceutical research and development: Elsevier; 2014. p. 103-19.
43. Zeng W, Liu G, Ma H, Zhao D, Yang Y, Liu M, et al. Biochemical characterization of SARS-CoV-2 nucleocapsid protein. Biochemical and Biophysical Research Communications. 2020.
44. Chang M-S, Lu Y-T, Ho S-T, Wu C-C, Wei T-Y, Chen C-J, et al. Antibody detection of SARS-CoV spike and nucleocapsid protein. Biochemical and biophysical research communications. 2004;314(4):931-6.
45. He R, Leeson A, Ballantine M, Andonov A, Baker L, Dobie F, et al. Characterization of protein–protein interactions between the nucleocapsid protein and membrane protein of the SARS coronavirus. Virus research. 2004;105(2):121-5.
46. Decroly E, Debarnot C, Ferron F, Bouvet M, Coutard B, Imbert I, et al. Crystal structure and functional analysis of the SARS-coronavirus RNA cap 2'-O-methyltransferase nsp10/nsp16 complex. PLoS Pathog. 2011 May;7(5):e1002059. PubMed PMID: 21637813. Pubmed Central PMCID: 3102710.
47. Mahmoudvand H, Kheirandish F, Mirbadie SR, Kayedi MH, Rezaei Riabi T, Ghasemi AA, et al. The Potential Use of Methotrexate in the Treatment of Cutaneous Leishmaniasis: In Vitro Assays against Sensitive and Meglumine Antimoniate-resistant Strains of Leishmania tropica. Iran J Parasitol. 2017 Jul-Sep;12(3):339-47. PubMed PMID: 28979343. eng.
48. Beck S, Zhu Z, Oliveira MF, Smith DM, Rich JN, Bernatchez JA, et al. Mechanism of Action of Methotrexate Against Zika Virus. Viruses. 2019 Apr 10;11(4). PubMed PMID: 30974762. Pubmed Central PMCID: 6521145.
49. Lewis KA, Eugster EA. Experience with the once-yearly histrelin (GnRHa) subcutaneous implant in the treatment of central precocious puberty. Drug design, development and therapy. 2009;3:1.
50. Lee H, Cao S, Hevener KE, Truong L, Gatuz JL, Patel K, et al. Synergistic inhibitor binding to the papain-like protease of human SARS coronavirus: mechanistic and inhibitor design implications. ChemMedChem. 2013 Aug;8(8):1361-72. PubMed PMID: 23788528. Pubmed Central PMCID: 3954986.

51. Ghosh AK, Brindisi M, Shahabi D, Chapman ME, Mesecar AD. Drug Development and Medicinal Chemistry Efforts toward SARS-Coronavirus and Covid-19 Therapeutics. ChemMedChem. 2020 Jun 4;15(11):907-32. PubMed PMID: 32324951. Pubmed Central PMCID: 7264561.
52. Liu Y, Liang C, Xin L, Ren X, Tian L, Ju X, et al. The development of Coronavirus 3C-Like protease (3CL(pro)) inhibitors from 2010 to 2020. European journal of medicinal chemistry. 2020 Aug 6;206:112711. PubMed PMID: 32810751. Pubmed Central PMCID: 7409838.
53. Zhang L, Lin D, Sun X, Curth U, Drosten C, Sauerhering L, et al. Crystal structure of SARS-CoV-2 main protease provides a basis for design of improved alpha-ketoamide inhibitors. Science. 2020 Apr 24;368(6489):409-12. PubMed PMID: 32198291. Pubmed Central PMCID: 7164518.
54. Cao B, Wang Y, Wen D, Liu W, Wang J, Fan G, et al. A Trial of Lopinavir-Ritonavir in Adults Hospitalized with Severe Covid-19. The New England journal of medicine. 2020 May 7;382(19):1787-99. PubMed PMID: 32187464. Pubmed Central PMCID: 7121492.
55. Zhang L, Lin D, Kusov Y, Nian Y, Ma Q, Wang J, et al. Alpha-ketoamides as broad-spectrum inhibitors of coronavirus and enterovirus replication. bioRxiv. 2020.
56. Chen YW, Yiu C-PB, Wong K-Y. Prediction of the SARS-CoV-2 (2019-nCoV) 3C-like protease (3CL pro) structure: virtual screening reveals velpatasvir, ledipasvir, and other drug repurposing candidates. F1000Research. 2020;9.
57. Hayden FG, Turner RB, Gwaltney JM, Chi-Burris K, Gersten M, Hsyu P, et al. Phase II, randomized, double-blind, placebo-controlled studies of ruprintrivir nasal spray 2-percent suspension for prevention and treatment of experimentally induced rhinovirus colds in healthy volunteers. Antimicrobial agents and chemotherapy. 2003 Dec;47(12):3907-16. PubMed PMID: 14638501. Pubmed Central PMCID: 296196.
58. Anand K, Ziebuhr J, Wadhwani P, Mesters JR, Hilgenfeld R. Coronavirus Main Proteinase (3CL^{pro}) Structure: Basis for Design of Anti-SARS Drugs. Science. 2003;300(5626):1763-7.
59. Plosker GL, Noble S. Indinavir. Drugs. 1999;58(6):1165-203.
60. Esmadi M, Ahmad D, Hewlett A. Efficacy of naldemedine for the treatment of opioid-induced constipation: A meta-analysis. Journal of Gastrointestinal & Liver Diseases. 2019;28(1).
61. Wu C, Liu Y, Yang Y, Zhang P, Zhong W, Wang Y, et al. Analysis of therapeutic targets for SARS-CoV-2 and discovery of potential drugs by computational methods. Acta Pharmaceutica Sinica B. 2020 2020/05/01/;10(5):766-88.
62. Lin MH, Moses DC, Hsieh CH, Cheng SC, Chen YH, Sun CY, et al. Disulfiram can inhibit MERS and SARS coronavirus papain-like proteases via different modes. Antiviral research. 2018 Feb;150:155-63. PubMed PMID: 29289665. Pubmed Central PMCID: PMC7113793. Epub 2018/01/01. eng.
63. Eyer L, Nougairède A, Uhlířová M, Driouich J-S, Zouharová D, Valdés JJ, et al. An E460D Substitution in the NS5 Protein of Tick-Borne Encephalitis Virus Confers Resistance to the Inhibitor Galidesivir (BCX4430) and Also Attenuates the Virus for Mice. Journal of Virology. 2019;93(16):e00367-19.

64. Filion L, Logan D, Gaudreault R, Izaguirre C. Inhibition of HIV-1 replication by daunorubicin. Clinical and investigative medicine Medecine clinique et experimentale. 1993;16(5):339-47.
65. Ash RJ, Diekema KA. Inhibition of herpes simplex virus replication by anthracycline compounds. Antiviral research. 1987;8(2):71-83.
66. Chen X, Zhang X, Pan J. Effect of Montelukast on Bronchopulmonary Dysplasia (BPD) and Related Mechanisms. Medical science monitor : international medical journal of experimental and clinical research. 2019 Mar 13;25:1886-93. PubMed PMID: 30862773. Pubmed Central PMCID: 6427930.
67. Sarzi-Puttini P, Giorgi V, Sirotti S, Marotto D, Ardizzone S, Rizzardini G, et al. COVID-19, cytokines and immunosuppression: what can we learn from severe acute respiratory syndrome? Clinical and experimental rheumatology. 2020 Mar-Apr;38(2):337-42. PubMed PMID: 32202240.
68. Chen Y, Li Y, Wang X, Zou P. Montelukast, an Anti-asthmatic Drug, Inhibits Zika Virus Infection by Disrupting Viral Integrity. Front Microbiol. 2019;10:3079. PubMed PMID: 32082265. Pubmed Central PMCID: PMC7002393. Epub 2020/02/23.
69. Wu C, Liu Y, Yang Y, Zhang P, Zhong W, Wang Y, et al. Analysis of therapeutic targets for SARS-CoV-2 and discovery of potential drugs by computational methods. Acta pharmaceutica Sinica B. 2020 May;10(5):766-88. PubMed PMID: 32292689. Pubmed Central PMCID: 7102550.
70. Adedeji AO, Marchand B, te Velthuis AJ, Snijder EJ, Weiss S, Eoff RL, et al. Mechanism of nucleic acid unwinding by SARS-CoV helicase. PloS one. 2012;7(5).
71. Habtemariam S, Nabavi SF, Banach M, Berindan-Neagoe I, Sarkar K, Sil PC, et al. Should We Try SARS-CoV-2 Helicase Inhibitors for COVID-19 Therapy? Archives of medical research. 2020 May 31. PubMed PMID: 32536457. Pubmed Central PMCID: 7261434.
72. Daly MB, Roth ME, Bonnac L, Maldonado JO, Xie J, Clouser CL, et al. Dual anti-HIV mechanism of clofarabine. Retrovirology. 2016 Mar 24;13:20. PubMed PMID: 27009333. Pubmed Central PMCID: 4806454.
73. Cotter TG, Jensen DM. Glecaprevir/pibrentasvir for the treatment of chronic hepatitis C: design, development, and place in therapy. Drug design, development and therapy. 2019;13:2565.
74. Wu C, Liu Y, Yang Y, Zhang P, Zhong W, Wang Y, et al. Analysis of therapeutic targets for SARS-CoV-2 and discovery of potential drugs by computational methods. Acta pharmaceutica Sinica B. 2020 Feb 27. PubMed PMID: 32292689. Pubmed Central PMCID: 7102550.
75. Gao Y, Yan L, Huang Y, Liu F, Zhao Y, Cao L, et al. Structure of the RNA-dependent RNA polymerase from COVID-19 virus. Science. 2020 May 15;368(6492):779-82. PubMed PMID: 32277040. Pubmed Central PMCID: 7164392.
76. Gil C, Ginex T, Maestro I, Nozal V, Barrado-Gil L, Cuesta-Geijo MA, et al. COVID-19: Drug Targets and Potential Treatments. Journal of medicinal chemistry. 2020 Jun 26. PubMed PMID: 32511912. Pubmed Central PMCID: 7323060.
77. Fan S, Xiao D, Wang Y, Liu L, Zhou X, Zhong W. Research progress on repositioning drugs and specific therapeutic drugs for SARS-CoV-2. Future medicinal chemistry. 2020 Jul 8. PubMed PMID: 32638628. Pubmed Central PMCID: 7341957.

78. Choudhury S, Moulick D, Saikia P, Mazumder MK. Evaluating the potential of different inhibitors on RNA-dependent RNA polymerase of severe acute respiratory syndrome coronavirus 2: A molecular modeling approach. Medical journal, Armed Forces India. 2020 May 30. PubMed PMID: 32836709. Pubmed Central PMCID: 7261222.
79. Ramírez-Olivencia G, Estébanez M, Membrillo FJ, Ybarra MdC. Use of ribavirin in viruses other than hepatitis C. A review of the evidence. Enfermedades infecciosas y microbiologia clinica (English ed). 2019;37(9):602-8. PubMed PMID: PMC7195261. Epub 06/15. eng.
80. von Hentig N. Clinical use of cobicistat as a pharmacoenhancer of human immunodeficiency virus therapy. HIV/AIDS (Auckland, NZ). 2016;8:1.
81. Mendoza-Martinez C, Rodriguez-Lezama A. Identification of Potential Inhibitors of SARS-CoV-2 Main Protease via a Rapid In-Silico Drug Repurposing Approach. 2020.
82. Bhardwaj K, Sun J, Holzenburg A, Guarino LA, Kao CC. RNA recognition and cleavage by the SARS coronavirus endoribonuclease. Journal of molecular biology. 2006;361(2):243-56.
83. Plosker GL, Noble S. Indinavir: a review of its use in the management of HIV infection. Drugs. 1999 Dec;58(6):1165-203. PubMed PMID: 10651394.
84. Bhardwaj K, Sun J, Holzenburg A, Guarino LA, Kao CC. RNA recognition and cleavage by the SARS coronavirus endoribonuclease. J Mol Biol. 2006 Aug 11;361(2):243-56. PubMed PMID: 16828802. Pubmed Central PMCID: 7118729.
85. Deng X, Hackbart M, Mettelman RC, O'Brien A, Mielech AM, Yi G, et al. Coronavirus nonstructural protein 15 mediates evasion of dsRNA sensors and limits apoptosis in macrophages. Proceedings of the National Academy of Sciences. 2017;114(21):E4251-E60.
86. Vaduganathan M, Vardeny O, Michel T, McMurray JJV, Pfeffer MA, Solomon SD. Renin–Angiotensin–Aldosterone System Inhibitors in Patients with Covid-19. New England Journal of Medicine. 2020;382(17):1653-9. PubMed PMID: 32227760.
87. Shakoor H, Feehan J, Mikkelsen K, Al Dhaheri AS, Ali HI, Platat C, et al. Be well: A potential role for vitamin B in COVID-19. Maturitas. 2020 Aug 15. PubMed PMID: 32829981. Pubmed Central PMCID: 7428453.
88. Morrey JD, Sidwell RW, Noble RL, Barnett BB, Mahoney AW. Effects of folic acid malnutrition on rotaviral infection in mice. Proceedings of the Society for Experimental Biology and Medicine Society for Experimental Biology and Medicine. 1984 May;176(1):77-83. PubMed PMID: 6324227.
89. Zahra S, Maryam Heydari D, Manica N, Mehdi D, Hassan Z, Mohsen M, et al. The Role of Folic Acid in the Management of Respiratory Disease Caused by COVID-192020.
90. Garcia JM, Swerdloff R, Wang C, Kyle M, Kipnes M, Biller BM, et al. Macimorelin (AEZS-130)-stimulated growth hormone (GH) test: validation of a novel oral stimulation test for the diagnosis of adult GH deficiency. The Journal of clinical endocrinology and metabolism. 2013 Jun;98(6):2422-9. PubMed PMID: 23559086. Pubmed Central PMCID: 4207947.
91. arun k, Sharanya CS, Abhithaj J, Dileep F, Sadasivan C. Drug Repurposing Against SARS-CoV-2 Using E-Pharmacophore Based Virtual Screening and Molecular Docking with Main Protease as the

Target2020.

92. Lam S, Lombardi A, Ouanounou A. COVID-19: A review of the proposed pharmacological treatments. European journal of pharmacology. 2020 Aug 6;886:173451. PubMed PMID: 32768505. Pubmed Central PMCID: 7406477.
93. Graepel KW, Lu X, Case JB, Sexton NR, Smith EC, Denison MR. Proofreading-deficient coronaviruses adapt for increased fitness over long-term passage without reversion of exoribonuclease-inactivating mutations. MBio. 2017;8(6):e01503-17.
94. Minskaia E, Hertzig T, Gorbalenya AE, Campanacci V, Cambillau C, Canard B, et al. Discovery of an RNA virus 3'→ 5' exoribonuclease that is critically involved in coronavirus RNA synthesis. Proceedings of the National Academy of Sciences. 2006;103(13):5108-13.
95. Karlas A, Berre S, Couderc T, Varjak M, Braun P, Meyer M, et al. A human genome-wide loss-of-function screen identifies effective chikungunya antiviral drugs. Nature communications. 2016;7(1):1-14.
96. Perin PM, Haid S, Brown RJ, Doerrbecker J, Schulze K, Zeilinger C, et al. Flunarizine prevents hepatitis C virus membrane fusion in a genotype-dependent manner by targeting the potential fusion peptide within E1. Hepatology. 2016;63(1):49-62.
97. Tsuji M. Potential anti-SARS-CoV-2 drug candidates identified through virtual screening of the ChEMBL database for compounds that target the main coronavirus protease. FEBS open bio. 2020 Jun;10(6):995-1004. PubMed PMID: 32374074. Pubmed Central PMCID: PMC7262888. Epub 2020/05/07. eng.
98. Lucifora J, Esser K, Protzer U. Ezetimibe blocks hepatitis B virus infection after virus uptake into hepatocytes. Antiviral research. 2013;97(2):195-7.
99. Osuna-Ramos JF, Reyes-Ruiz JM, Bautista-Carbajal P, Cervantes-Salazar M, Farfan-Morales CN, De Jesús-González LA, et al. Ezetimibe inhibits Dengue virus infection in Huh-7 cells by blocking the cholesterol transporter Niemann–Pick C1-like 1 receptor. Antiviral research. 2018;160:151-64.
100. Incorvaia C, Ridolo E, Riario-Sforza E, Montagni M, G Riario-Sforza G. Indacaterol in the treatment of chronic obstructive pulmonary disease: from clinical trials to daily practice. Reviews on recent clinical trials. 2014;9(2):96-101.
101. Yan D, Hamed O, Joshi T, Mostafa MM, Jamieson KC, Joshi R, et al. Analysis of the Indacaterol-Regulated Transcriptome in Human Airway Epithelial Cells Implicates Gene Expression Changes in the Adverse and Therapeutic Effects of beta2-Adrenoceptor Agonists. The Journal of pharmacology and experimental therapeutics. 2018 Jul;366(1):220-36. PubMed PMID: 29653961.
102. Alvarez RA, Berra L, Gladwin MT. Home Nitric Oxide Therapy for COVID-19. American journal of respiratory and critical care medicine. 2020 Jul 1;202(1):16-20. PubMed PMID: 32437250. Pubmed Central PMCID: 7328337.
103. Theodoridou A, Gika H, Diza E, Garyfallos A, Settas L. In vivo study of pro-inflammatory cytokine changes in serum and synovial fluid during treatment with celecoxib and etoricoxib and correlation with VAS pain change and synovial membrane penetration index in patients with inflammatory

arthritis. Mediterranean journal of rheumatology. 2017 Mar;28(1):33-40. PubMed PMID: 32185252. Pubmed Central PMCID: 7045925.

104. Raaben M, Einerhand AW, Taminiau LJ, van Houdt M, Bouma J, Raatgeep RH, et al. Cyclooxygenase activity is important for efficient replication of mouse hepatitis virus at an early stage of infection. Virology journal. 2007 Jun 7;4:55. PubMed PMID: 17555580. Pubmed Central PMCID: 1892777.
105. Novakova I, Subileau E-A, Toegel S, Gruber D, Lachmann B, Urban E, et al. Transport Rankings of Non-Steroidal Antiinflammatory Drugs across Blood-Brain Barrier In Vitro Models. PloS one. 2014;9(1):e86806.
106. Toblli JE, DiGennaro F, Giani JF, Dominici FP. Nebivolol: impact on cardiac and endothelial function and clinical utility. Vasc Health Risk Manag. 2012;8:151-60. PubMed PMID: 22454559. Epub 03/13. eng.
107. Ogando NS, Zevenhoven-Dobbe JC, Posthuma CC, Snijder EJ. The enzymatic activity of the nsp14 exoribonuclease is critical for replication of Middle East respiratory syndrome-coronavirus. bioRxiv. 2020:2020.06.19.162529.
108. Richters A, Basu D, Engel J, Ercanoglu MS, Balke-Want H, Tesch R, et al. Identification and further development of potent TBK1 inhibitors. ACS chemical biology. 2015 Jan 16;10(1):289-98. PubMed PMID: 25540906.
109. Chen X, Yang X, Zheng Y, Yang Y, Xing Y, Chen Z. SARS coronavirus papain-like protease inhibits the type I interferon signaling pathway through interaction with the STING-TRAF3-TBK1 complex. Protein & cell. 2014 May;5(5):369-81. PubMed PMID: 24622840. Pubmed Central PMCID: 3996160.
110. Wu S, Zhang Q, Zhang F, Meng F, Liu S, Zhou R, et al. HER2 recruits AKT1 to disrupt STING signalling and suppress antiviral defence and antitumour immunity. Nature cell biology. 2019 Aug;21(8):1027-40. PubMed PMID: 31332347.
111. Sachin P, Jeremy H, Pedro J. B, Elena F, Juliette D, Autumn C, et al. Drug Repurposing for Covid-19: Discovery of Potential Small-Molecule Inhibitors of Spike Protein-ACE2 Receptor Interaction Through Virtual Screening and Consensus Scoring2020.
112. Hao L, Tao J, Wenlang L, Zheng Z. Computational Evaluation of the COVID-19 3c-like Protease Inhibition Mechanism, and Drug Repurposing Screening2020.
113. Kume H, Hojo M, Hashimoto N. Eosinophil Inflammation and Hyperresponsiveness in the Airways as Phenotypes of COPD, and Usefulness of Inhaled Glucocorticosteroids. Frontiers in pharmacology. 2019;10:765. PubMed PMID: 31404293. Pubmed Central PMCID: 6676333.
114. Gill SK, Marriott HM, Suvarna SK, Peachell PT. Evaluation of the anti-inflammatory effects of beta-adrenoceptor agonists on human lung macrophages. European journal of pharmacology. 2016 Dec 15;793:49-55. PubMed PMID: 27832943.
115. Scola AM, Loxham M, Charlton SJ, Peachell PT. The long-acting beta-adrenoceptor agonist, indacaterol, inhibits IgE-dependent responses of human lung mast cells. British journal of pharmacology. 2009 Sep;158(1):267-76. PubMed PMID: 19371332. Pubmed Central PMCID: 2795262.

116. Mizutani T. Signaling Pathways of SARS-CoV In Vitro and In Vivo. Molecular Biology of the SARS-Coronavirus: Springer; 2010. p. 305-22.
117. Eferl R, Hasselblatt P, Rath M, Popper H, Zenz R, Komnenovic V, et al. Development of pulmonary fibrosis through a pathway involving the transcription factor Fra-2/AP-1. Proceedings of the National Academy of Sciences. 2008;105(30):10525-30.
118. Rahman I, MacNee W. Role of transcription factors in inflammatory lung diseases. Thorax. 1998;53(7):601-12.
119. Camoretti-Mercado B, Karrar E, Nuñez L, Bowman MAH. S100a12 and the airway smooth muscle: beyond inflammation and constriction. Journal of allergy & therapy. 2012;3(Suppl 1).
120. Hofmann MA, Drury S, Fu C, Qu W, Taguchi A, Lu Y, et al. RAGE mediates a novel proinflammatory axis: a central cell surface receptor for S100/calgranulin polypeptides. Cell. 1999;97(7):889-901.
121. Díaz L, Muñoz MD, González L, Lira-Albarrán S, Larrea F, Méndez I. Prolactin in the immune system. Prolactin Intech, Wiltshire. 2013:53-82.
122. Daher R, Manceau H, Karim Z. Iron metabolism and the role of the iron-regulating hormone hepcidin in health and disease. Presse medicale. 2017 Dec;46(12 Pt 2):e272-e8. PubMed PMID: 29129410.
123. Kell DB, Pretorius E. Serum ferritin is an important inflammatory disease marker, as it is mainly a leakage product from damaged cells. Metallomics : integrated biometal science. 2014 Apr;6(4):748-73. PubMed PMID: 24549403.
124. Perricone C, Bartoloni E, Bursi R, Cafaro G, Guidelli GM, Shoenfeld Y, et al. COVID-19 as part of the hyperferritinemic syndromes: the role of iron depletion therapy. Immunologic research. 2020 Aug;68(4):213-24. PubMed PMID: 32681497. Pubmed Central PMCID: 7366458.
125. Edeas M, Saleh J, Peyssonnaux C. Iron: Innocent bystander or vicious culprit in COVID-19 pathogenesis? International journal of infectious diseases : IJID : official publication of the International Society for Infectious Diseases. 2020 Aug;97:303-5. PubMed PMID: 32497811. Pubmed Central PMCID: 7264936.

Figures

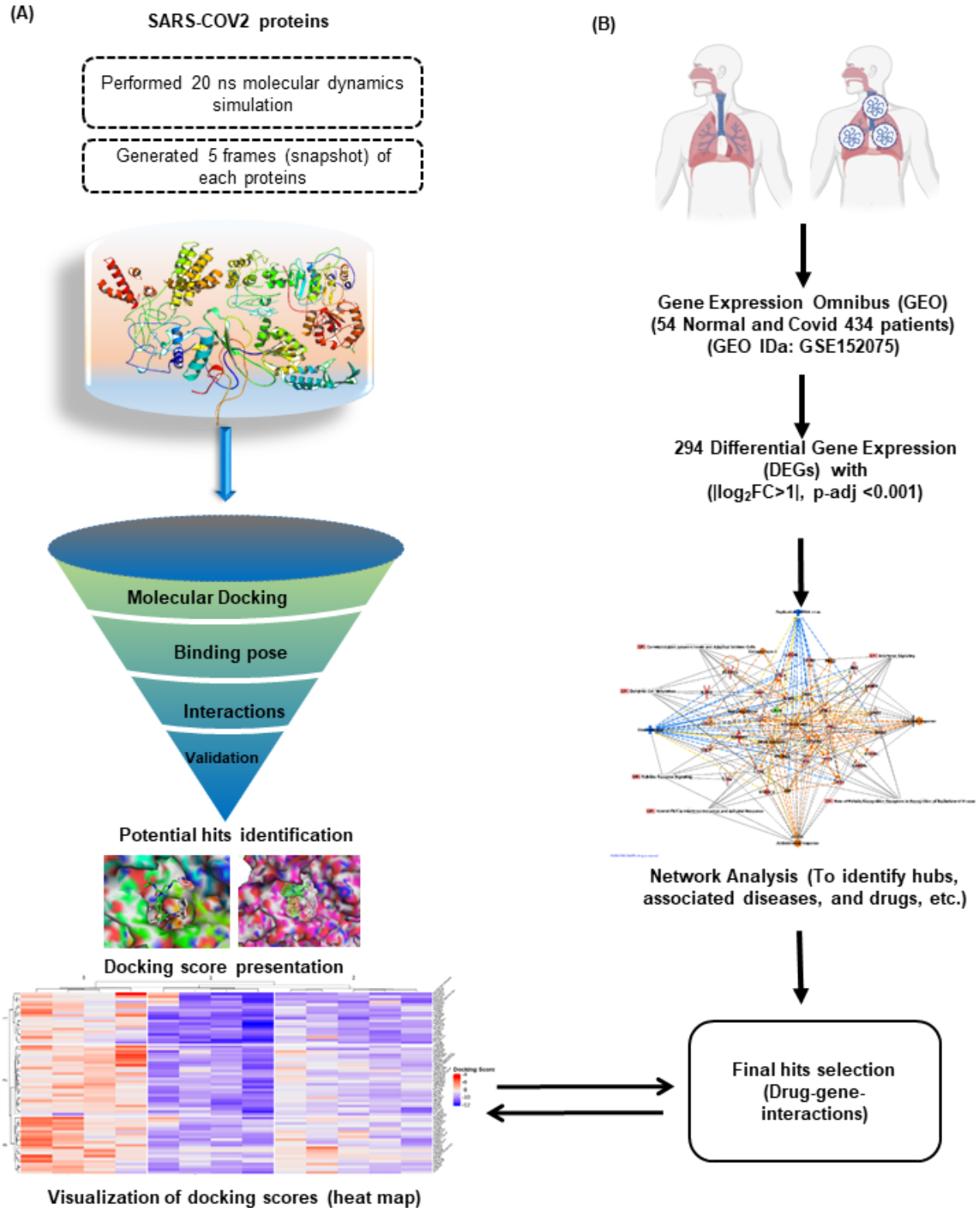

Figure 1

Outline of the repurposing work. (A) Nine SARS-CoV2 proteins structures were obtained from either PDB or modeled. The protein structures were subjected to 20ns MD run (total 180 ns) to explore the flexibility of the binding site. Snapshots were generated at equal time points during MD simulation for each protein. The FDA approved drug library was docked in the generated snapshots using Glide. The MMGBSA score was also calculated for each of the ligand in individual snapshots. (B) Transcriptomics data from SARS-

CoV2 infected and normal human samples identified significantly differentially expressed genes (|log2FC>1|, Adj. p-value<0.001) as a result of infection. A protein-protein-interaction network was created using these genes. They were also analyzed for their involvement in biological pathways using Ingenuity Pathways Analysis (IPA).

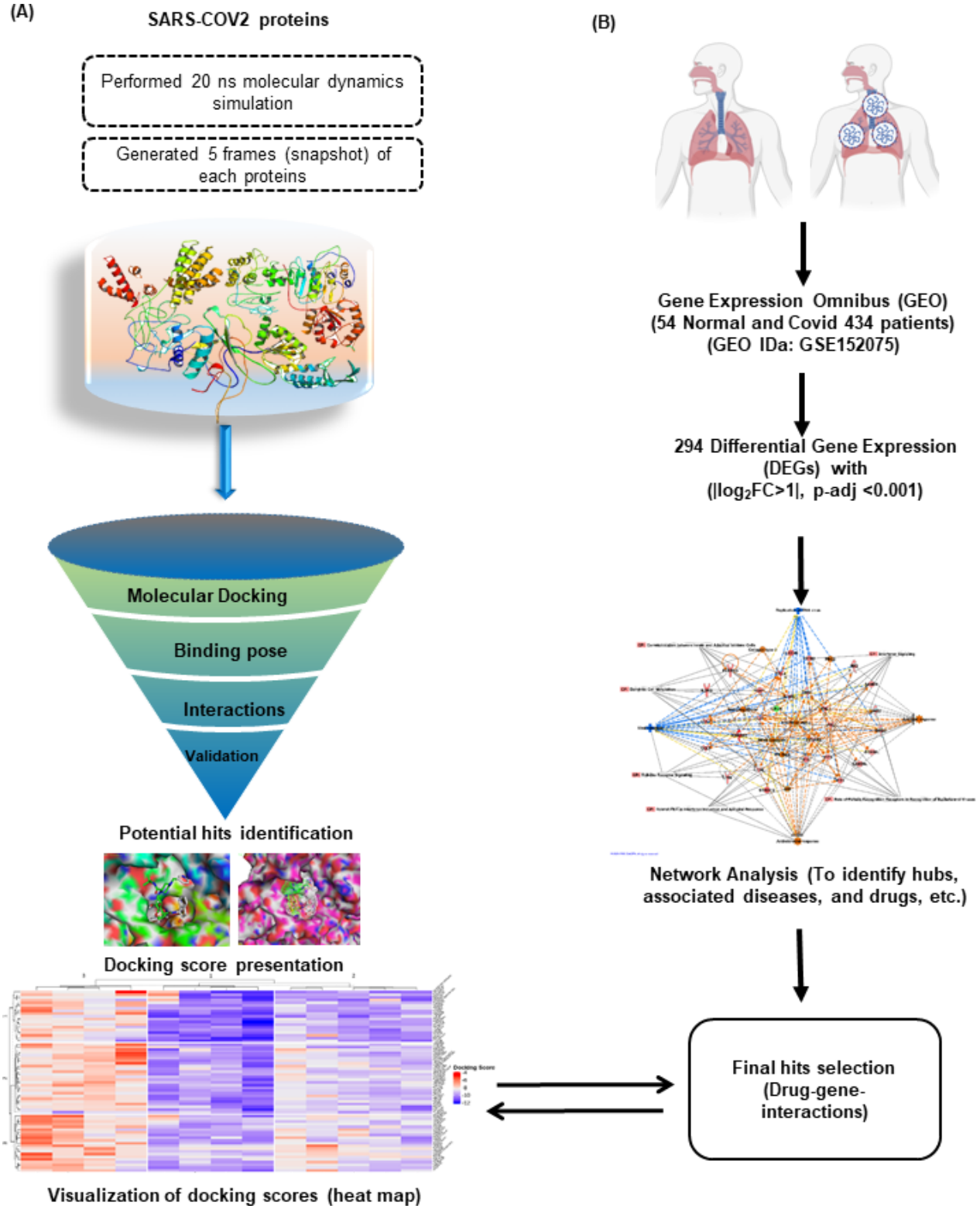

Figure 1

Outline of the repurposing work. (A) Nine SARS-CoV2 proteins structures were obtained from either PDB or modeled. The protein structures were subjected to 20ns MD run (total 180 ns) to explore the flexibility of the binding site. Snapshots were generated at equal time points during MD simulation for each protein. The FDA approved drug library was docked in the generated snapshots using Glide. The MMGBSA score was also calculated for each of the ligand in individual snapshots. (B) Transcriptomics data from SARS-CoV2 infected and normal human samples identified significantly differentially expressed genes (|log2FC>1|, Adj. p-value<0.001) as a result of infection. A protein-protein-interaction network was created using these genes. They were also analyzed for their involvement in biological pathways using Ingenuity Pathways Analysis (IPA).

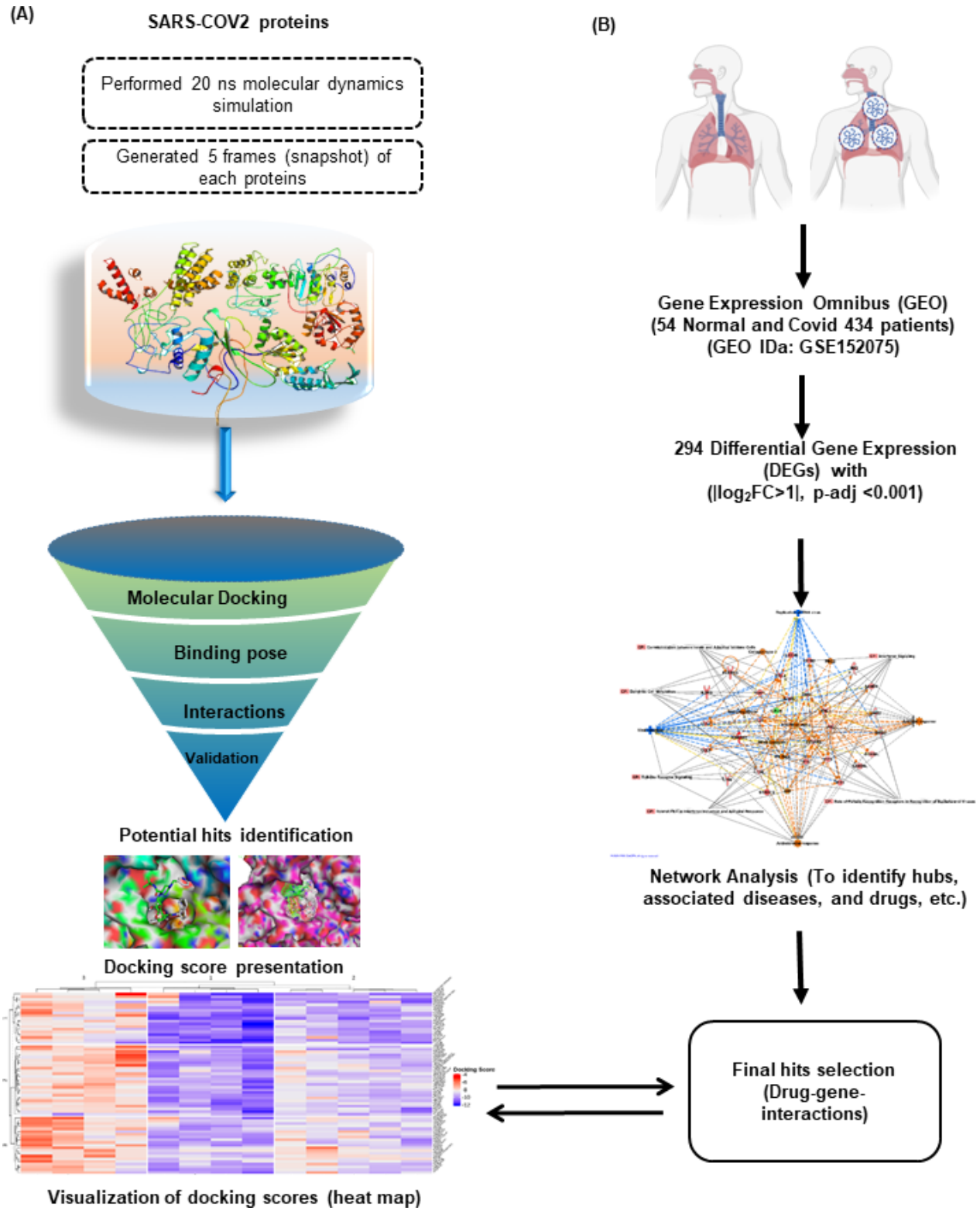

Figure 1

Outline of the repurposing work. (A) Nine SARS-CoV2 proteins structures were obtained from either PDB or modeled. The protein structures were subjected to 20ns MD run (total 180 ns) to explore the flexibility of the binding site. Snapshots were generated at equal time points during MD simulation for each protein. The FDA approved drug library was docked in the generated snapshots using Glide. The MMGBSA score was also calculated for each of the ligand in individual snapshots. (B) Transcriptomics data from SARS-

CoV2 infected and normal human samples identified significantly differentially expressed genes (|log2FC>1|, Adj. p-value<0.001) as a result of infection. A protein-protein-interaction network was created using these genes. They were also analyzed for their involvement in biological pathways using Ingenuity Pathways Analysis (IPA).

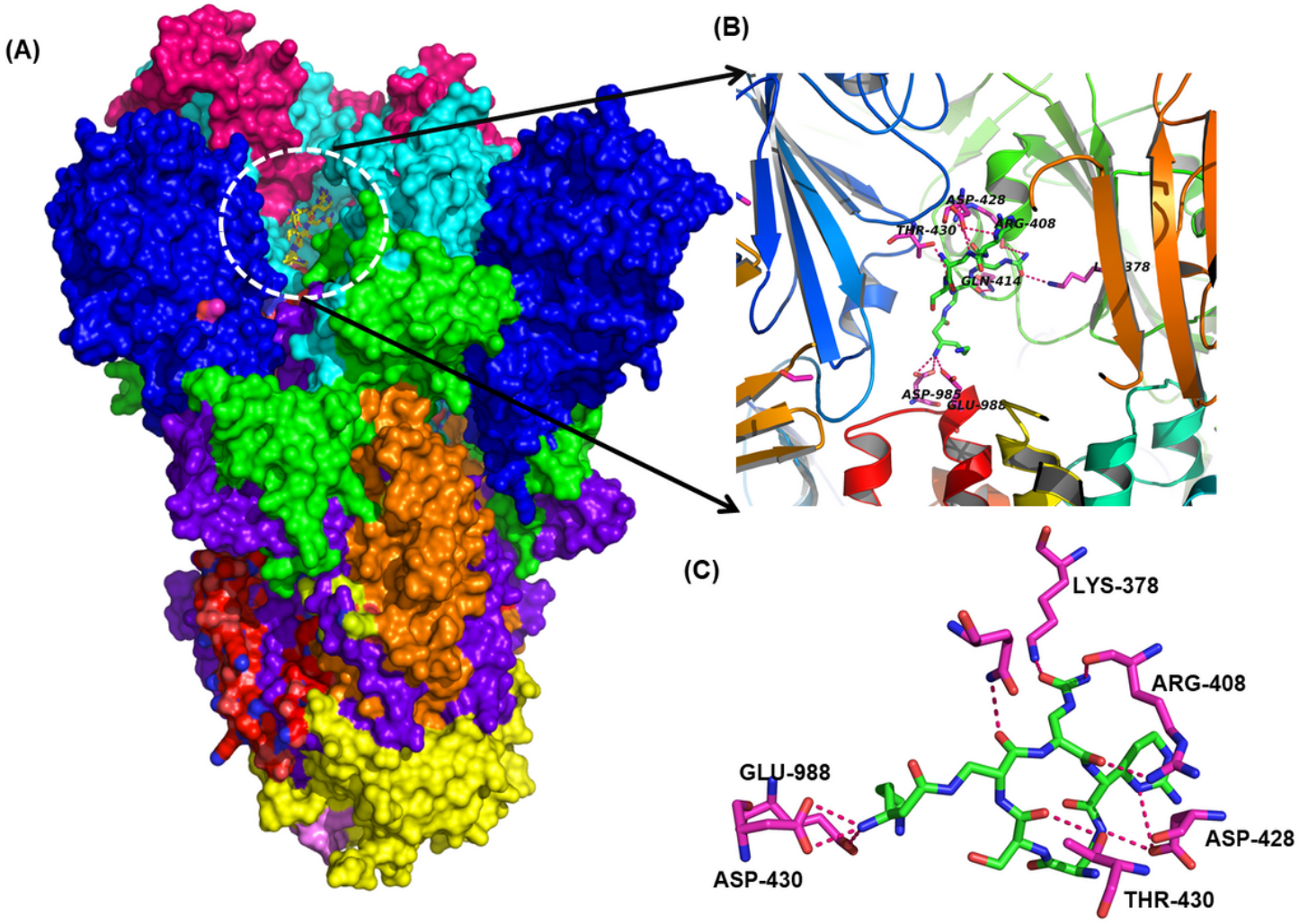

Figure 2

Virtual screening of FDA drugs against Spike protein. (A) The surface view of spike protein where domains are represented in different colors. The ligand binding site is shown inside white dotted circle at RBD (receptor binding domain) of the spike protein. (B) Cartoon depiction of the RBD showing the secondary structure elements and binding of capreomycin. (C) Closeup of RBD-capreomycin interaction showing residues making hydrogen bonds interactions (red dotted lines) with capreomycin.

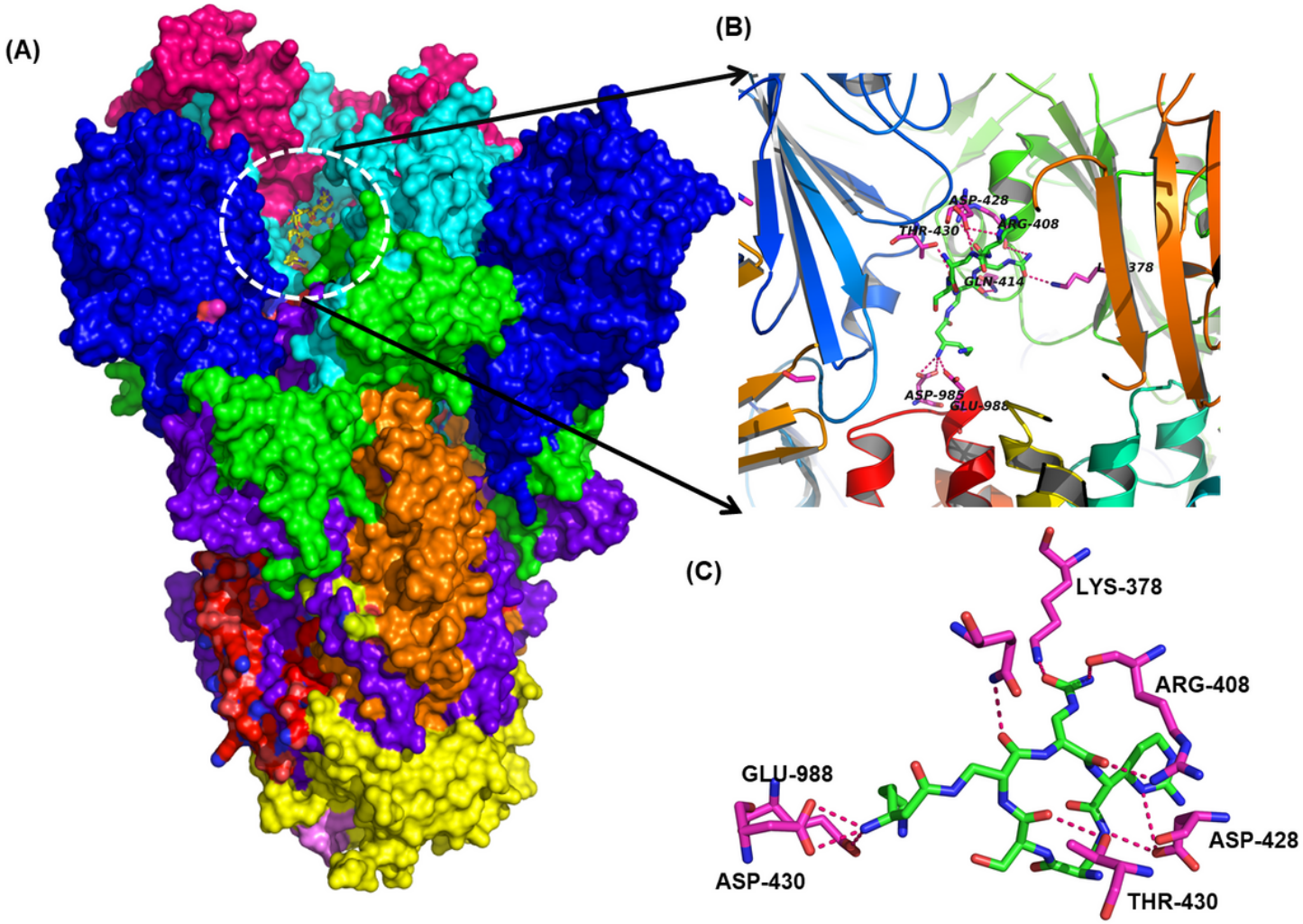

Figure 2

Virtual screening of FDA drugs against Spike protein. (A) The surface view of spike protein where domains are represented in different colors. The ligand binding site is shown inside white dotted circle at RBD (receptor binding domain) of the spike protein. (B) Cartoon depiction of the RBD showing the secondary structure elements and binding of capreomycin. (C) Closeup of RBD-capreomycin interaction showing residues making hydrogen bonds interactions (red dotted lines) with capreomycin.

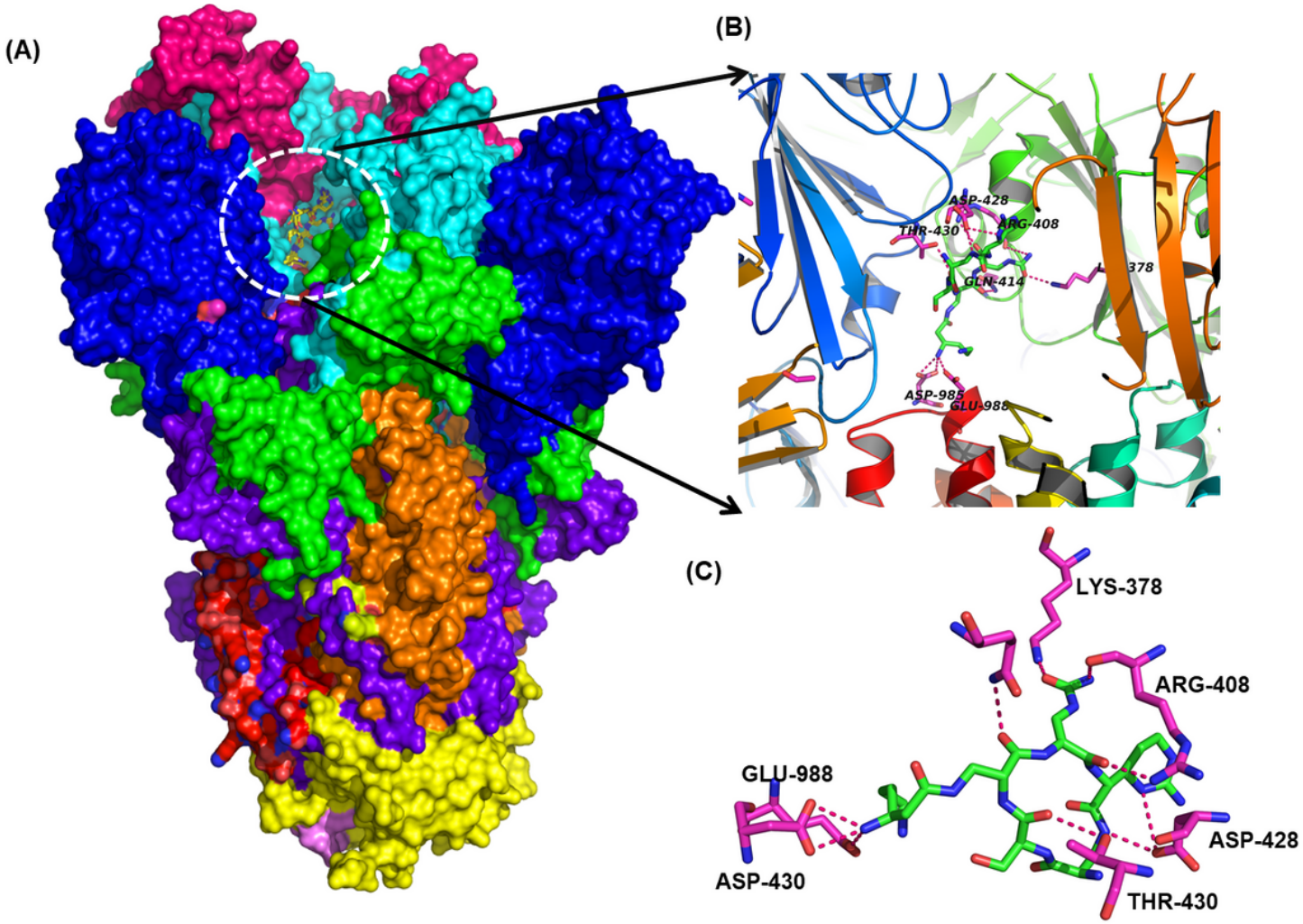

Figure 2

Virtual screening of FDA drugs against Spike protein. (A) The surface view of spike protein where domains are represented in different colors. The ligand binding site is shown inside white dotted circle at RBD (receptor binding domain) of the spike protein. (B) Cartoon depiction of the RBD showing the secondary structure elements and binding of capreomycin. (C) Closeup of RBD-capreomycin interaction showing residues making hydrogen bonds interactions (red dotted lines) with capreomycin.

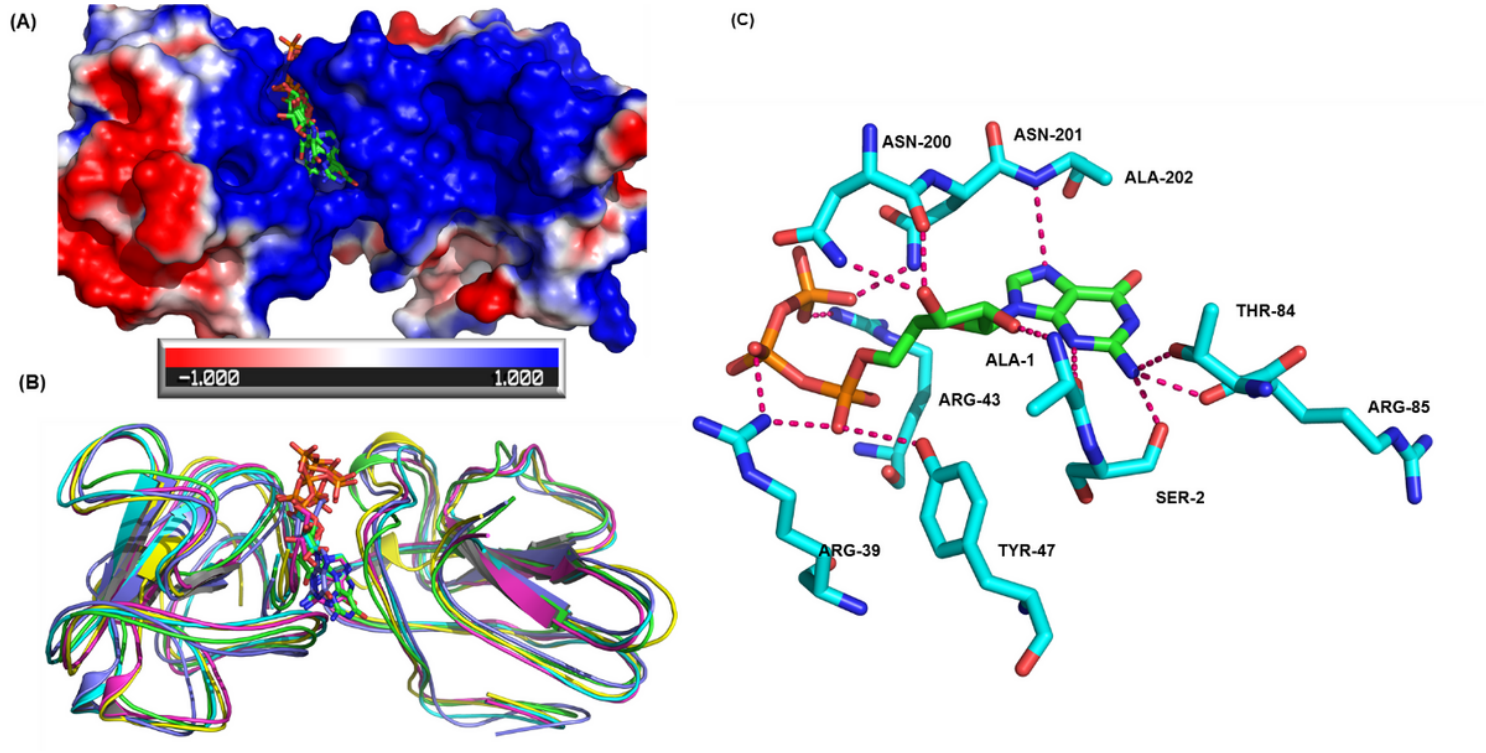

Figure 3

Nelarabine binding to nucleocapsid (N) protein of SARS-CoV2. (A) The surface is coloured by the charge on the amino acids. The red, white and blue surface area depict negative, neutral and positive surface respectively. Nelarabine binds in a predominantly positive area at the nucleocapsid homodimer interface. (B) Nelarabine docked in five MD snapshots of N-protein. (C) Ligand-protein interaction showing nelarabine makes multiple hydrogen bond interactions with N-protein.

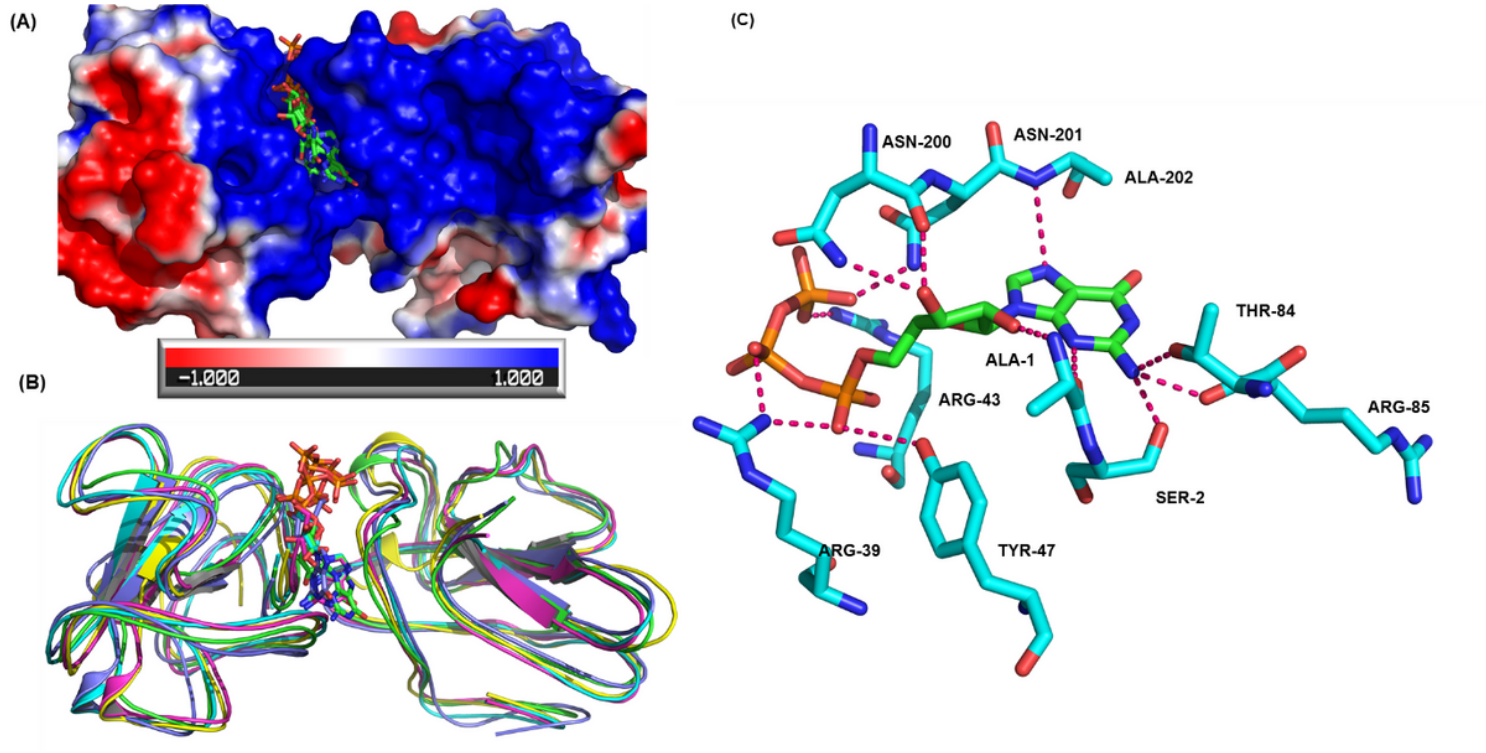

Figure 3

Nelarabine binding to nucleocapsid (N) protein of SARS-CoV2. (A) The surface is coloured by the charge on the amino acids. The red, white and blue surface area depict negative, neutral and positive surface respectively. Nelarabine binds in a predominantly positive area at the nucleocapsid homodimer interface. (B) Nelarabine docked in five MD snapshots of N-protein. (C) Ligand-protein interaction showing nelarabine makes multiple hydrogen bond interactions with N-protein.

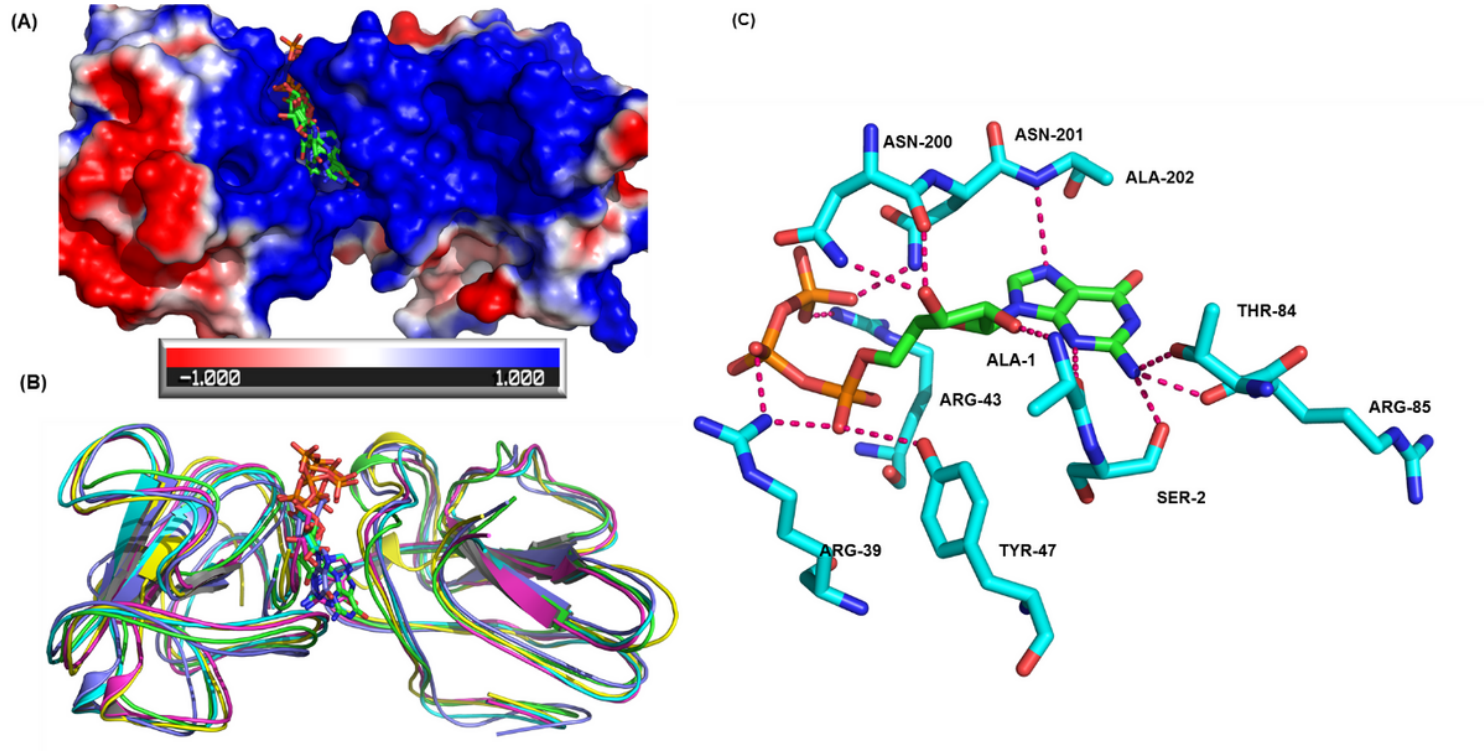

Figure 3

Nelarabine binding to nucleocapsid (N) protein of SARS-CoV2. (A) The surface is coloured by the charge on the amino acids. The red, white and blue surface area depict negative, neutral and positive surface respectively. Nelarabine binds in a predominantly positive area at the nucleocapsid homodimer interface. (B) Nelarabine docked in five MD snapshots of N-protein. (C) Ligand-protein interaction showing nelarabine makes multiple hydrogen bond interactions with N-protein.

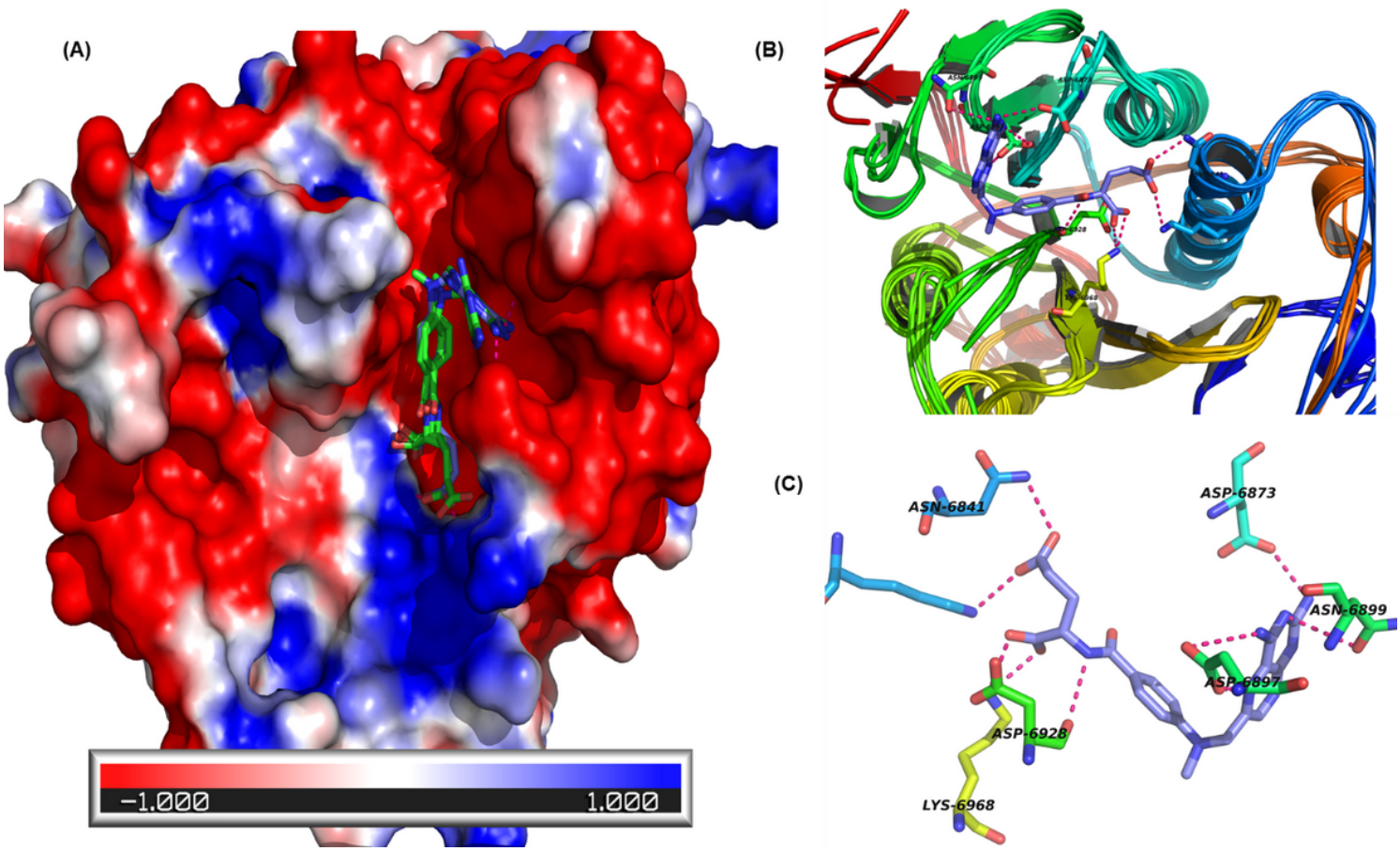

Figure 4

Methotrexate binding with methyltransferase (NSP16) (A) Representation of the NSP16 surface coloured by electrostatic charges on amino acids. The red, white and blue surface area depict negative, neutral and positive surface respectively. Methotrexate bind with methyltransferase in a predominantly negative cavity. (B) The cartoon representation shows active site flexibility during MD simulation. (C) Ligands interaction plot shows methotrexate (purple sticks) forms hydrogen bonds with Asn6841, Asp6928, Lys6968, Asp6897, Asn6899 and Asp6876 of NSP16.

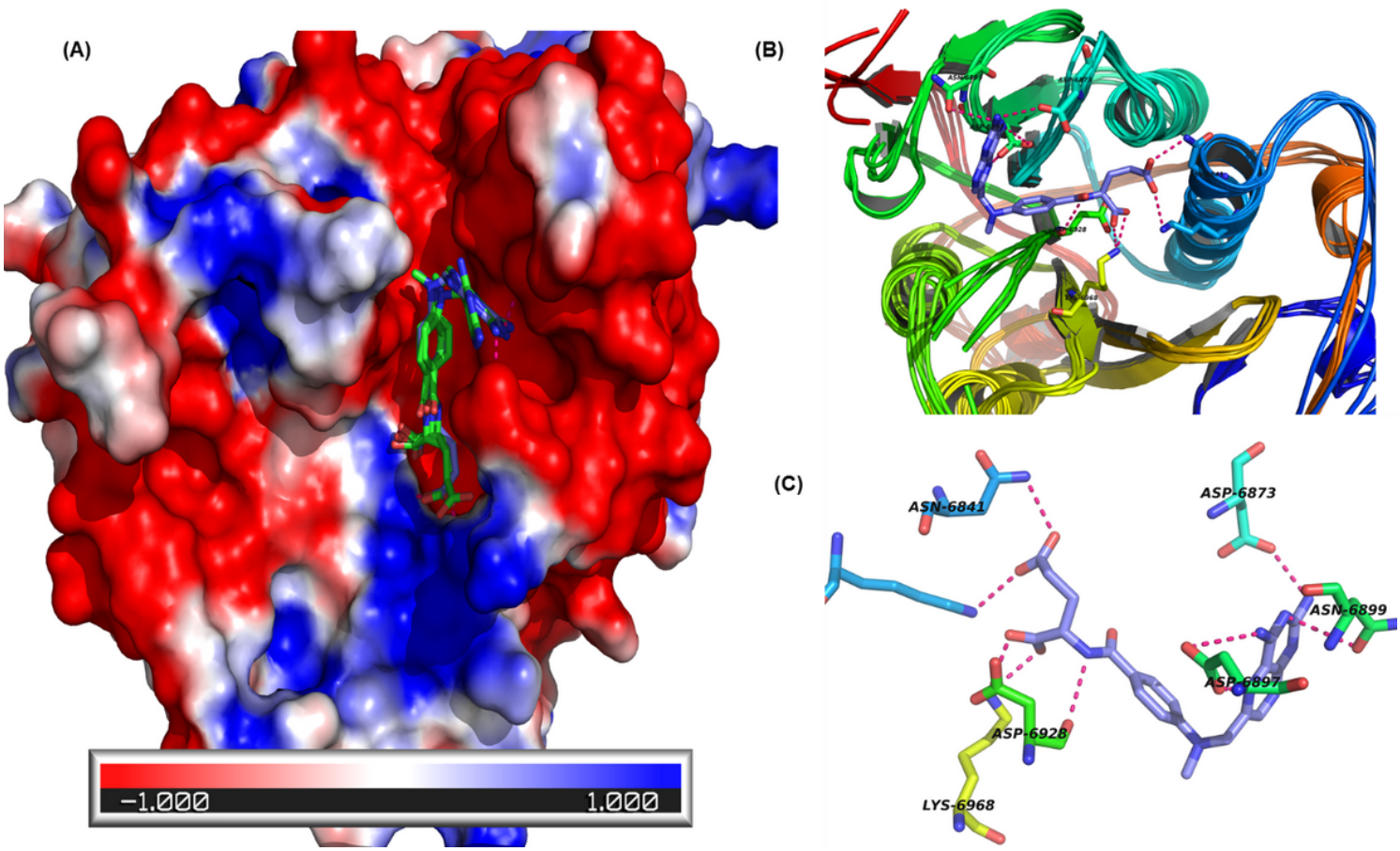

Figure 4

Methotrexate binding with methyltransferase (NSP16) (A) Representation of the NSP16 surface coloured by electrostatic charges on amino acids. The red, white and blue surface area depict negative, neutral and positive surface respectively. Methotrexate bind with methyltransferase in a predominantly negative cavity. (B) The cartoon representation shows active site flexibility during MD simulation. (C) Ligands interaction plot shows methotrexate (purple sticks) forms hydrogen bonds with Asn6841, Asp6928, Lys6968, Asp6897, Asn6899 and Asp6876 of NSP16.

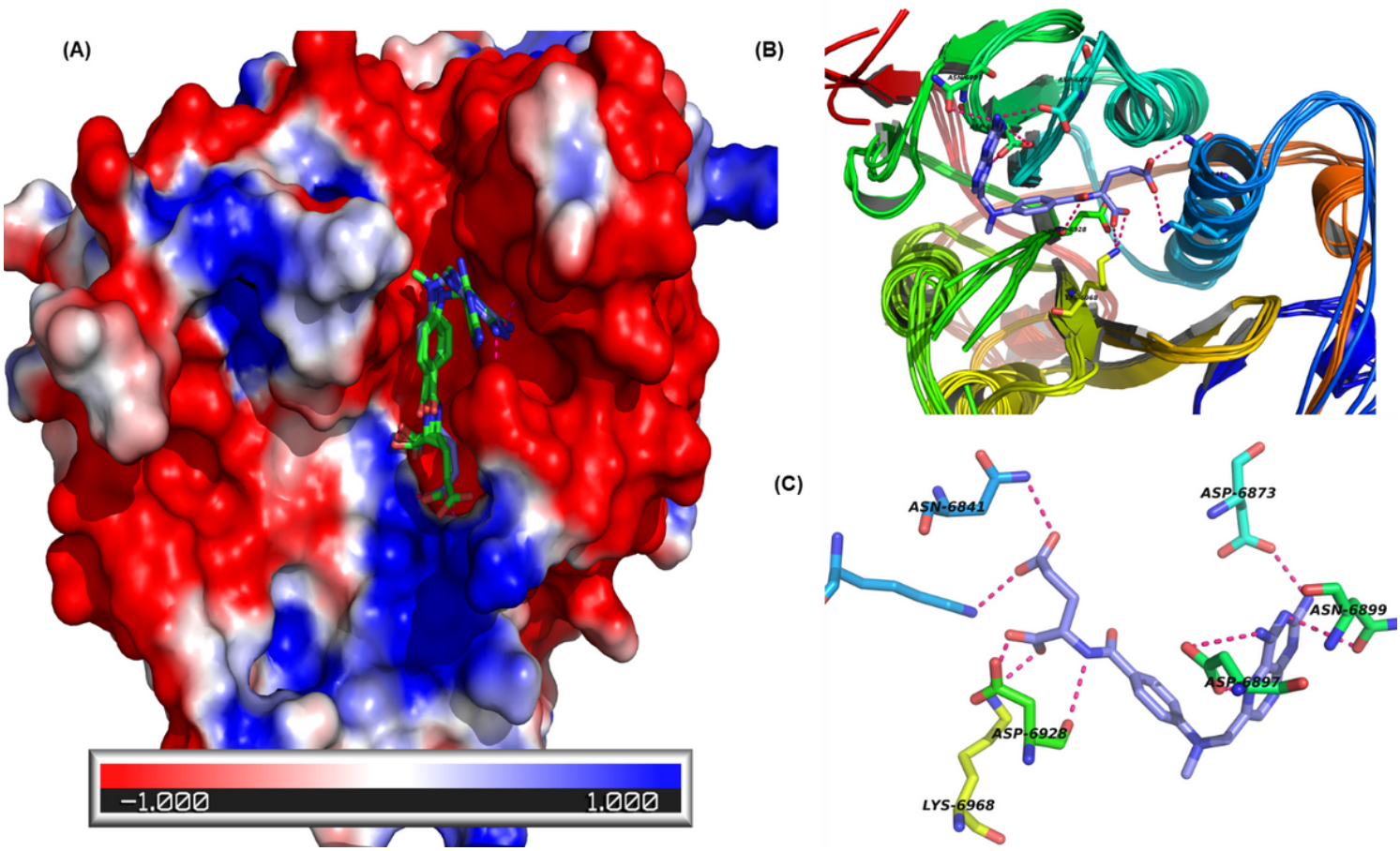

Figure 4

Methotrexate binding with methyltransferase (NSP16) (A) Representation of the NSP16 surface coloured by electrostatic charges on amino acids. The red, white and blue surface area depict negative, neutral and positive surface respectively. Methotrexate bind with methyltransferase in a predominantly negative cavity. (B) The cartoon representation shows active site flexibility during MD simulation. (C) Ligands interaction plot shows methotrexate (purple sticks) forms hydrogen bonds with Asn6841, Asp6928, Lys6968, Asp6897, Asn6899 and Asp6876 of NSP16.

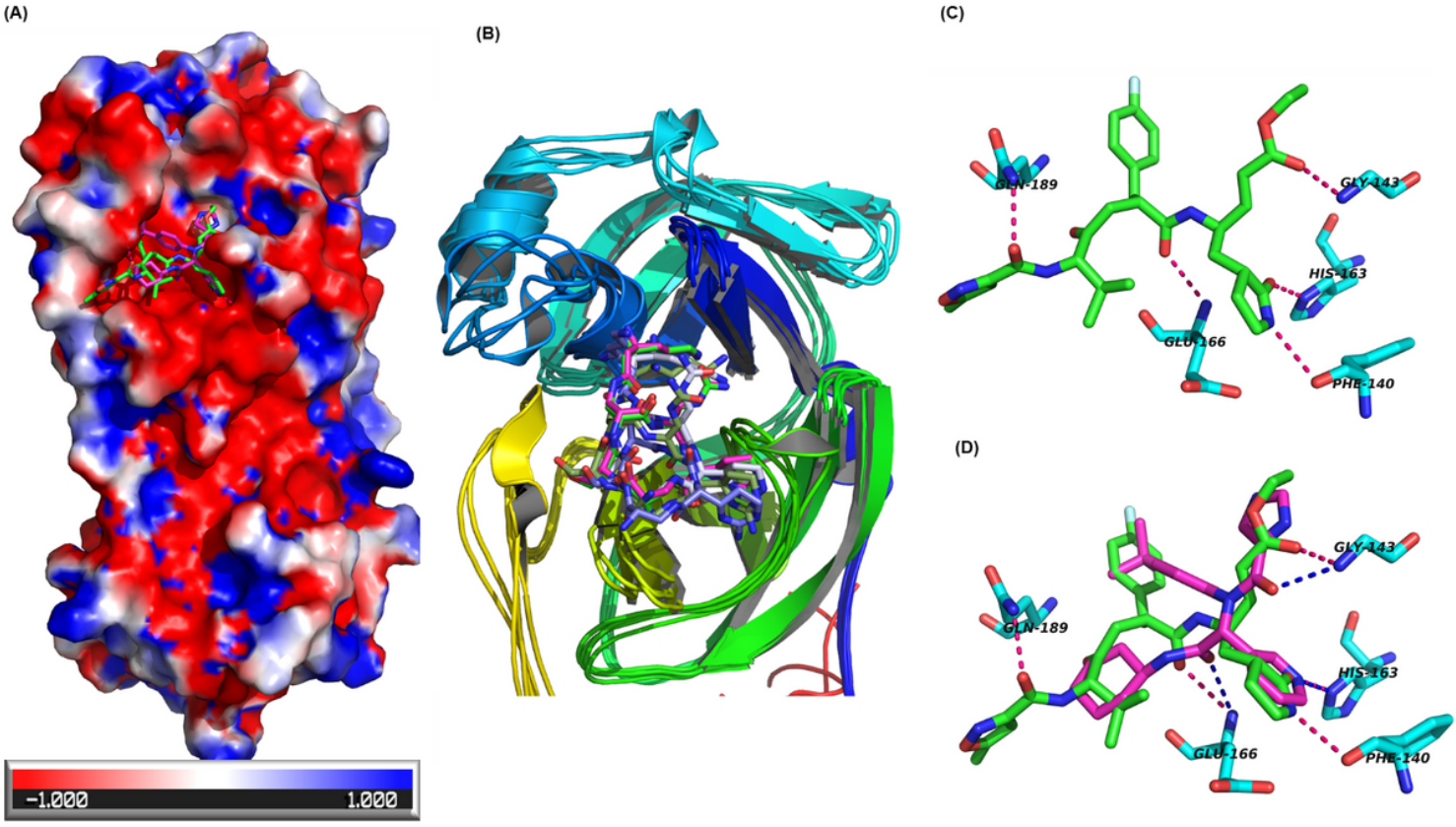

Figure 5

Binding of rupintrivir with the main protease of SARS-CoV2. (A) The red white and blue surface area depict negative, neutral and positive charged surface respectively on the main protease. Rupintrivir is shown in green sticks while the co-crystallized ligand is shown in maroon. (B) The docking of rupintrivir in MD snapshots of the receptor. (C) The hydrogen bonding interactions (dotted lines) between rupintrivir (green sticks) and active site residues of main protease (cyan sticks). (D) Binding pose comparison of rupintrivir (green sticks) with co-crystallized ligand (maroon sticks). The receptor residues are shown in cyan sticks. The dotted line shows hydrogen bond interaction with the receptor.

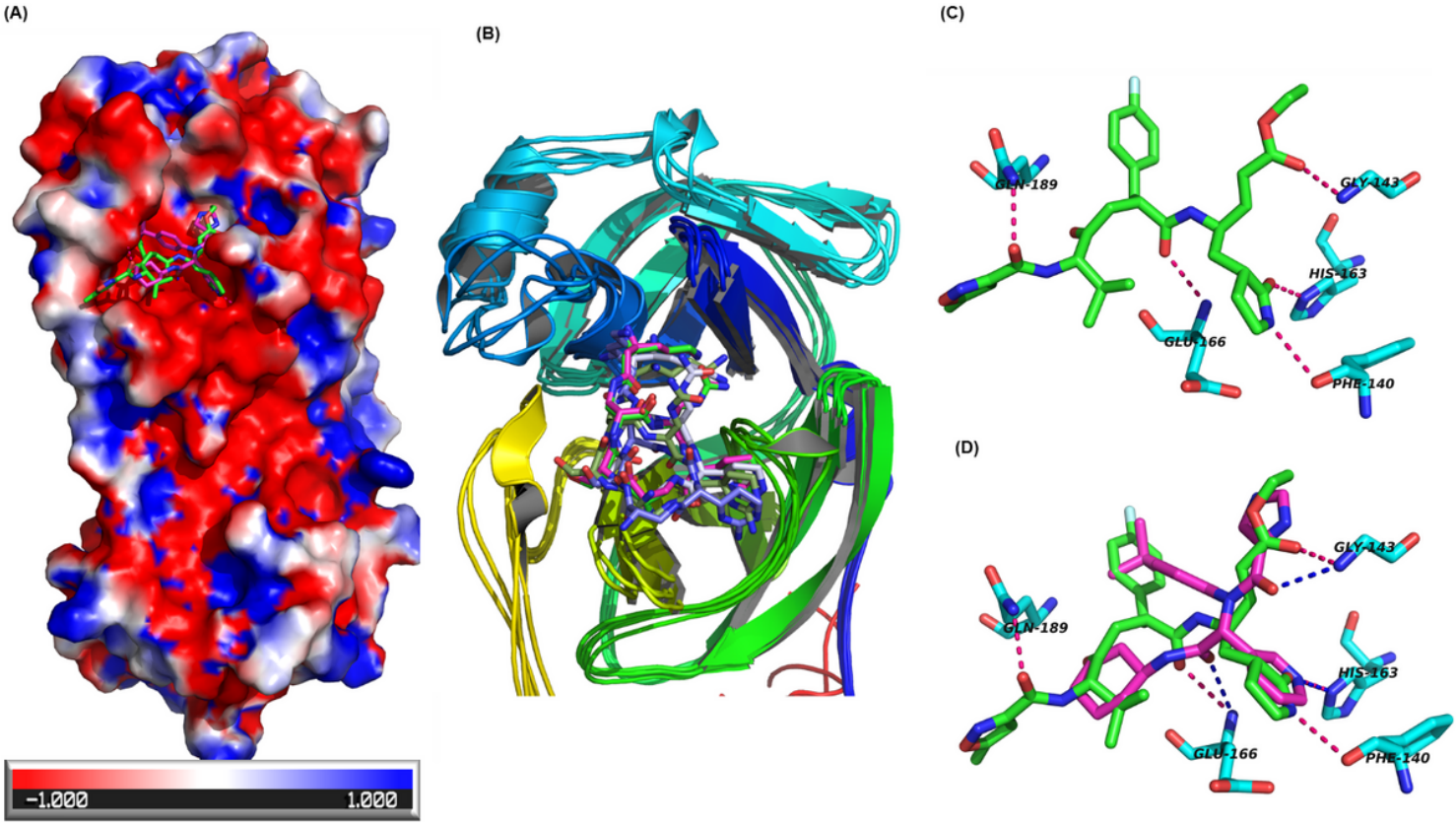

Figure 5

Binding of rupintrivir with the main protease of SARS-CoV2. (A) The red white and blue surface area depict negative, neutral and positive charged surface respectively on the main protease. Rupintrivir is shown in green sticks while the co-crystallized ligand is shown in maroon. (B) The docking of rupintrivir in MD snapshots of the receptor. (C) The hydrogen bonding interactions (dotted lines) between rupintrivir (green sticks) and active site residues of main protease (cyan sticks). (D) Binding pose comparison of rupintrivir (green sticks) with co-crystallized ligand (maroon sticks). The receptor residues are shown in cyan sticks. The dotted line shows hydrogen bond interaction with the receptor.

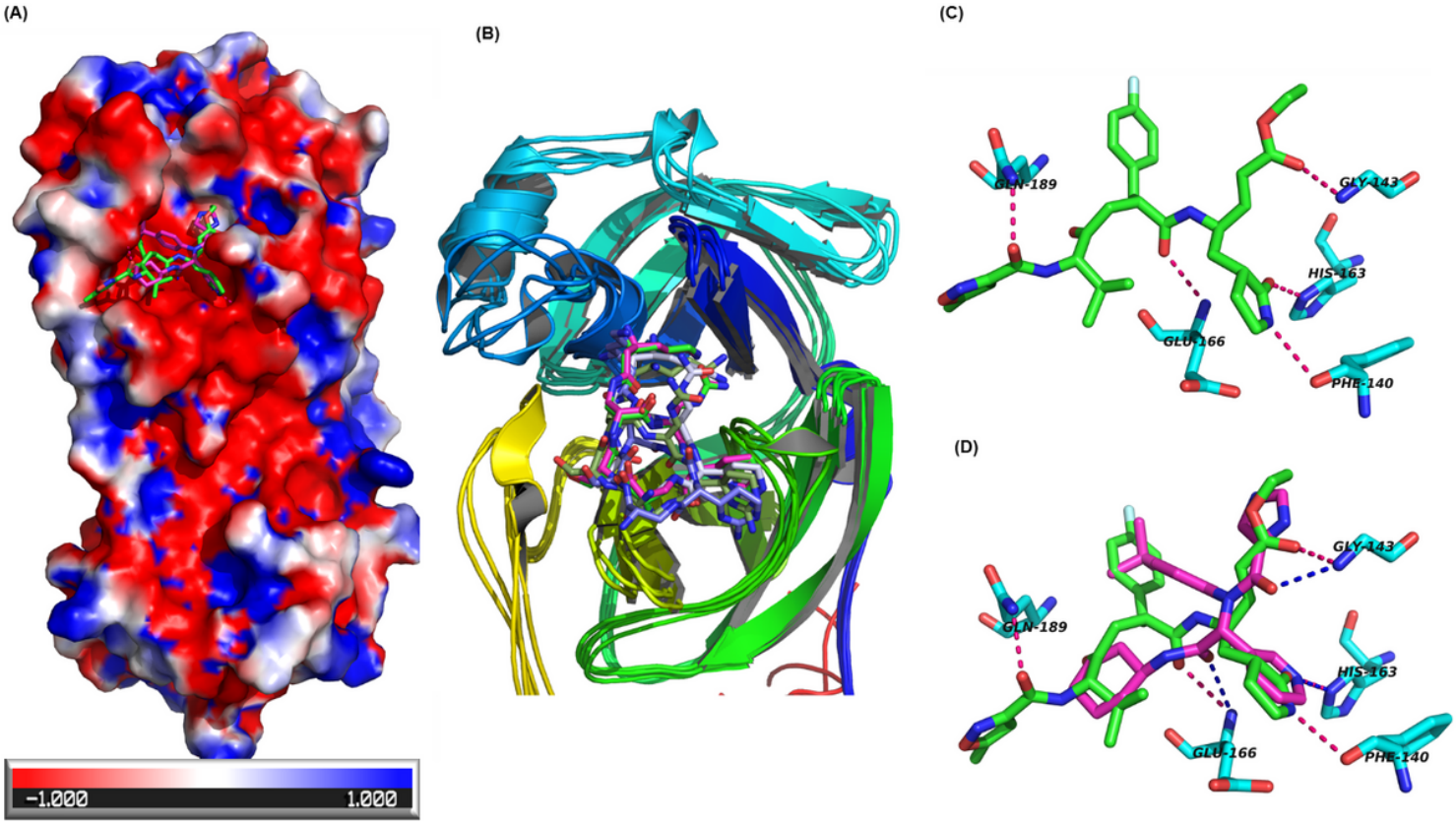

Figure 5

Binding of rupintrivir with the main protease of SARS-CoV2. (A) The red white and blue surface area depict negative, neutral and positive charged surface respectively on the main protease. Rupintrivir is shown in green sticks while the co-crystallized ligand is shown in maroon. (B) The docking of rupintrivir in MD snapshots of the receptor. (C) The hydrogen bonding interactions (dotted lines) between rupintrivir (green sticks) and active site residues of main protease (cyan sticks). (D) Binding pose comparison of rupintrivir (green sticks) with co-crystallized ligand (maroon sticks). The receptor residues are shown in cyan sticks. The dotted line shows hydrogen bond interaction with the receptor.

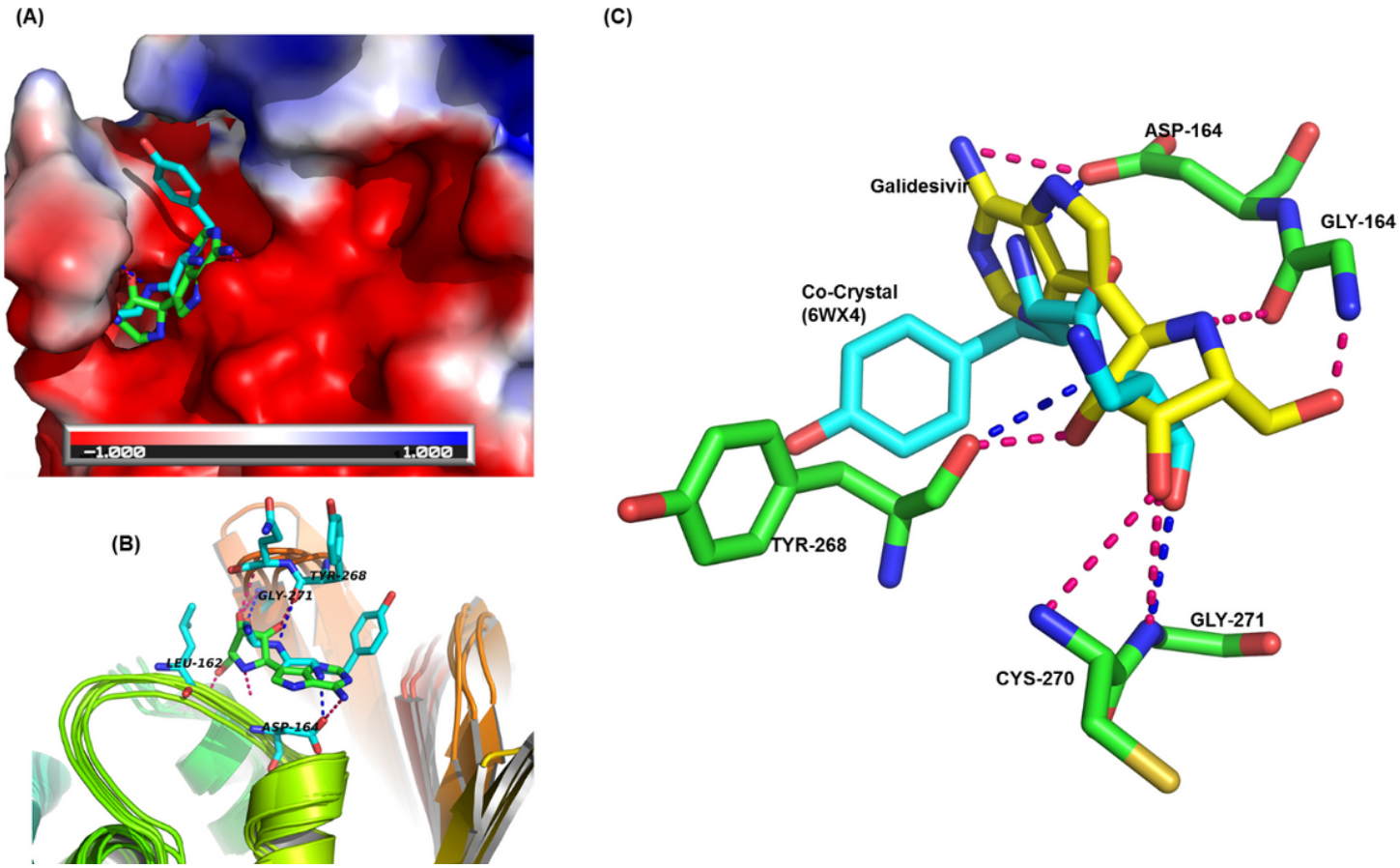

Figure 6

Binding of galidesivir with PLpro (NSP3). (A) The surface is colored as a function of electrostatic charge on the residues. The co-crystallized ligand (cyan sticks) and galidesivir (green sticks). (B) Superimposition of the snapshots and binding of galidesivir. (C) A close up of galidesivir-PLpro interactions. Hydrogen bonding interactions are shown for galidesivir (yellow sticks) and co-crystallized ligand (cyan). The pink and blue dotted lines show hydrogen bonds galidesivir and co-crystallized ligand respectively.

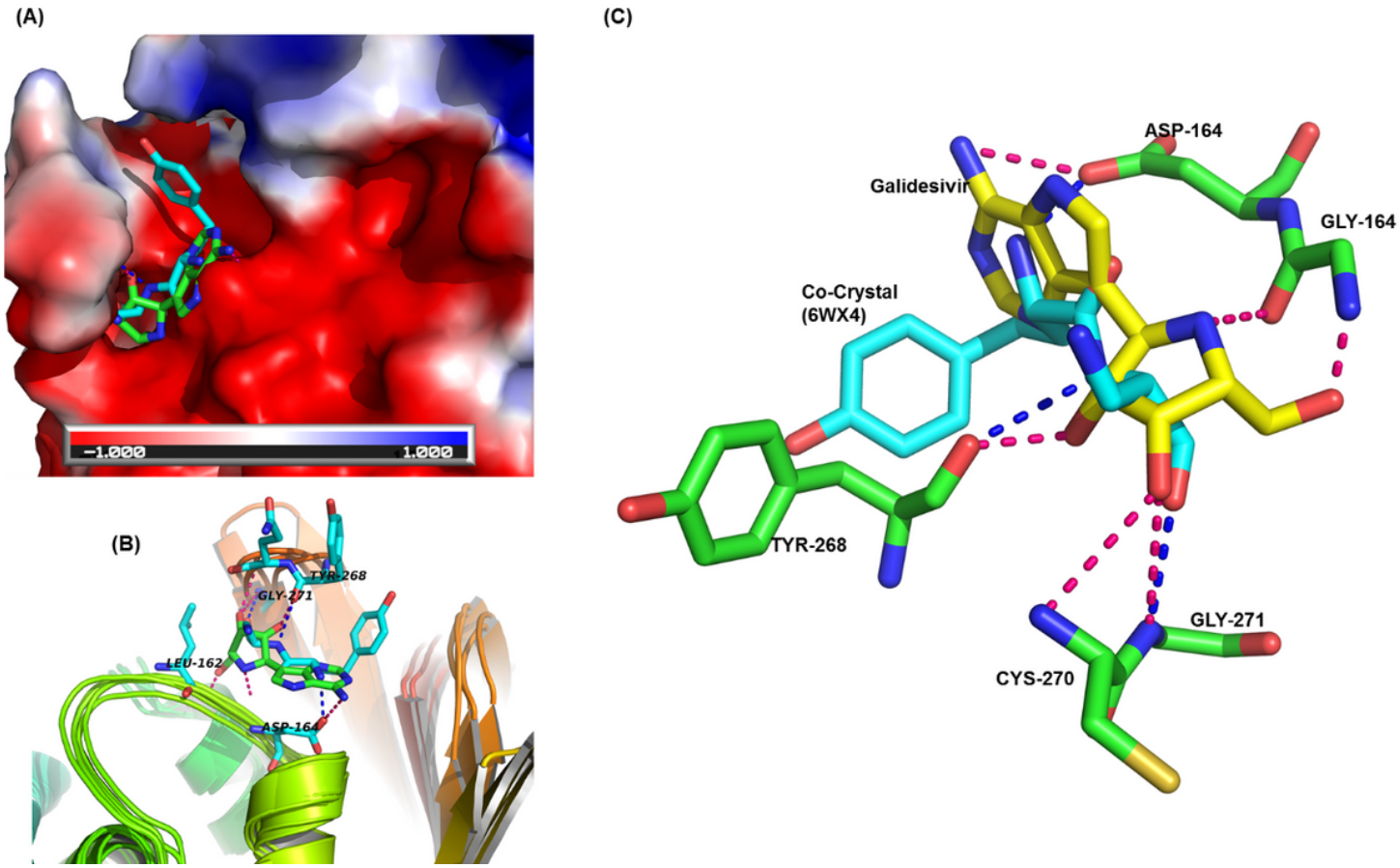

Figure 6

Binding of galidesivir with PLpro (NSP3). (A) The surface is colored as a function of electrostatic charge on the residues. The co-crystallized ligand (cyan sticks) and galidesivir (green sticks). (B) Superimposition of the snapshots and binding of galidesivir. (C) A close up of galidesivir-PLpro interactions. Hydrogen bonding interactions are shown for galidesivir (yellow sticks) and co-crystallized ligand (cyan). The pink and blue dotted lines show hydrogen bonds galidesivir and co-crystallized ligand respectively.

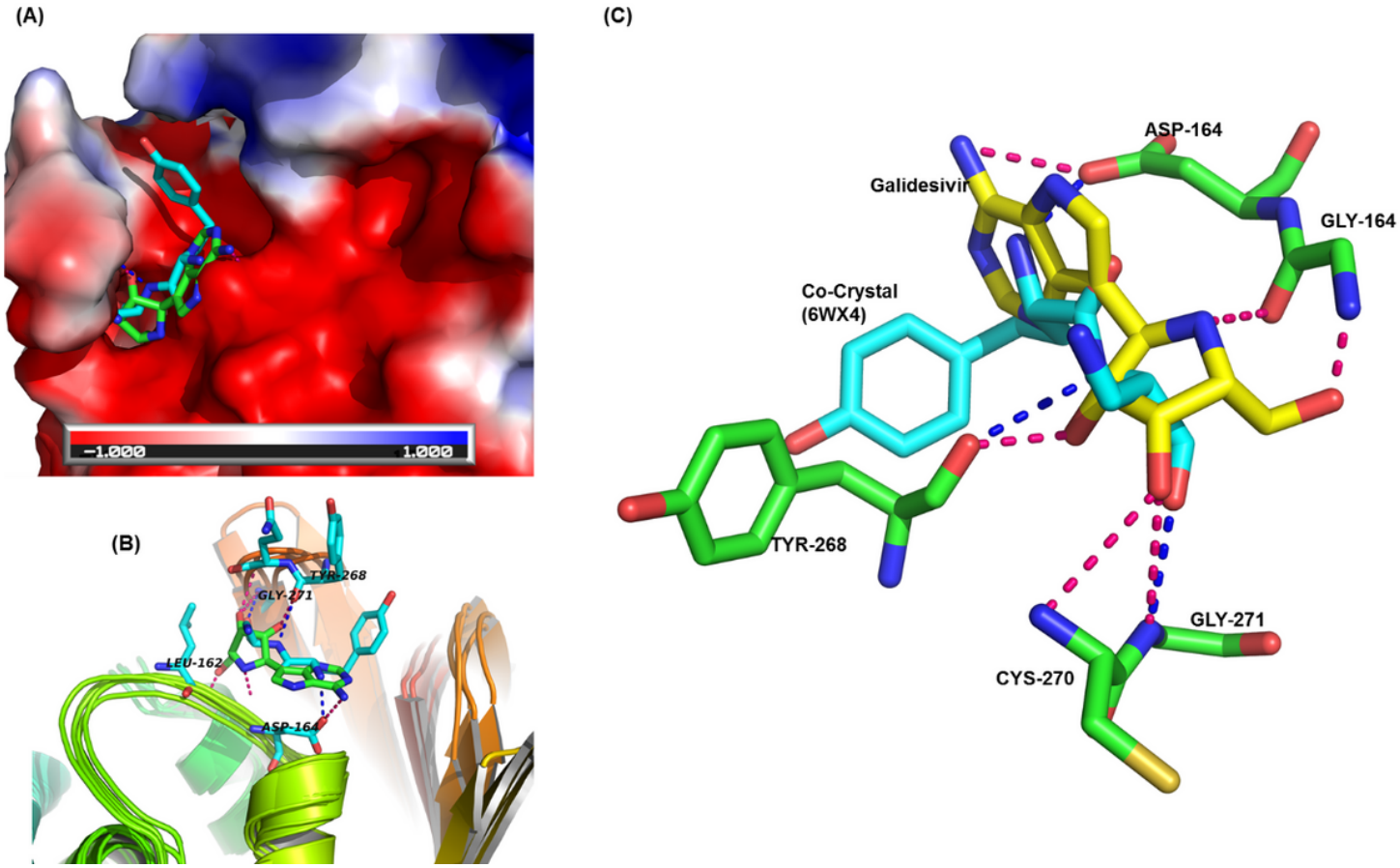

Figure 6

Binding of galidesivir with PLpro (NSP3). (A) The surface is colored as a function of electrostatic charge on the residues. The co-crystallized ligand (cyan sticks) and galidesivir (green sticks). (B) Superimposition of the snapshots and binding of galidesivir. (C) A close up of galidesivir-PLpro interactions. Hydrogen bonding interactions are shown for galidesivir (yellow sticks) and co-crystallized ligand (cyan). The pink and blue dotted lines show hydrogen bonds galidesivir and co-crystallized ligand respectively.

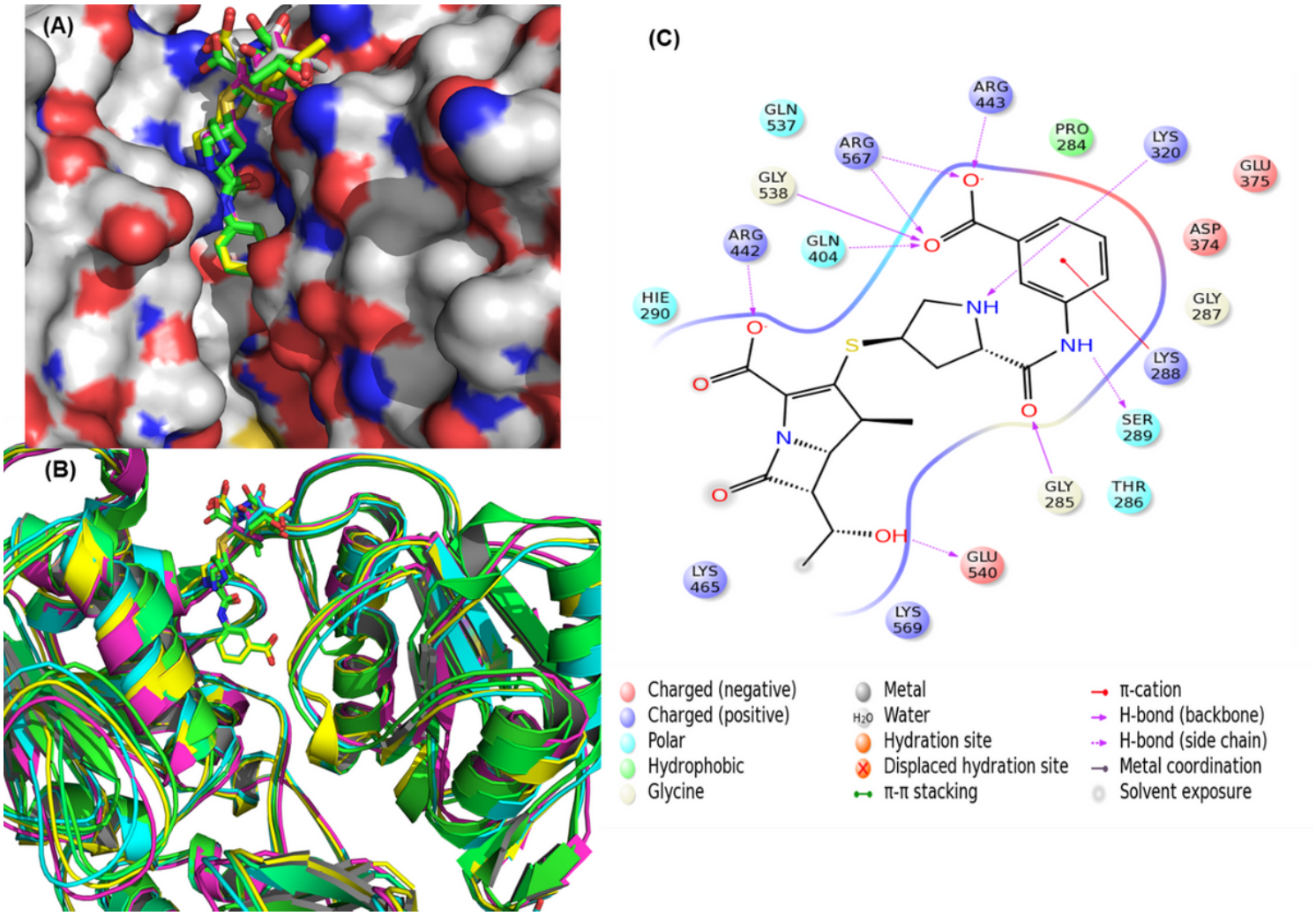

Figure 7

(A) Binding of eratapenem (average docking score -9.86) at the helicase protein of SARS-CoV2. (B) The five receptor frames are shown with docked eratapenem. (C) The ligand plot is showing interactions between eratapenem and helicase binding site.

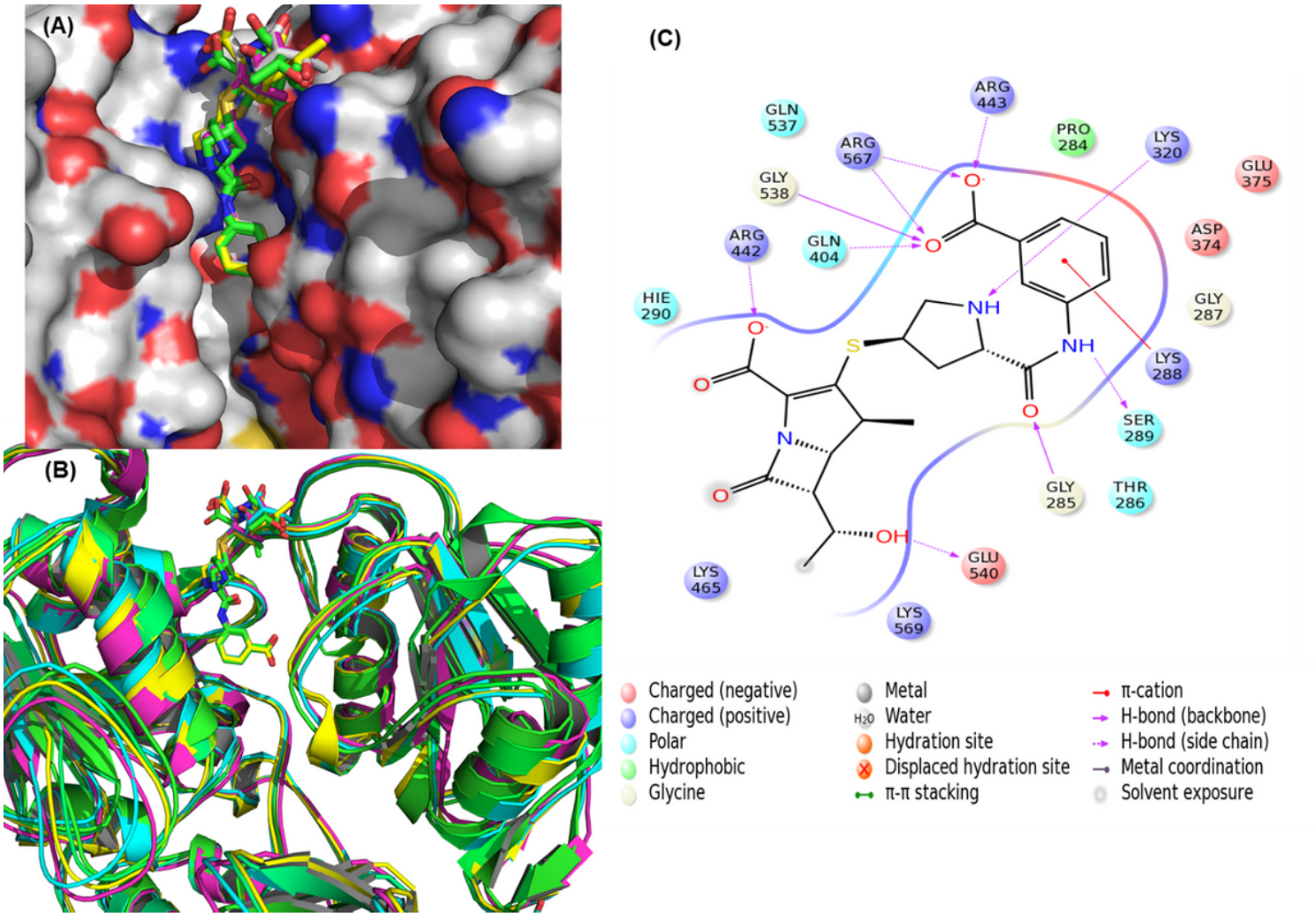

Figure 7

(A) Binding of eratapenem (average docking score -9.86) at the helicase protein of SARS-CoV2. (B) The five receptor frames are shown with docked eratapenem. (C) The ligand plot is showing interactions between eratapenem and helicase binding site.

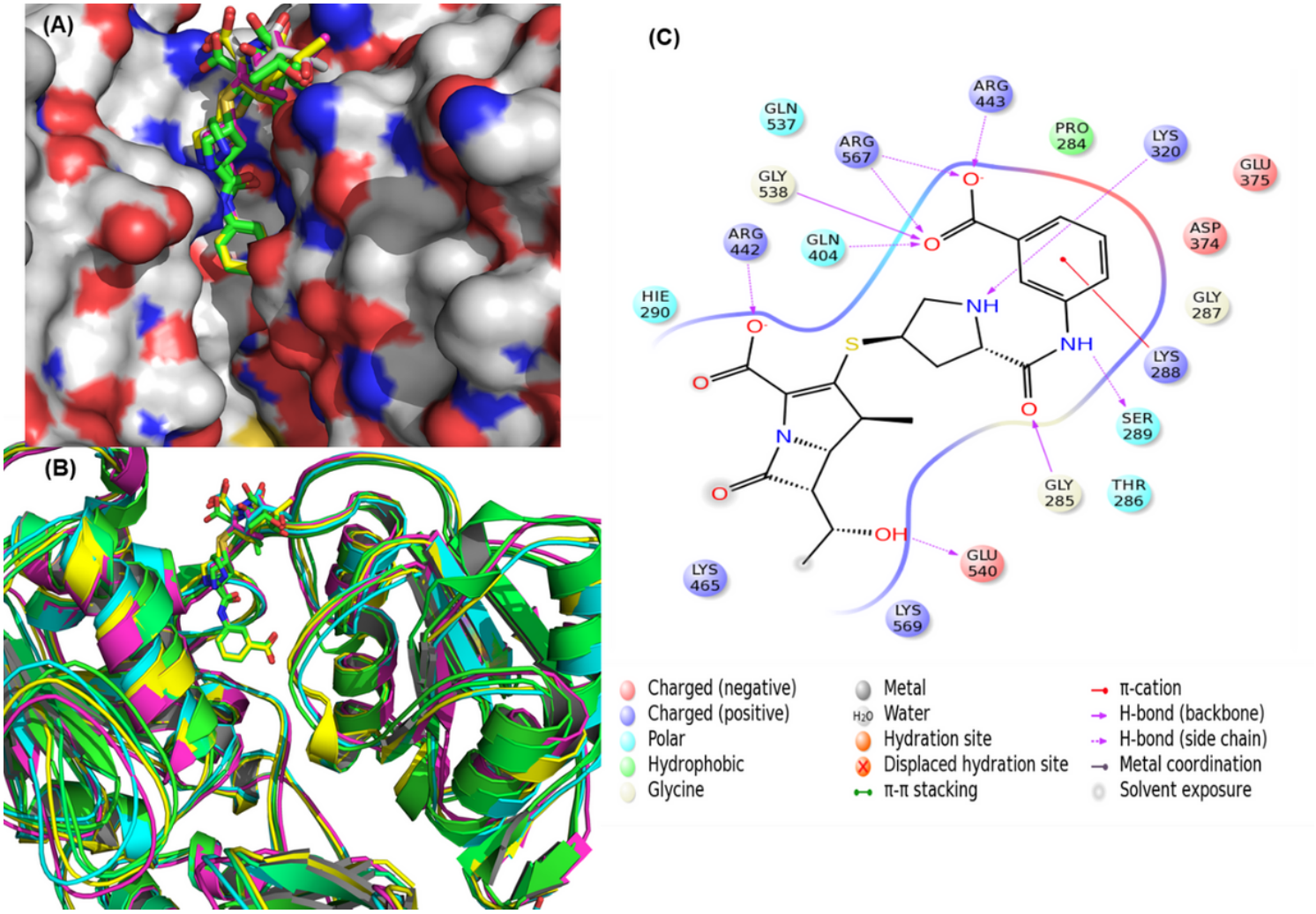

Figure 7

(A) Binding of eratapenem (average docking score -9.86) at the helicase protein of SARS-CoV2. (B) The five receptor frames are shown with docked eratapenem. (C) The ligand plot is showing interactions between eratapenem and helicase binding site.

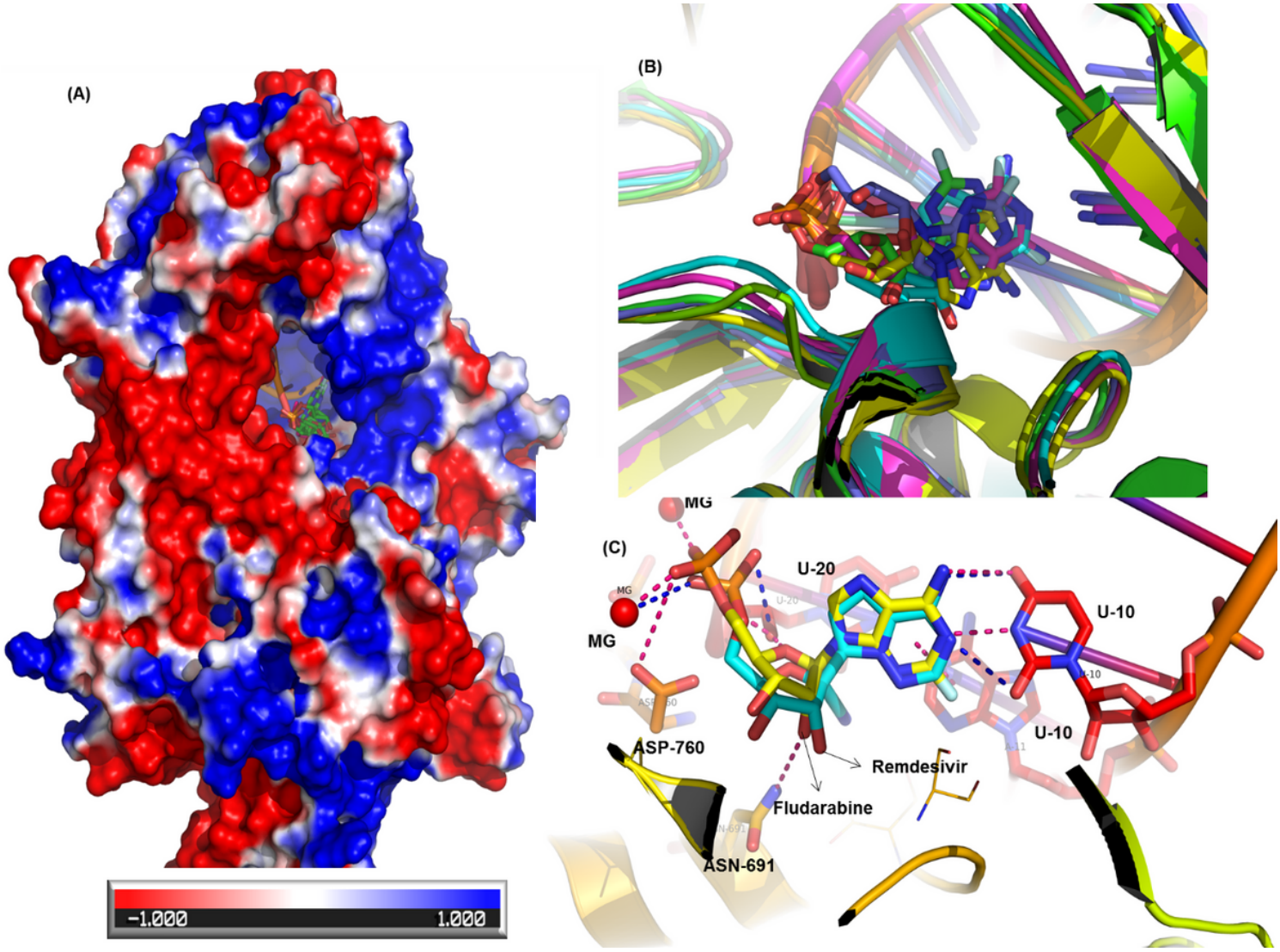

Figure 8

Binding of fludarabine with RNA-dependent RNA polymerase (RdRp) of SARS-CoV2. (A) The surface view of RdRp protein with co-crystallized ligand (remdesivir). The red white and blue surface area depict negative, neutral and positive charged surface respectively. (B) Fludarabine docked into MD snapshots of RdRp. (C) Fludarabine (yellow sticks) and remdesivir (blue sticks) in RdRp active site. The hydrogen bonding interactions are shown in dotted lines (blue-remdesivir, red-fludarabine). It is clear from the binding pose and interactions that fludarabine binds to RdRp quite similar as remdesivir.

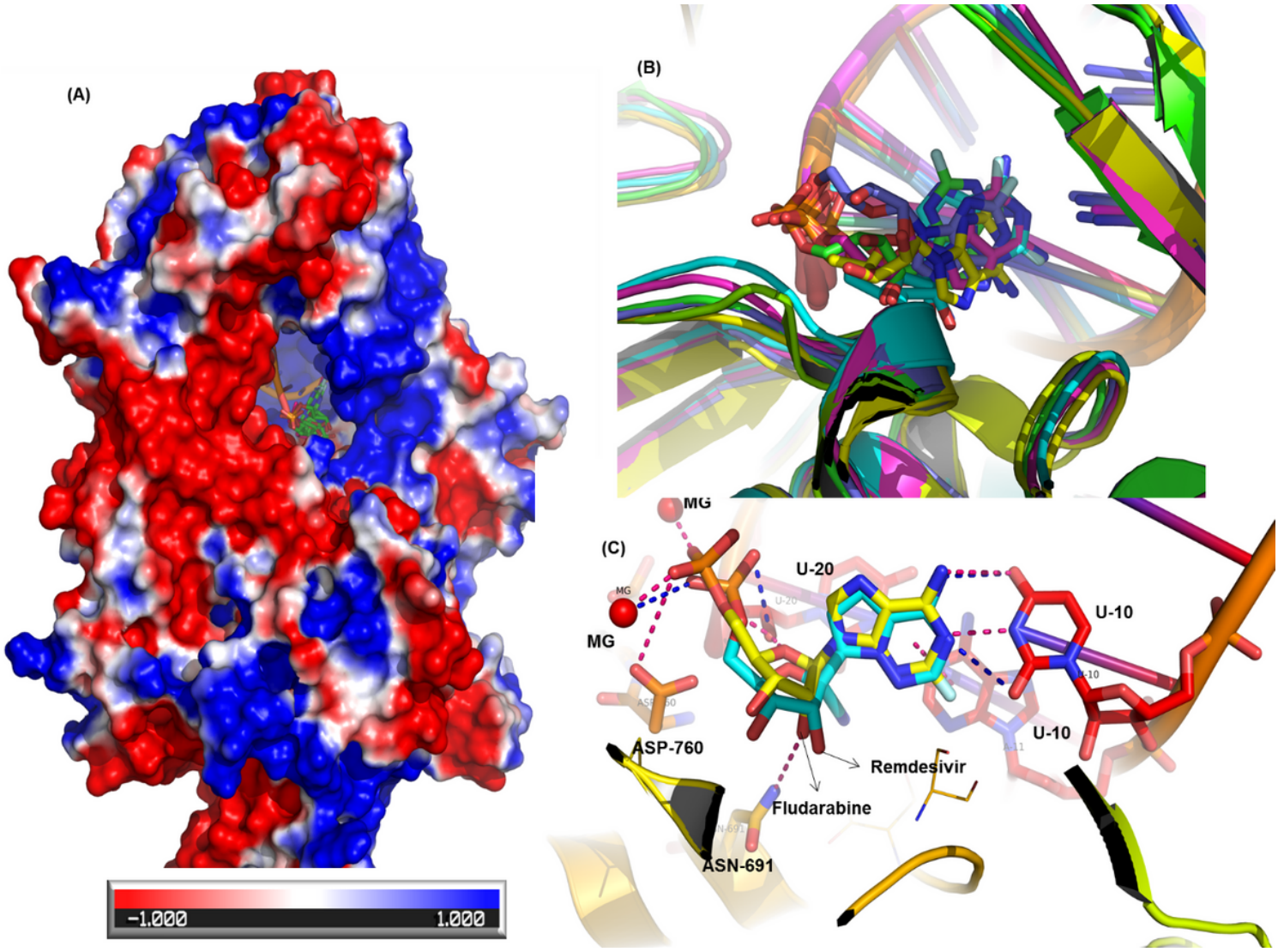

Figure 8

Binding of fludarabine with RNA-dependent RNA polymerase (RdRp) of SARS-CoV2. (A) The surface view of RdRp protein with co-crystallized ligand (remdesivir). The red white and blue surface area depict negative, neutral and positive charged surface respectively. (B) Fludarabine docked into MD snapshots of RdRp. (C) Fludarabine (yellow sticks) and remdesivir (blue sticks) in RdRp active site. The hydrogen bonding interactions are shown in dotted lines (blue-remdesivir, red-fludarabine). It is clear from the binding pose and interactions that fludarabine binds to RdRp quite similar as remdesivir.

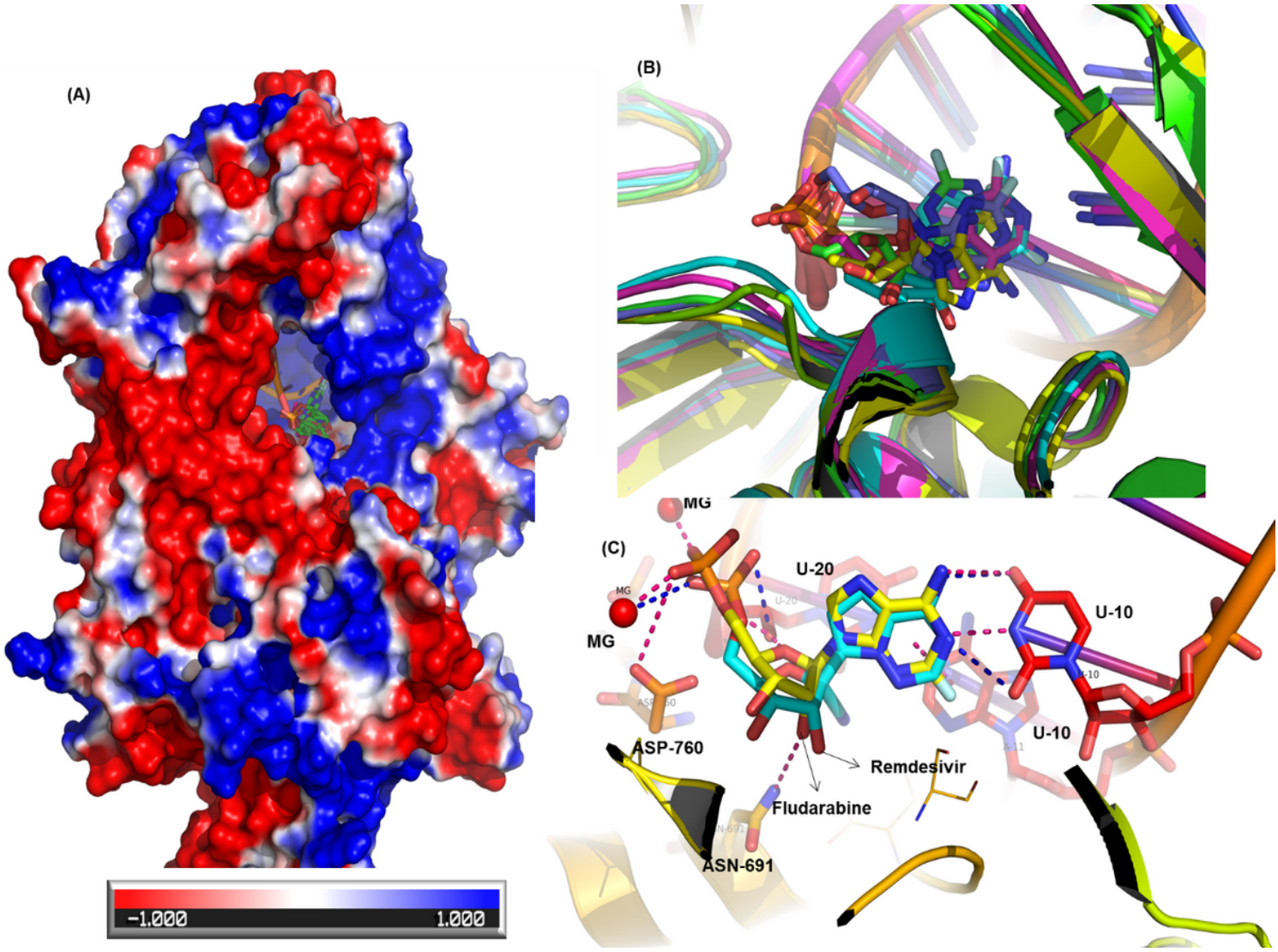

Figure 8

Binding of fludarabine with RNA-dependent RNA polymerase (RdRp) of SARS-CoV2. (A) The surface view of RdRp protein with co-crystallized ligand (remdesivir). The red white and blue surface area depict negative, neutral and positive charged surface respectively. (B) Fludarabine docked into MD snapshots of RdRp. (C) Fludarabine (yellow sticks) and remdesivir (blue sticks) in RdRp active site. The hydrogen bonding interactions are shown in dotted lines (blue-remdesivir, red-fludarabine). It is clear from the binding pose and interactions that fludarabine binds to RdRp quite similar as remdesivir.

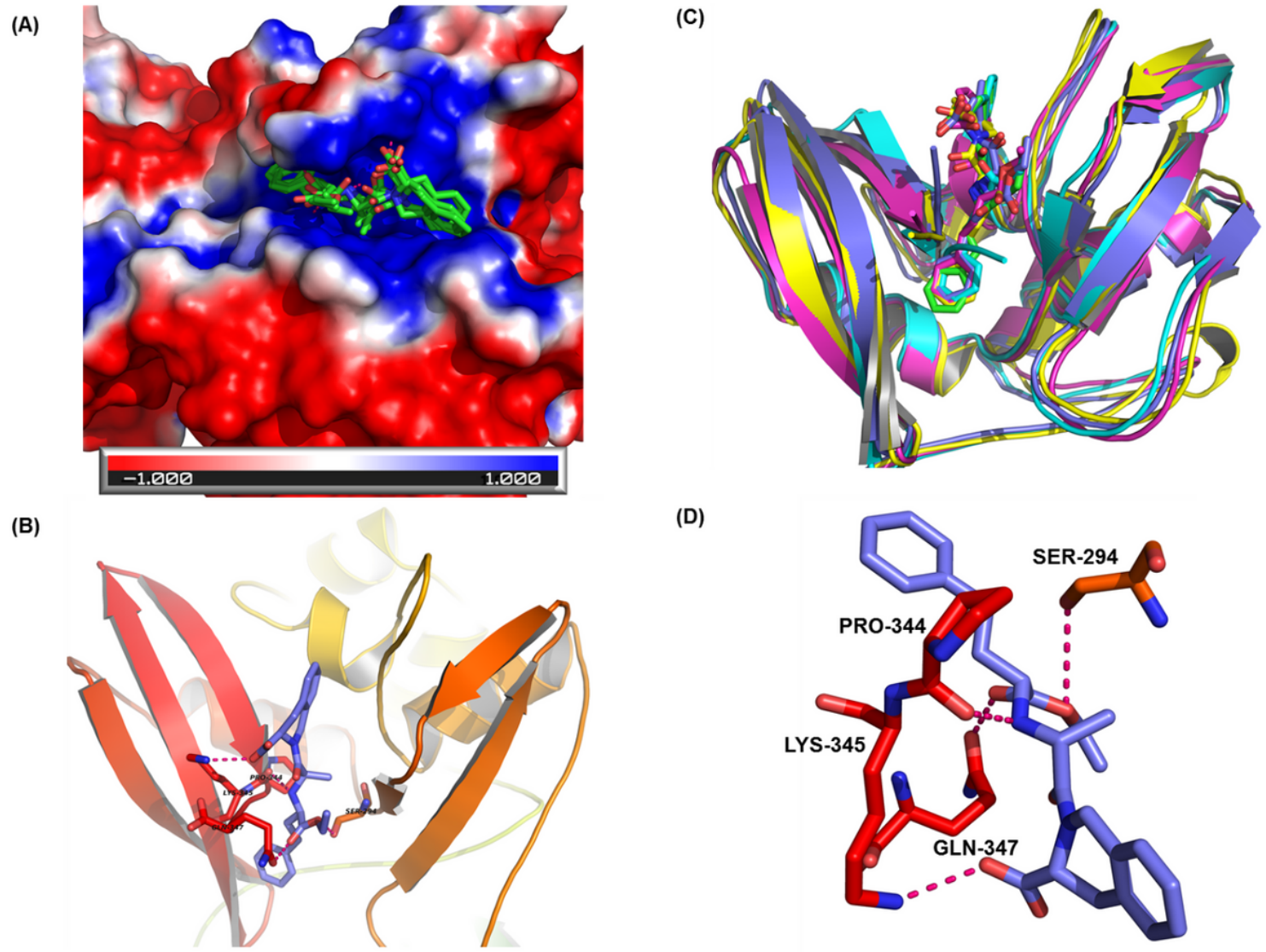

Figure 9

Quinapril binding to endonuclease protein: (A) The surface view of endonuclease with docked ligands. The red white and blue surface area depict negative,neutral and positive charged surface respectively. Ligands bind to the predominantly positive cavity. (B) The MD frames with ligand. (C) The secondary structural elements of the binding site (cyan) and quinapril (purple). (D) Hydrogen bonding interactions between quinapril (purple) and receptor residues Gln347, Lys345, and Ser294 (red).

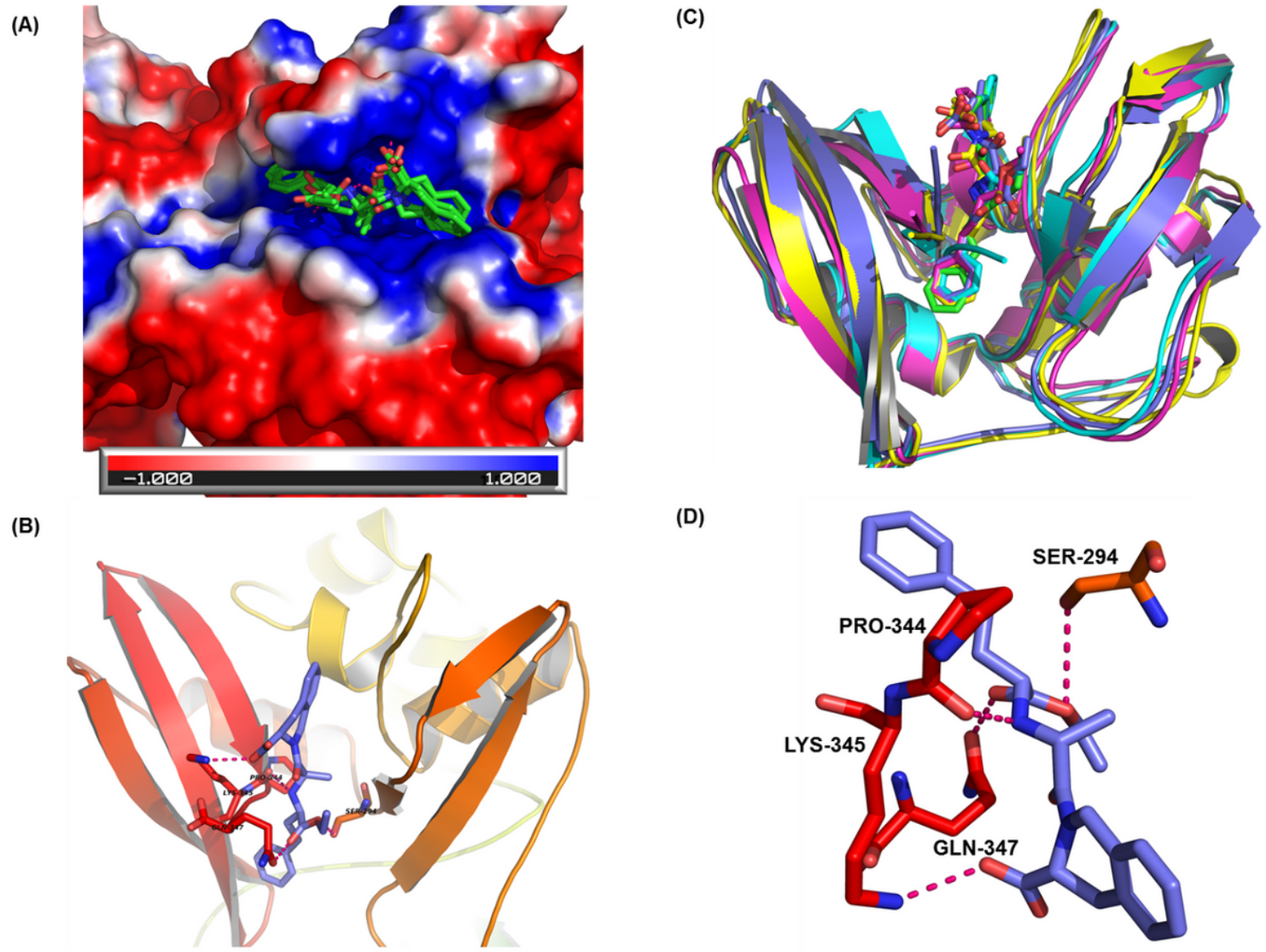

Figure 9

Quinapril binding to endonuclease protein: (A) The surface view of endonuclease with docked ligands. The red white and blue surface area depict negative,neutral and positive charged surface respectively. Ligands bind to the predominantly positive cavity. (B) The MD frames with ligand. (C) The secondary structural elements of the binding site (cyan) and quinapril (purple). (D) Hydrogen bonding interactions between quinapril (purple) and receptor residues Gln347, Lys345, and Ser294 (red).

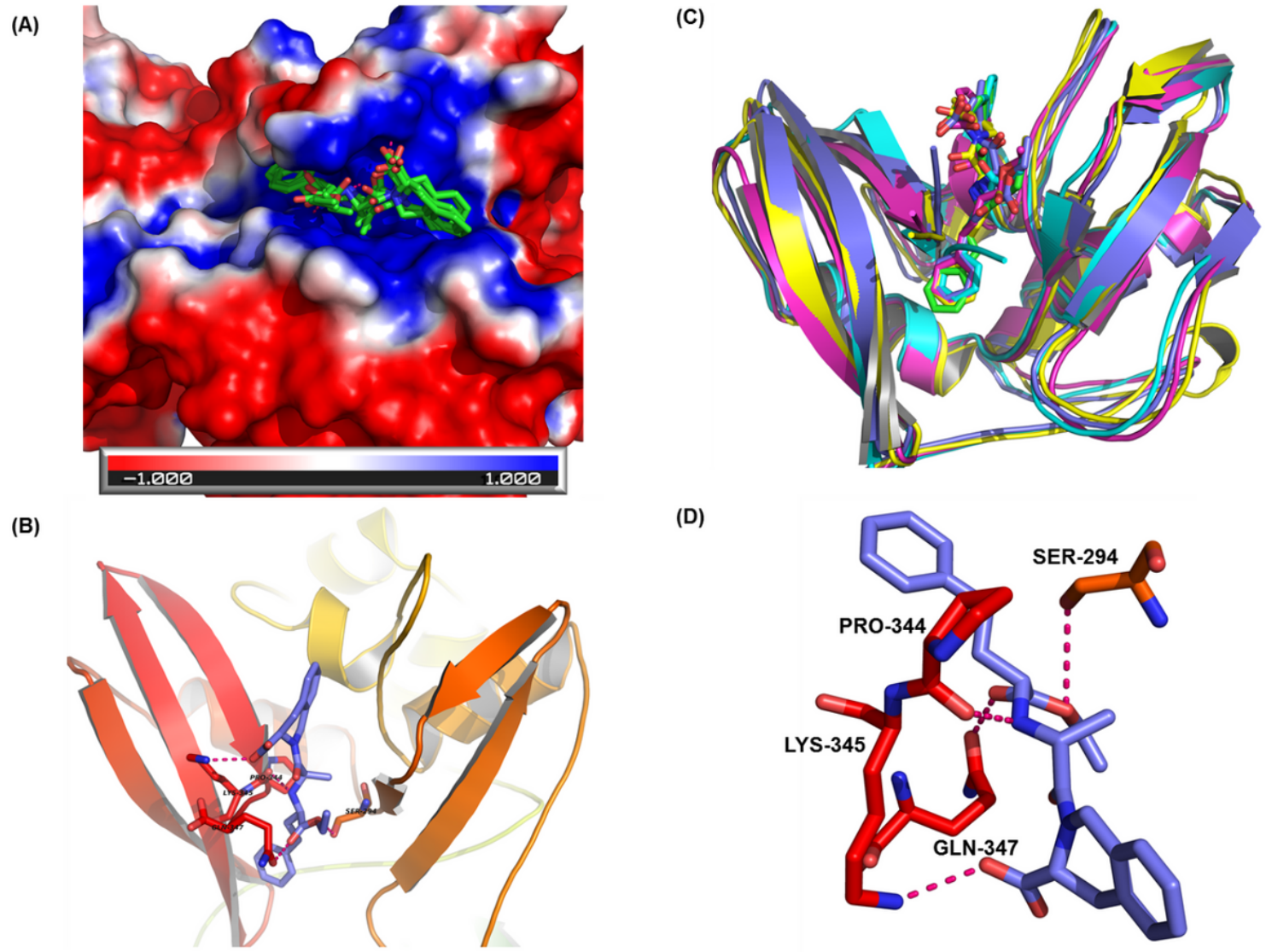

Figure 9

Quinapril binding to endonuclease protein: (A) The surface view of endonuclease with docked ligands. The red white and blue surface area depict negative,neutral and positive charged surface respectively. Ligands bind to the predominantly positive cavity. (B) The MD frames with ligand. (C) The secondary structural elements of the binding site (cyan) and quinapril (purple). (D) Hydrogen bonding interactions between quinapril (purple) and receptor residues Gln347, Lys345, and Ser294 (red).

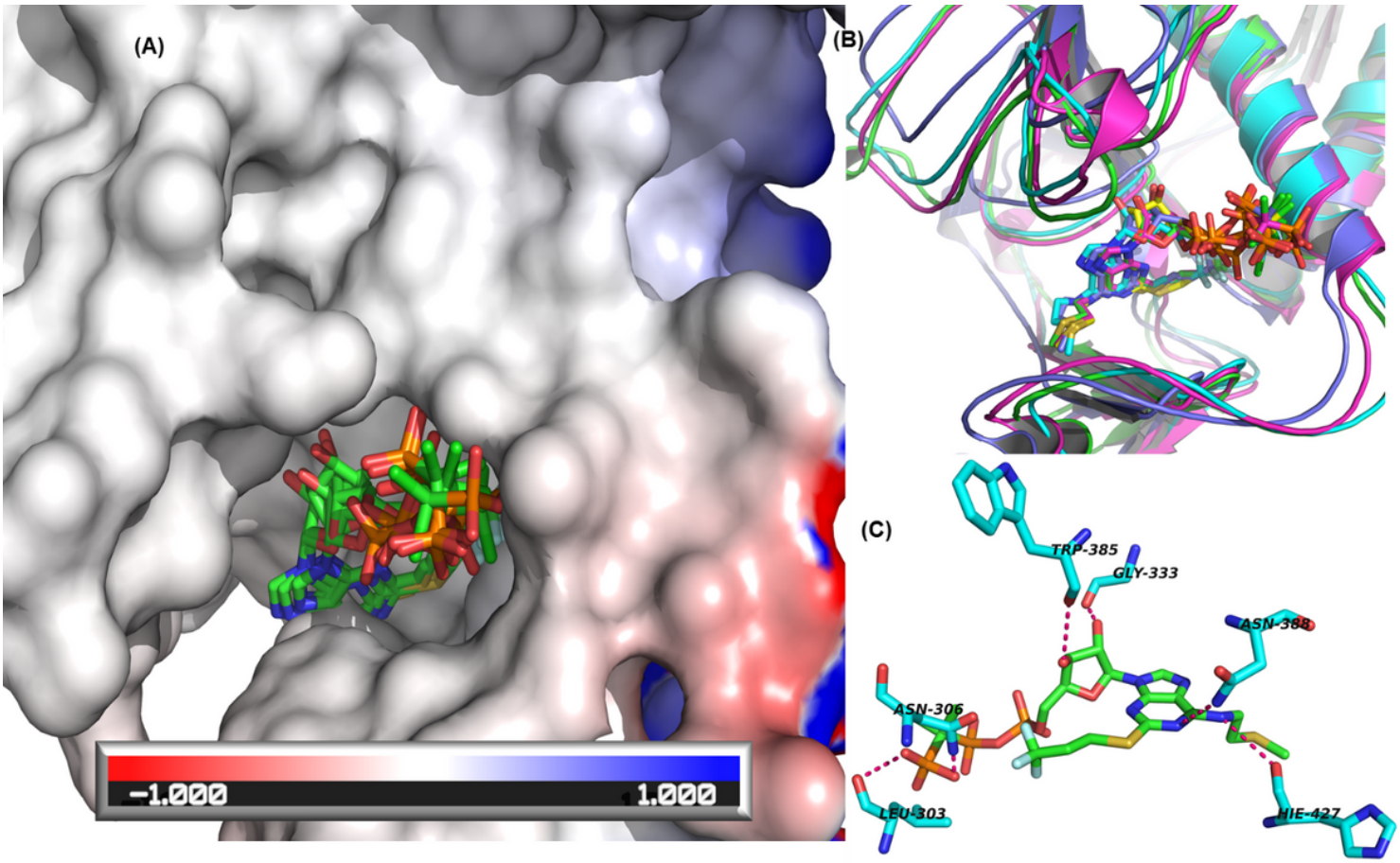

Figure 10

Cangrelor binding to ExoNulease: (A) The surface view of the protein and cangrelor binding. (B) The MD frames showing the flexibility of the active site and binding of ligand in the MD snapshots (C) The hydrogen bonding interactions of cangrelor with ExoNuclease protein.

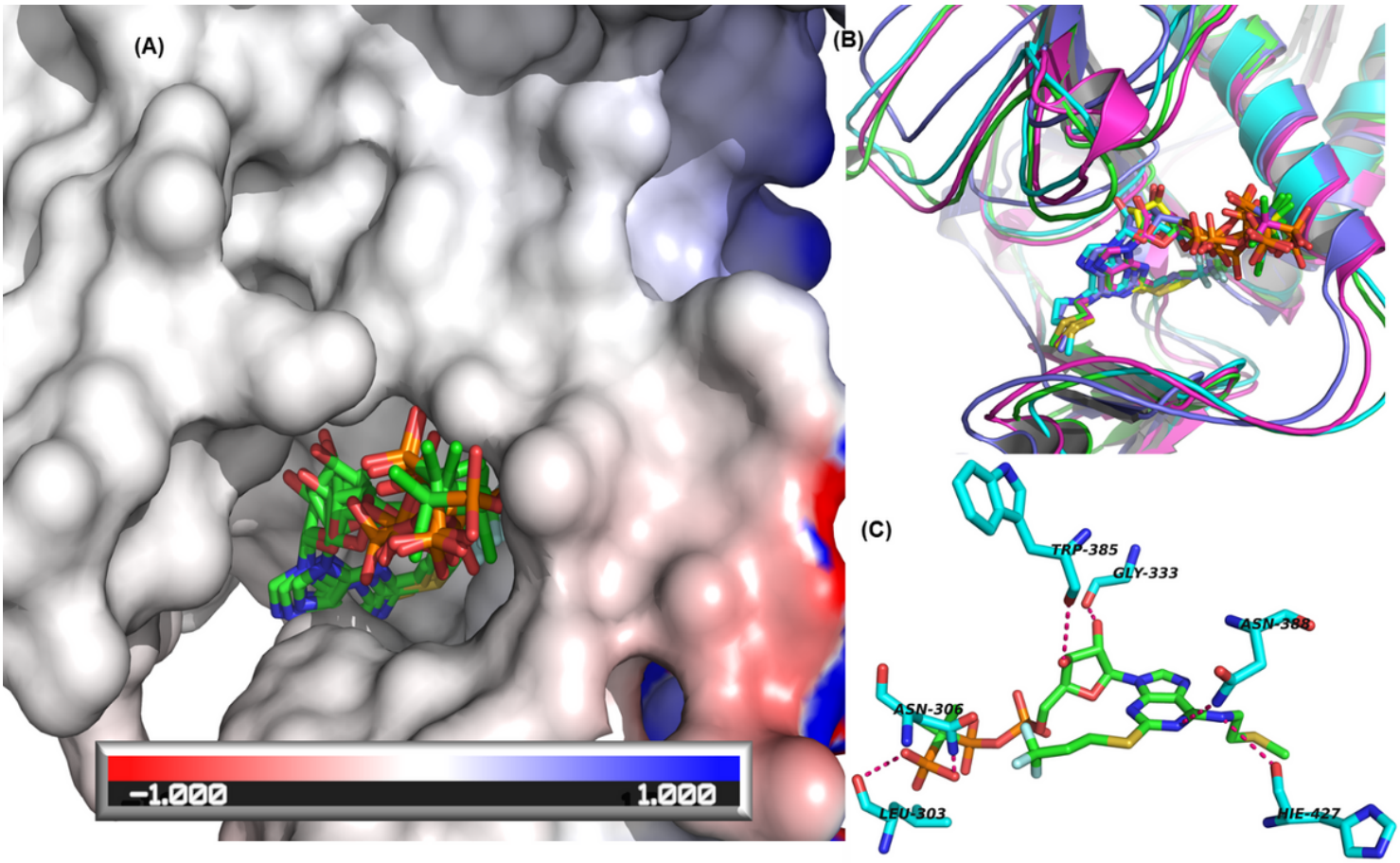

Figure 10

Cangrelor binding to ExoNulease: (A) The surface view of the protein and cangrelor binding. (B) The MD frames showing the flexibility of the active site and binding of ligand in the MD snapshots (C) The hydrogen bonding interactions of cangrelor with ExoNuclease protein.

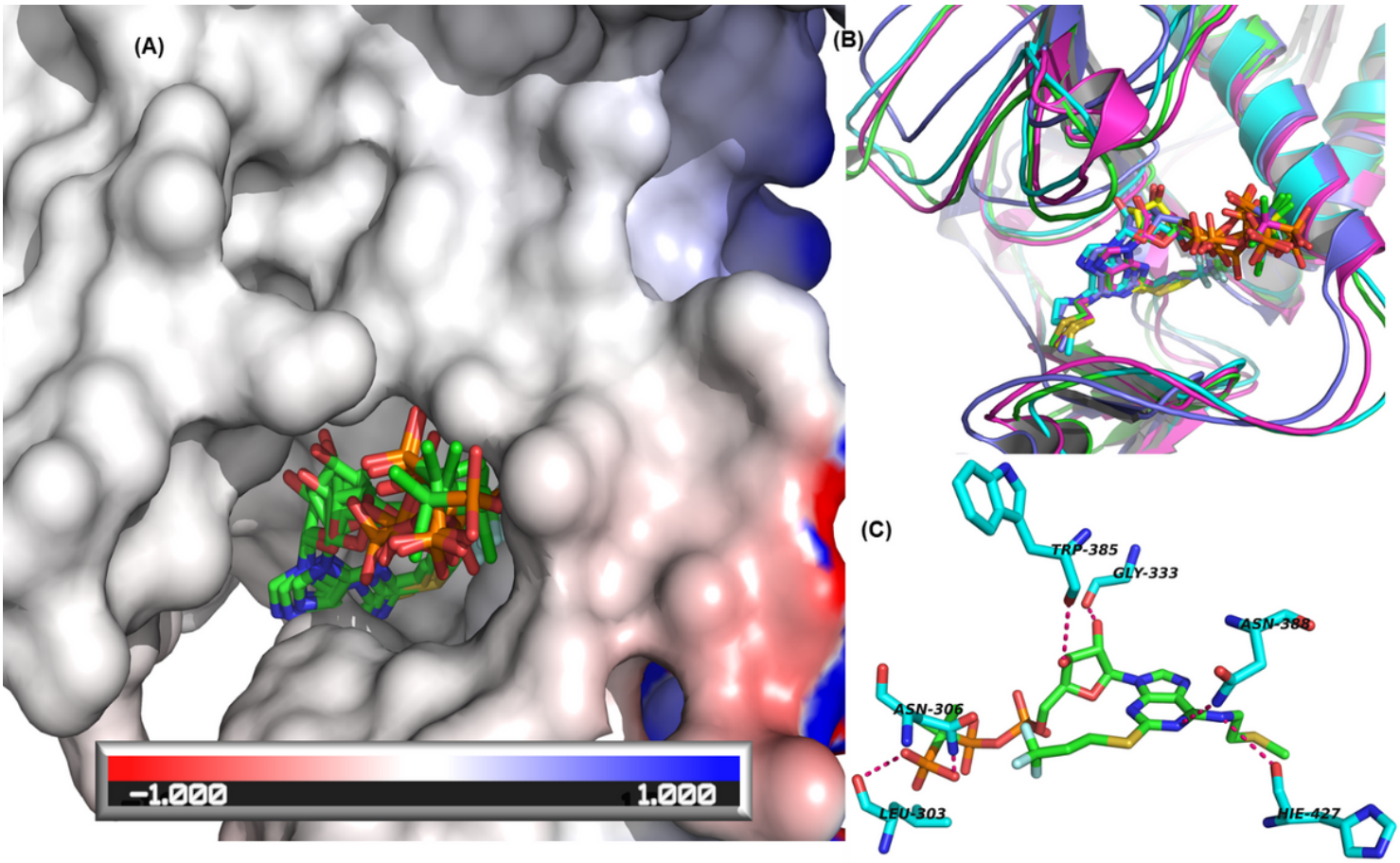

Figure 10

Cangrelor binding to ExoNulease: (A) The surface view of the protein and cangrelor binding. (B) The MD frames showing the flexibility of the active site and binding of ligand in the MD snapshots (C) The hydrogen bonding interactions of cangrelor with ExoNuclease protein.

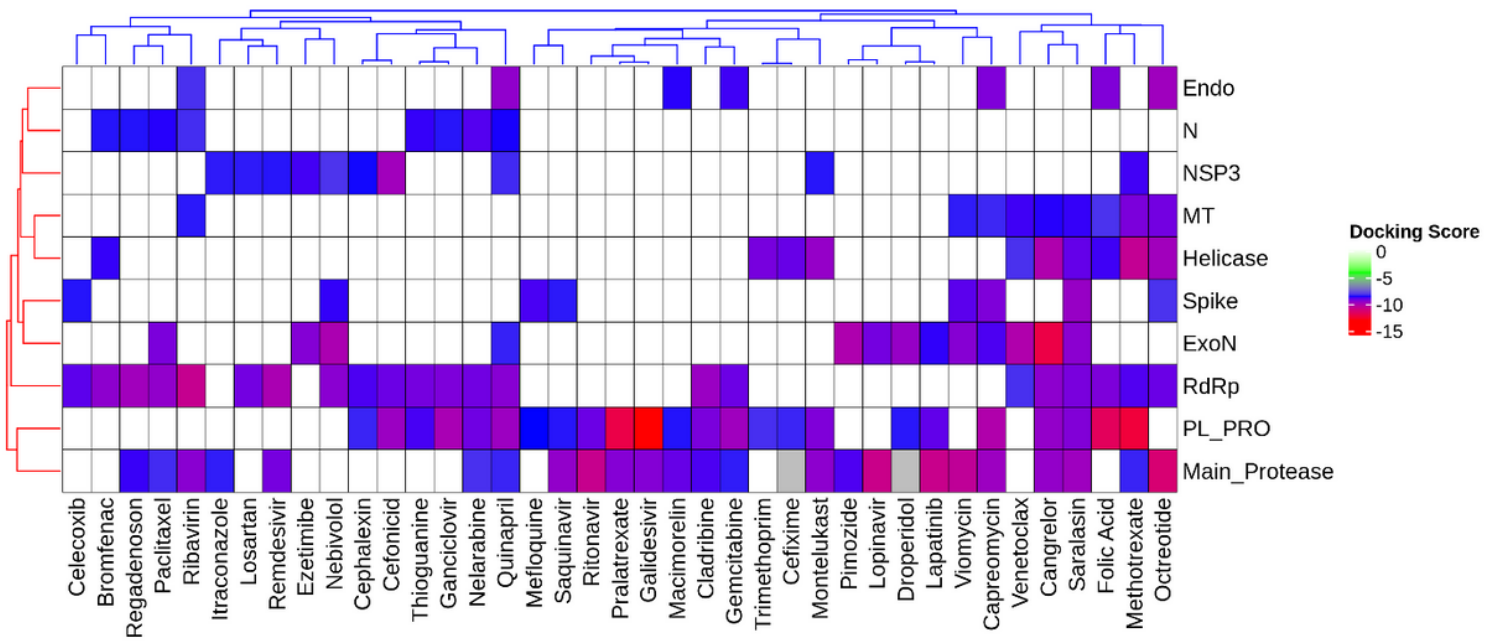

Figure 11

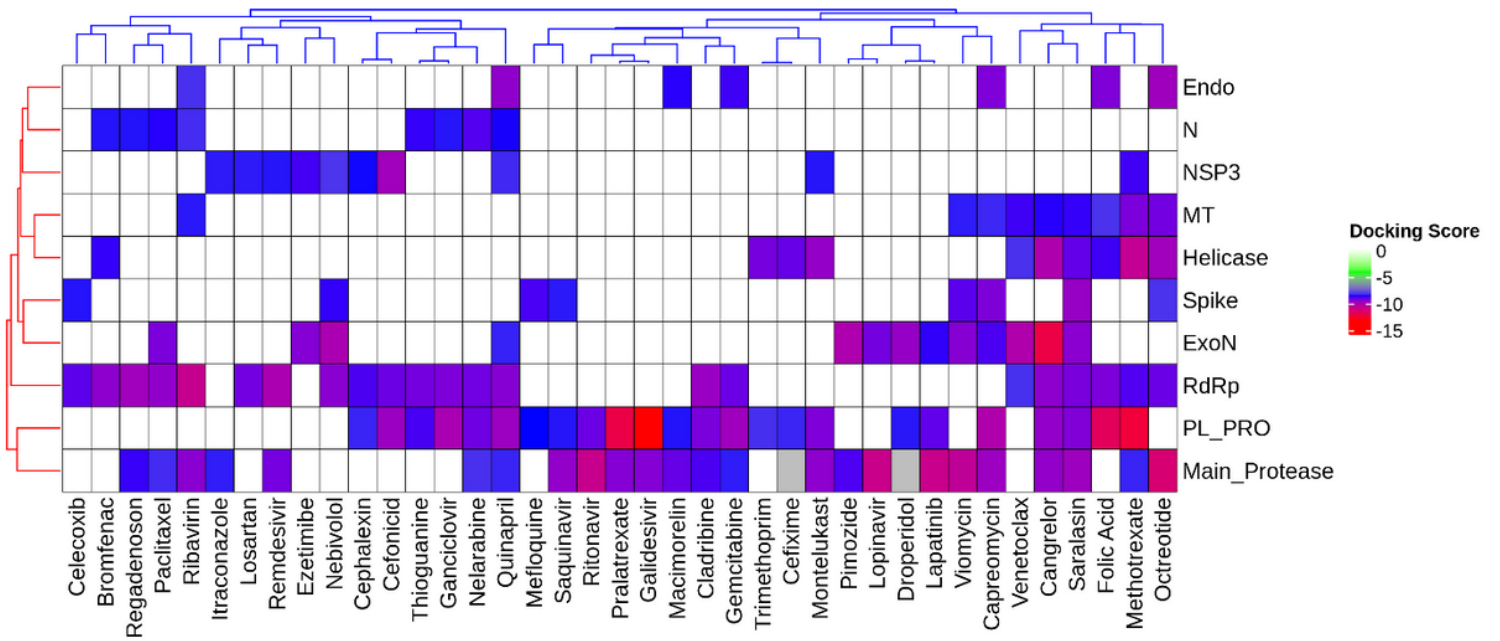

Figure 11

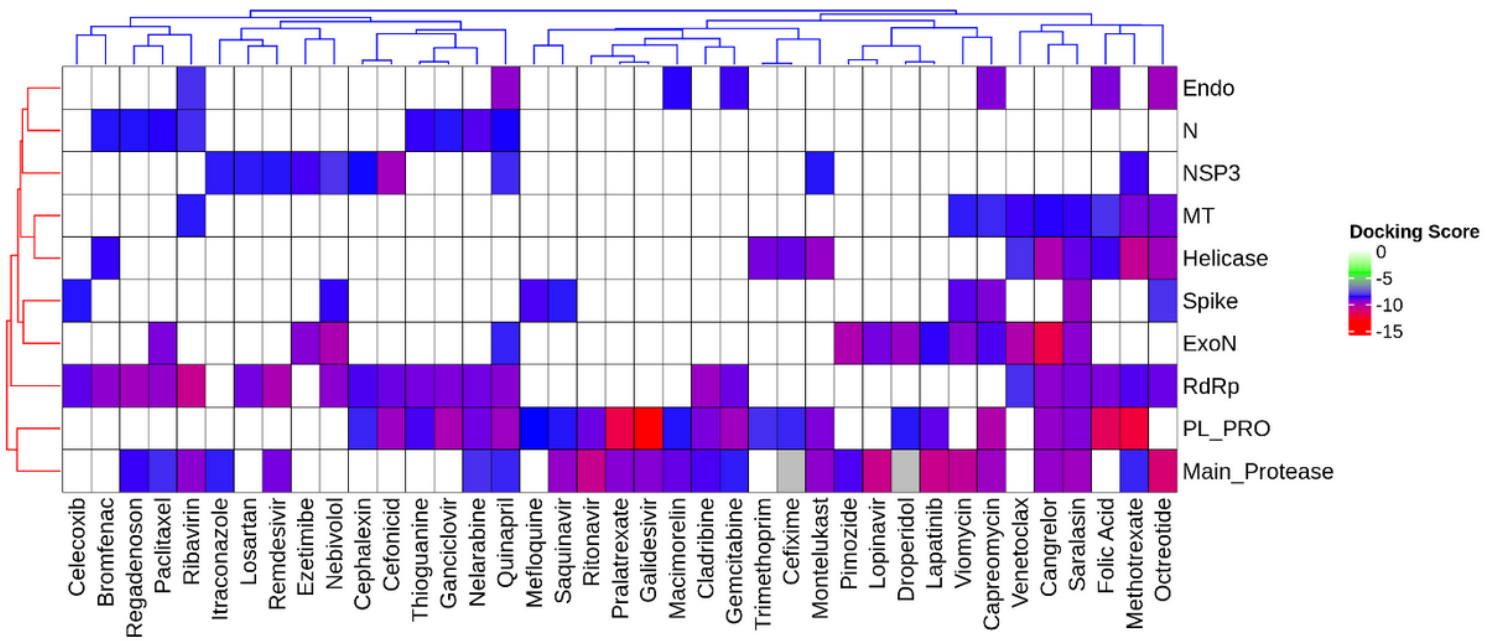
Endo
N
NSP3
MT
Helicase
Spike
ExoN
RdRp
PL_PRO
Main_Protease
Docking Score
0
-5
-10
-15
Celecoxib
Bromfenac
Regadenoson
Paclitaxel
Ribavirin
Itraconazole
Losartan
Remdesivir
Ezetimibe
Nebivolol
Cephalexin
Cefonicid
Thioguanine
Ganciclovir
Nelarabine
Quinapril
Mefloquine
Saquinavir
Ritonavir
Pralatrexate
Galidesivir
Macimorelin
Cladribine
Gemcitabine
Trimethoprim
Cefixime
Montelukast
Pimozide
Lopinavir
Droperidol
Lapatinib
Viomycin
Capreomycin
Venetoclax
Cangrelor
Saralasin
Folic Acid
Methotrexate
Octreotide

Figure 11

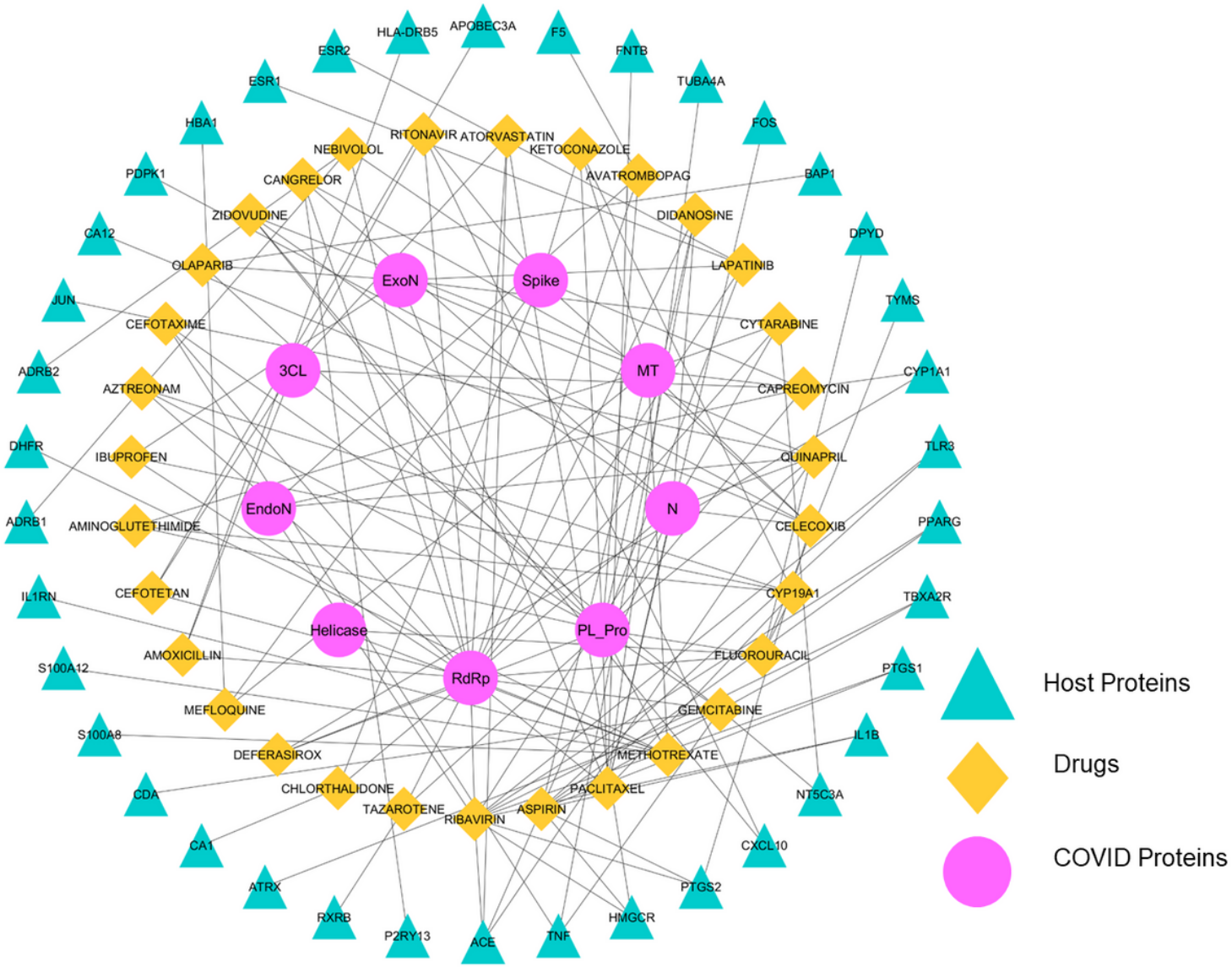

Figure 12

Human host and SARS-CoV2 protein drug interactions. Drugs capable of binding to multiple viral as well as human proteins related with SARS-CoV2 infection. The pink circles show the name of the SARS-CoV2 proteins, the green squares depict the drugs and the triangles show the name of the human proteins. The lines show the interaction between drugs and target protein.

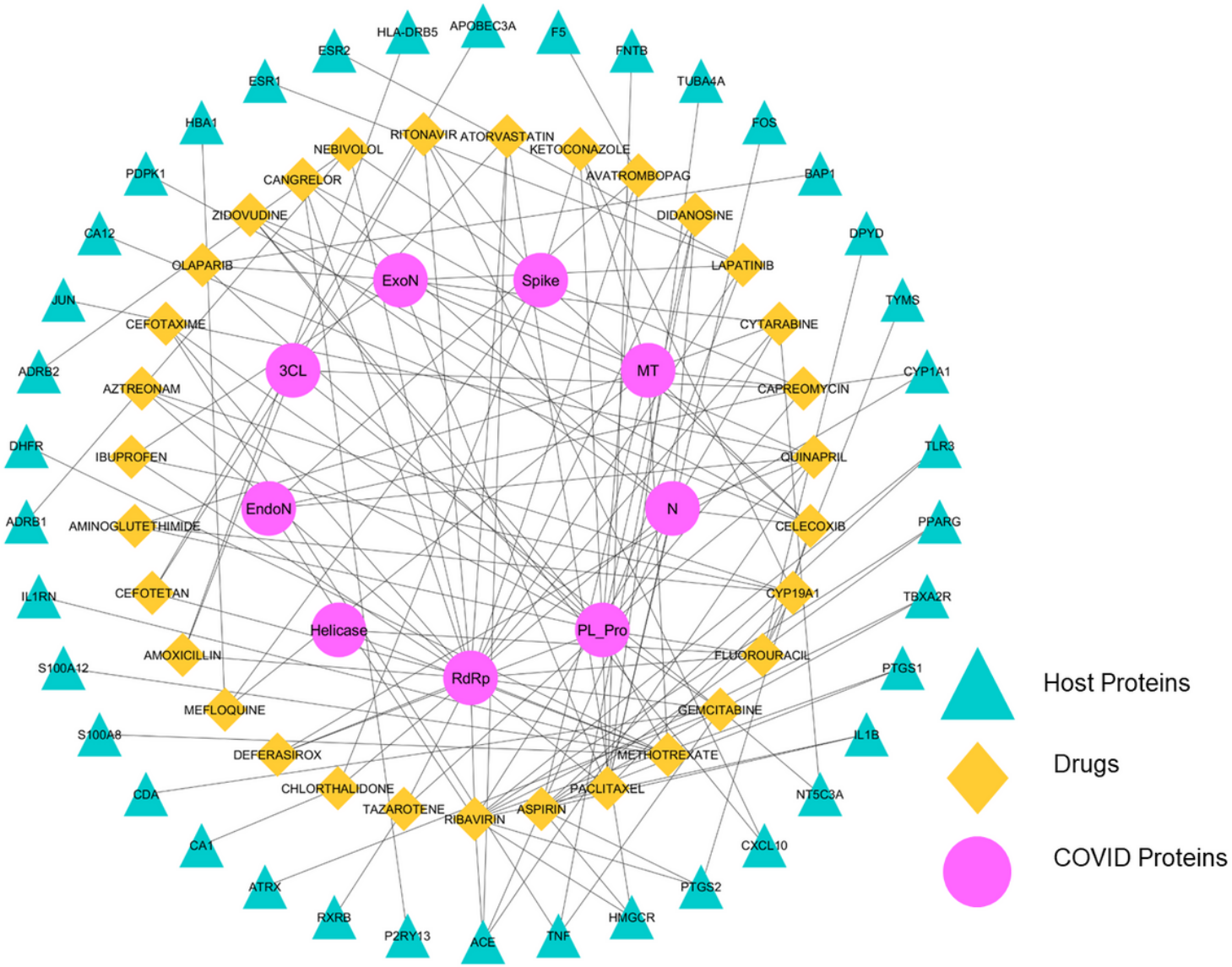

Figure 12

Human host and SARS-CoV2 protein drug interactions. Drugs capable of binding to multiple viral as well as human proteins related with SARS-CoV2 infection. The pink circles show the name of the SARS-CoV2 proteins, the green squares depict the drugs and the triangles show the name of the human proteins. The lines show the interaction between drugs and target protein.

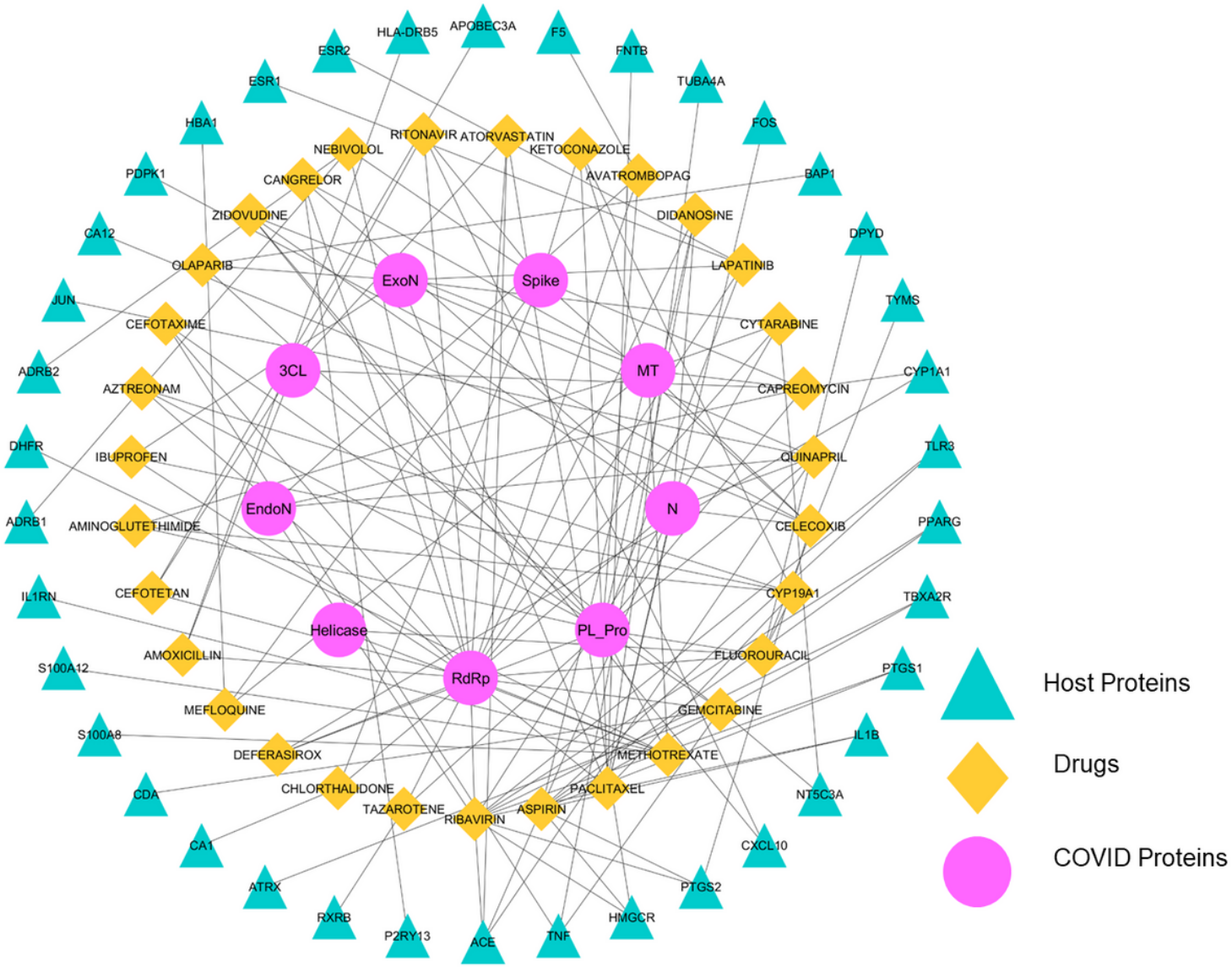

Figure 12

Human host and SARS-CoV2 protein drug interactions. Drugs capable of binding to multiple viral as well as human proteins related with SARS-CoV2 infection. The pink circles show the name of the SARS-CoV2 proteins, the green squares depict the drugs and the triangles show the name of the human proteins. The lines show the interaction between drugs and target protein.

Supplementary Files

This is a list of supplementary files associated with this preprint. Click to download.

- SupplementaryTable1.xlsx
- SupplementaryTable1.xlsx
- SupplementaryTable1.xlsx
- SupplementaryTable2.xlsx

- SupplementaryTable2.xlsx
- SupplementaryTable2.xlsx
- SupplementaryTable3.xlsx
- SupplementaryTable3.xlsx
- SupplementaryTable3.xlsx
- SupplementaryTable4.xlsx
- SupplementaryTable4.xlsx
- SupplementaryTable4.xlsx
- SupplementaryTable5.xlsx
- SupplementaryTable5.xlsx
- SupplementaryTable5.xlsx